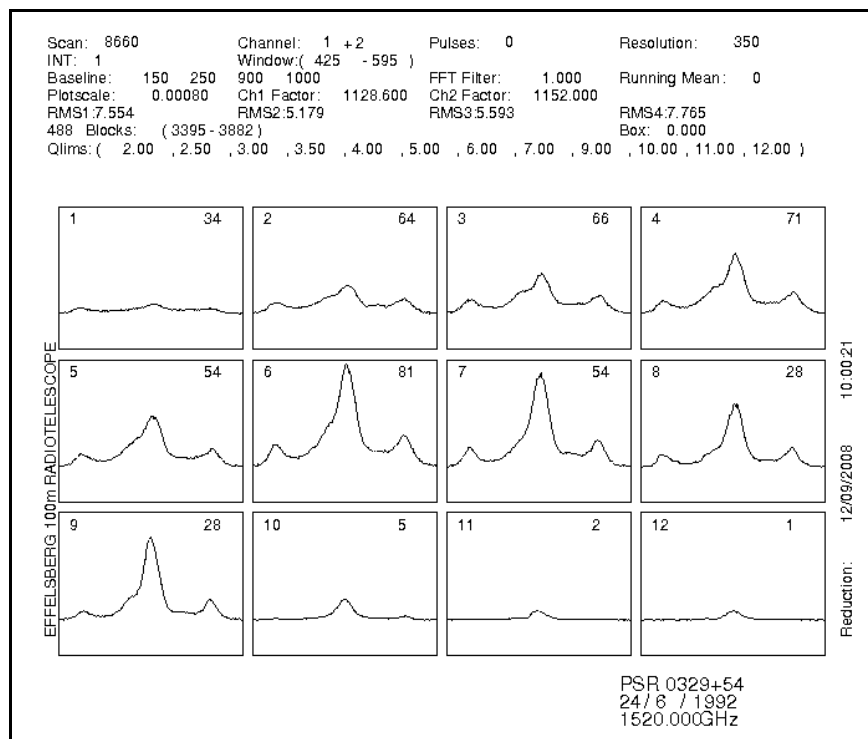


*Aristotle University of Thessaloniki*  
*Department of Physics*  
*Section of Astrophysics, Astronomy and Mechanics*  
*Astronomy Lab*

*Study of single pulses of pulsars in correlation to their emitted radiation*

*Elisavet Proedrou*



*Supervisor:*  
*John-Hugh Seiradakis*

*Thessaloniki, October 2008*



## **Abstract**

*The subject of this theses is the study of the single pulses of pulsars Pulsar PSR 0525+21, Pulsar PSR 0329+54 and Pulsar PSR 1822-09 in correlation to their emitted radiation. The behaviour of the core (main) components and conal (first & second) components in connection with their intensity, is investigated. The pulses are distributed to twelve categories according to their maximum intensities. The resulting profiles are studied and the maximum values of each component recorded. The study reveals that the First to Main and Second to Main component's ratio decreases as the fractionated intensity (*sigma*) increases. The same phenomenon occurs for the Second to First component's ratio for two out of the three scans from PSR 0329+54. Increase instead of decrease is for the Second to First component's ratio with the increase of the *sigma* in contrast to the rest of the results. Study of more pulsars is needed for these results to be explained and theories created.*



## **Abstract in Greek - Περίληψη**

Αντικείμενο αυτής της Πτυχιακής Εργασίας είναι η μελέτη των μεμονωμένων παλμών των pulsars PSR 0525+21, PSR 0329+54 και PSR 1822-09 συναρτήσει της ακτινοβολίας τους. Η μελετάται η συμπεριφορά της κύριας συνιστώσας, της πρώτης και δεύτερης συνιστώσας ως συνάρτηση της έντασης των παλμών. Οι παλμοί χωρίζονται σε δώδεκα κατηγορίες σύμφωνα με την μέγιστη τιμή των παλμών τους. Τα προφίλ δημιουργούνται μελετώνται και οι μέγιστες τιμές των παλμών καταγράφονται. Η μελέτη καταδεικνύει ο λόγος της Πρώτης προς την Κύρια συνιστώσα και ο λόγος της Δεύτερης προς την Κύρια συνιστώσα ελαττώνεται με την αύξηση της κλασματικής έντασης (σίγμα). Το ίδιο φαινόμενο παρατηρείται για τον λόγο της Δεύτερης προς την Πρώτη συνιστώσα σε δύο από τις τρεις καταγραφές του πάλσαρ PSR 0329+54. Στην τρίτη καταγραφή παρατηρείται αύξηση αντί για μείωση με την αύξηση του σίγμα, κάτι που έρχεται σε αντίθεση με τις άλλες δύο καταγραφές. Μελέτη περισσότερων πάλσαρ είναι απαραίτητη για την καλύτερη κατανόηση και εξήγηση του φαινομένου.

**Table of Contents:**

**(A) Introduction:**

1. A brief History on the discovery of pulsars.....	7
2. Pulse Profiles	
(i) Integrated Profile.....	9
(ii) Individual Radio Pulses.....	14
(a) Beam components, core and cone.....	54
(b) Subpulses.....	55
(c) Intensity fluctuations.....	56
(d) Polarization.....	60
(e) Nulling and Moding.....	61
(f) Mode changing.....	61

**(B) Experimental Data:**

I. Pulsars examined

• (1.1) Pulsar PSR 0525+21 .....	23
• (1.2) Pulsar PSR 0329+54 .....	26
• (1.3) Pulsar PSR 0450+55 .....	29
• (1.4) Pulsar PSR 1822-09 .....	30
• (1.5) Pulsar PSR 0823+26 .....	32
• (1.6) Pulsar PSR 1133+73 .....	33

II. Data Processing Program

• (2.1) Main program.....	34
• (2.2) Submenu Quality.....	36
• (2.3) Submenu Plot.....	38

III. Data Analysis and Results

• (3.1) Pulsar PSR 0525+21 .....	39
• Scan 7699.....	39
• Scan 7700.....	41
• Scan 7702.....	42
• Scan 7833.....	48
• Scan 9008.....	51
• (3.2) Pulsar PSR 0329+54 .....	54
• Scan 8653.....	54
• Scan 8654.....	59
• Scan 8656.....	61
• Scan 8657.....	63
• Scan 8658.....	68
• Scan 8659.....	70
• Scan 8660.....	72

• (3.3)Pulsar PSR 0450+55 .....	77
• (3.4)Pulsar PSR 1822-09 .....	79
• (3.5)Pulsar PSR 0823+26 .....	82
• (3.6)Pulsar PSR 1133+73 .....	84
VI. Conclusion .....	87
(C) <b>Bibliography</b> .....	88

## (A) Introduction

### 1. A brief History on the discovery of pulsars

The word *pulsar* is a contraction for "pulsating star" and appeared for the first time in print, in 1968. The first pulsar was observed by Jocelyn Bell Burnell and Antony Hewish on July 1967. Initially baffled by the seemingly unnatural regularity of its emissions, they named their discovery LGM-1, (which stands for "Little Green Men"). The hypothesis that "pulsars were beacons from extraterrestrial civilizations" was never seriously considered. There was some however, some discussion on the far-reaching implications should it turned out to be true. Their pulsar was later dubbed CP 1919 (for Cambridge pulsar) and is now known by a number of designators including PSR 1919+21, PSR B1919+21 (B indicates 1950.0 equatorial coordinates) and PSR J1921+2153 (J indicates 2000.0 equatorial coordinates). Although CP 1919 emits in radio wavelengths, pulsars have, subsequently been found to emit in the X-ray and/or gamma ray wavelengths.

The theory that "pulsars were rotating neutron stars" was proposed independently by Thomas Gold and Franco Pacini in 1968, and was proven beyond doubt by the discovery of the Crab pulsar, a pulsar with a very short pulse (33-millisecond) period in the Crab nebula.

Many of the basic observational facts about radio pulsars were established shortly after their discovery by Jocelyn Bell and Anthony Hewish. In the following years, theoretical and observational progress flourished and though there are many questions remaining unanswered, particularly about the emission mechanism, the basic model was established beyond all reasonable doubt: "Pulsars are rapidly rotating, highly magnetised neutron stars formed during the supernova explosions of massive 5-10 the mass of the Sun stars."

An image of the lighthouse model, used to explain the basic pulsar phenomenon can be seen in Figure 1 below. As the neutron star spins, charged particles from the surface of the neutron star, move along the magnetic field lines in the magnetosphere, accelerated by it. The light blue cones in Figure 1 represent them. Electromagnetic radiation is emitted by the accelerated particles, which is mostly detected at radio frequencies, in the form of sequences of pulses, produced as the magnetic axis (and therefore the radiation beam) crosses the observer's line of site, at every rotation. The orange ball in Figure 1, shows the relationship between the observed intensity and the rotational phase of the pulsar.

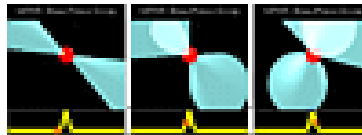


Figure 1: The rotating neutron star (or "lighthouse") model for pulsar emission.

In 1974, Joseph Hooton Taylor, Jr. and Russell Hulse discovered, a binary pulsar system, for the first time, PSR B1913+16. It orbits a neutron star with an orbital period of just eight hours. Einstein's theory of general relativity predicts that, the system should emit strong gravitational radiation, causing the orbit to continually contract as it loses orbital energy. Observations of the pulsar confirmed this prediction and provided the first evidence of the existence of gravitational waves, as observations of this pulsar continue to agree with general relativity. In 1993, the Nobel prize in physics was awarded to Taylor and Hulse for the discovery of this pulsar.

In 1982 Shri Kulkarni and Don Backer discovered a pulsar with rotation period of 1.6 milliseconds. Observations revealed that it possessed a magnetic field much weaker than that of ordinary pulsars and confirmed that a new class of object had been found. Those objects were named MSPs, which stands for "millisecond pulsars". They are believed to be the end product of X-ray binaries. Due to their extremely rapid and stable rotation, MSPs can be used as clocks, as stable as the atomic clocks on Earth. The factors affecting the arrival time of pulses on Earth by

*more than a few hundred nanoseconds can be easily detected and used to make precise measurements. Some of the physical parameters that are accessible through pulsar timing include:*

- *The 3D position of the pulsar*
- *The pulsar's proper motion*
- *The electron content of the interstellar medium along the propagation path]*
- *The orbital parameters of any binary companion*
- *The pulsar rotation period*
- *The pulsar's evolution with time*

*They are computed from the raw timing data by Tempo, a computer program specialized for this task.*

*The deviations between the observed arrival times and predictions made using the above parameters can be found (after they have been taken into account) and attributed to:*

- *Intrinsic variations in the spin period of the pulsar*  
*or*
- *Errors in the realization of Terrestrial time against which where measured*  
*or*
- *The presence background gravitational waves*

*Scientists are currently attempting to resolve these possibilities by forming a Pulsar Timing Array (they are comparing the deviations seen amongst several different pulsars). These efforts might lead to a time scale better than the one available at the moment (a factor of ten or better) and the first direct detection of gravitational waves.*

*The first extrasolar planet found was orbiting a MSP, (Aleksander Wolszczan ,made the observation). This discovery presented important evidence regarding the widespread existence of planets outside the solar system, although it is very unlikely that any life form could survive in an environment with such intense radiation.*

*It became clear after their discovery that pulsars are excellent celestial clocks. In the original discovery paper, the period of the first pulsar to be discovered, PSR B1919+21, was found to be stable to one part in  $10^7$  over a time-scale of a few months. Following the discovery of the millisecond pulsar B1937+21 in 1982, it was demonstrated that its period could be measured to one part in  $10^{13}$  or better. This stability leads to a number of applications which include: time keeping, probes of relativistic gravity and natural gravitational wave detectors. Nowadays a whole science has developed into measuring the pulse time-of-arrival with the highest accuracy possible.*

*Since their discovery in 1967, radio pulsars have provided insights into physics on length scales covering the range:*

- *1 m (giant pulses from the Crab pulsar)*
- *10 km (neutron star)*
- *kpc (Galactic) to hundreds*
- *Mpc (cosmological)*

*The exhibit extreme stellar environments, with matter at nuclear densities, magnetic fields of  $10^8$  G -  $10^{14}$  G, and spin periods ranging 1.5 s - 8.5 s. The regular pulses received from a pulsar correspond to a single rotation of the neutron star each. By measuring the deviations from perfect observed regularity we derive information about the neutron star itself, the interstellar medium it has crossed to reach Earth, and the effects due to gravitational interaction with binary companion stars.*

## **2. Pulse Profiles**

*Pulsars are weak radio sources with mean flux densities, (usually quoted in the literature at a radio frequency of 400 MHz), that vary between 1 and 100 mJy ( $1 \text{ Jy} = 10^{-26} \text{ Wm}^{-2}\text{Hz}^{-1}$ ). Therefore the addition of many thousands of pulses is required in order to produce a discernible profile. Although the individual pulses vary quite dramatically from pulse to pulse, the integrated profile at any particular observing frequency is very stable. The pulse profile can therefore act as a finger print of the emission beam.*

*Neutron stars are extremely stable rotators and are essentially equivalent to large celestial flywheels with moments of inertia  $\sim 10^{45}$ . The rotating neutron star model known as “lighthouse model”, correctly predicts that the pulse period should gradually increase as the outgoing radiation carries away rotational kinetic energy. Gold showed that “a rotating neutron star with a large magnetic field must be the dominant energy supply to the nebula” when a period increase of 36.5 ns per day was measured for the pulsar in the Crab nebula and the model became universally accepted.*

### **(i) Integrated Profile**

*The most striking characteristic of pulsars is the astonishing regularity of the pulsation period. This machine-like precision may suggest that the whole range of phenomena to be observed in pulsar radiation should follow equally simple patterns. On the other hand the individual pulses exhibit an almost bewildering range of variability in the characteristics of the pulses, which sometimes approach chaos. The actual time of arrival of the individual pulses varies over a considerable range, their strengths vary on several distinct time scales, and their polarization is variable. Also the individual pulses vary greatly in shape, intensity and longitude from one pulse to the next. The integrated profile clearly depends on the number of pulses included in it.*

*In general integrated profiles remain stable in shape and polarization on long time scales. This is the reason they are an important feature of pulsar emission.*

*Useful descriptions can be made by isolating typical properties of individual pulses, for example their average width or alternatively by using the integrated pulse profile.*

*The integrated pulse profiles are obtained by superimposing a sequence of some hundreds of individual pulses. This is achieved by taking sample of the radio signal at small time intervals, and superimposing the sequence of samples at the period of the pulsar. Since the individual pulses are often polarized, we must ensure that the total energy is recorded. For this to be achieved, the two orthogonal modes of polarization must be received, separately detected and added.*

*The signal-to-noise ratio in the integrated profile improves with larger receiver bandwidths and integration times; it is necessary however to restrict the bandwidth for pulsars with large dispersion measures, due to the smearing effect which would spoil the time resolution.*

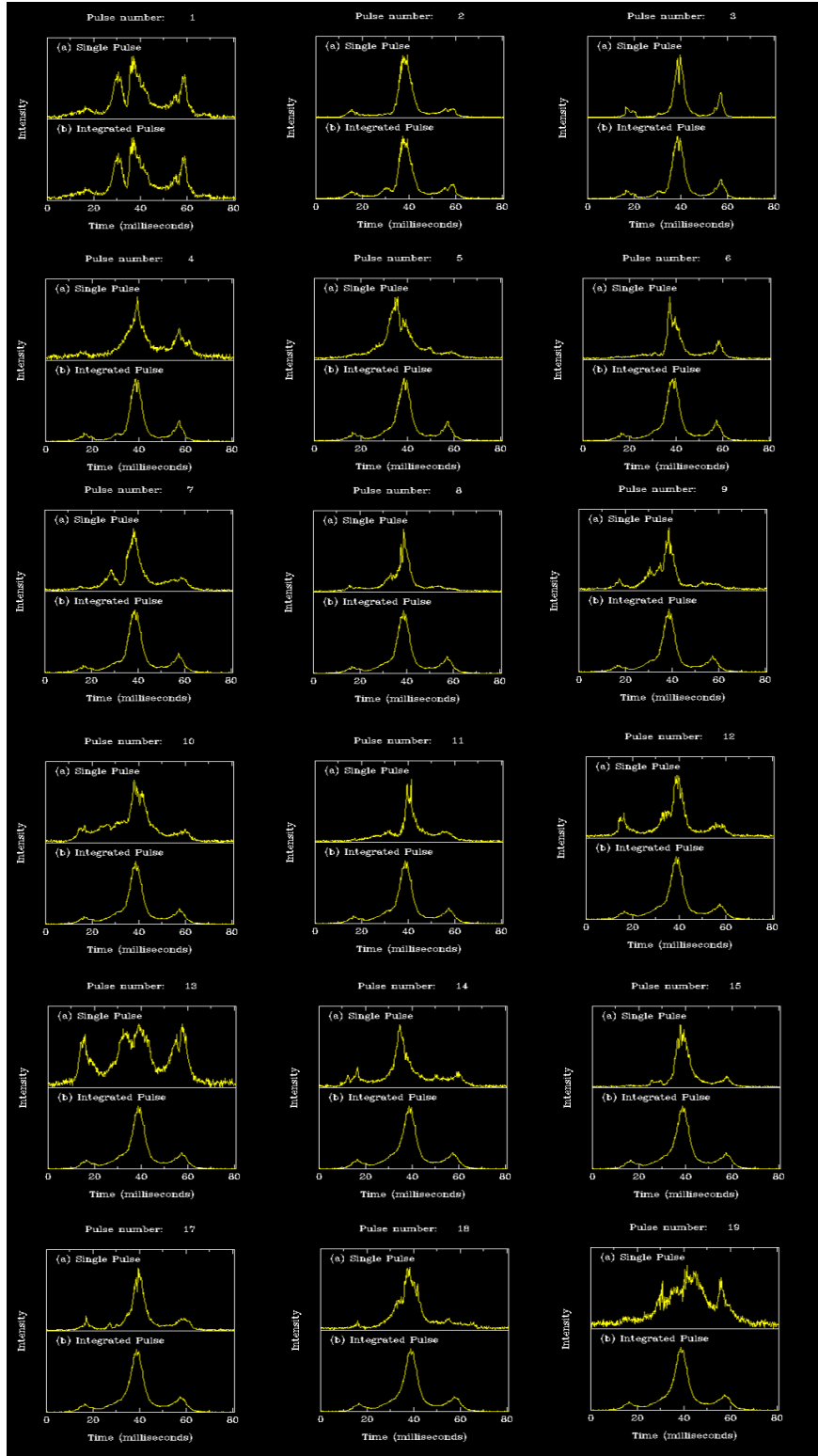


*Figure 2: Change of the integrated profile with the addition of pulses*

*It is known that the mean or integrated pulse profile for any given pulsar is very stable and has a characteristic shape. One of the most important properties of a pulsar is the shape of its integrated profile. The integrated profiles of most of the known pulsars have been obtained due to the improvement in the signal-to-noise ratio in several frequencies. A study of the observations reveal that are often rather complex, with several components or, and that each pulsar has a unique profile. Most profiles exhibit a single component, but multiple-components profiles are also*

common. The basic shape of multiple-component profiles is usually “double”,(two main peaks with steep outer edges separated by a saddle region. Integrated profiles of 45 pulsars, showing the wide variety of observed shapes, are given below.

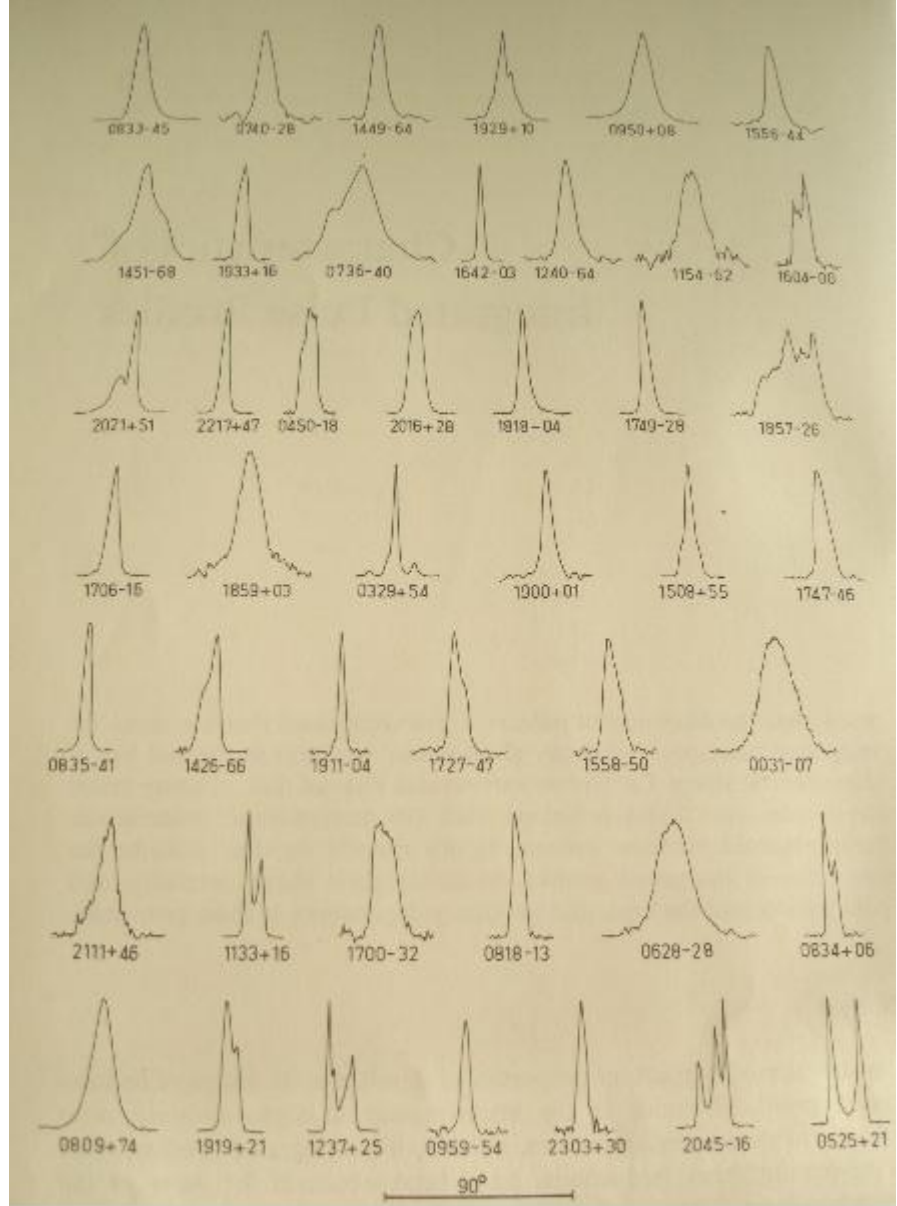


**Figure 3:** Integrated pulses for 45 pulsars, all plotted on the same longitude scale (a  $90^\circ$  bar is given in the bottom of the figure). These profiles were recorded at frequencies between 400 and 650 MHz, and are arranged in order of increasing pulse period.

The shape of integrated profiles is generally somewhat frequency-dependent (it is a useful generalization that the properties of the pulsars do not depend markedly on radio frequency, but there are some systematic changes to be found in a number of pulsars).

For pulsars with double profile Craft & Comella (1968) found that the separation between the two peaks tended to increase at lower frequencies and often the separation between identifiable components varies this way.

The basic character of a pulsar's profile is similar at all frequencies. Therefore pulsars may be divided into two categories, according to whether they have “single” or “double” profiles, called respectively Type S (simple) and Type C (complex) by Taylor & Huguenin (1971). More

*observations are available at frequencies around 400 MHz than at other frequencies, so profile shapes obtained at this frequency are used for purposes of classification.*

*Type C pulsars tend to have long periods, in most cases greater than one second they seldom have very small values of the parameter  $P\dot{P}$ . This phenomenon is related to the magnetic field strength at the surface of the neutron star. Neutron stars usually exhibit strong linear polarization and a smooth variation in the polarization position angle across the profile.*

*Type S pulsars, on the other hand, tend to have short periods and have often low values of  $P\dot{P}$ , weak polarization and discontinuous changes in the position angle across the profile.*

*Another characteristic feature of pulsars, which overlaps the above categories, is the phenomenon of drifting subpulses. Pulsars with drifting subpulses are called Type D or when more detail is required, Type SD or CD, to indicate a simple or complex mean profile. The most organized drifting patterns occur in Type SD pulsars.*

*The pulsed energy from most pulsars is confined to a small fraction of the period, there are a number of exceptions. In several pulsars an additional pulse component, the interpulse, is situated approximately half-way between the main pulses.*

*The pulsed emission is confined to a rather narrow longitude range, for most of the pulses but exceptions are observed. There may also be a nonvarying component to the emission from pulsars. In normal synchronous averaging such a component would be removed by the baseline-fitting procedure. A search for such emission by Huguenin & co-workers (1971) using interferometric techniques yielded upper limits comparable to the mean flux density (pulse energy divided by the period) for several pulsars; also in some pulsars the integrated profile is much broader than usual. These profiles are intrinsic to the pulsar and do not result from propagation effects in the interstellar medium. At low frequencies pulse profiles are often affected by scattering of the radiation by irregularities in interstellar electron density. Propagation delays result in a smearing of the pulse energy into an exponential decaying pulse tail. If the scattering is severe, delays can exceed the pulse period, thereby causing a nonvarying flux component and a decrease in pulsed period.*

*There is a tendency towards symmetry in all the integrated profiles, which are generally of the following types:*

- *a smooth single hump, e.g PSR 1642-03*
- *a double hump e.g PSR 1133+16*
- *a single hump with extensions or ‘outsiders’ e.g PSR 0329+54*
- *a double hump with structure between e.g PSR 1237+25*

*These profiles will be interpreted as distributions of emitting regions over a range of longitude in the pulsar magnetosphere.*

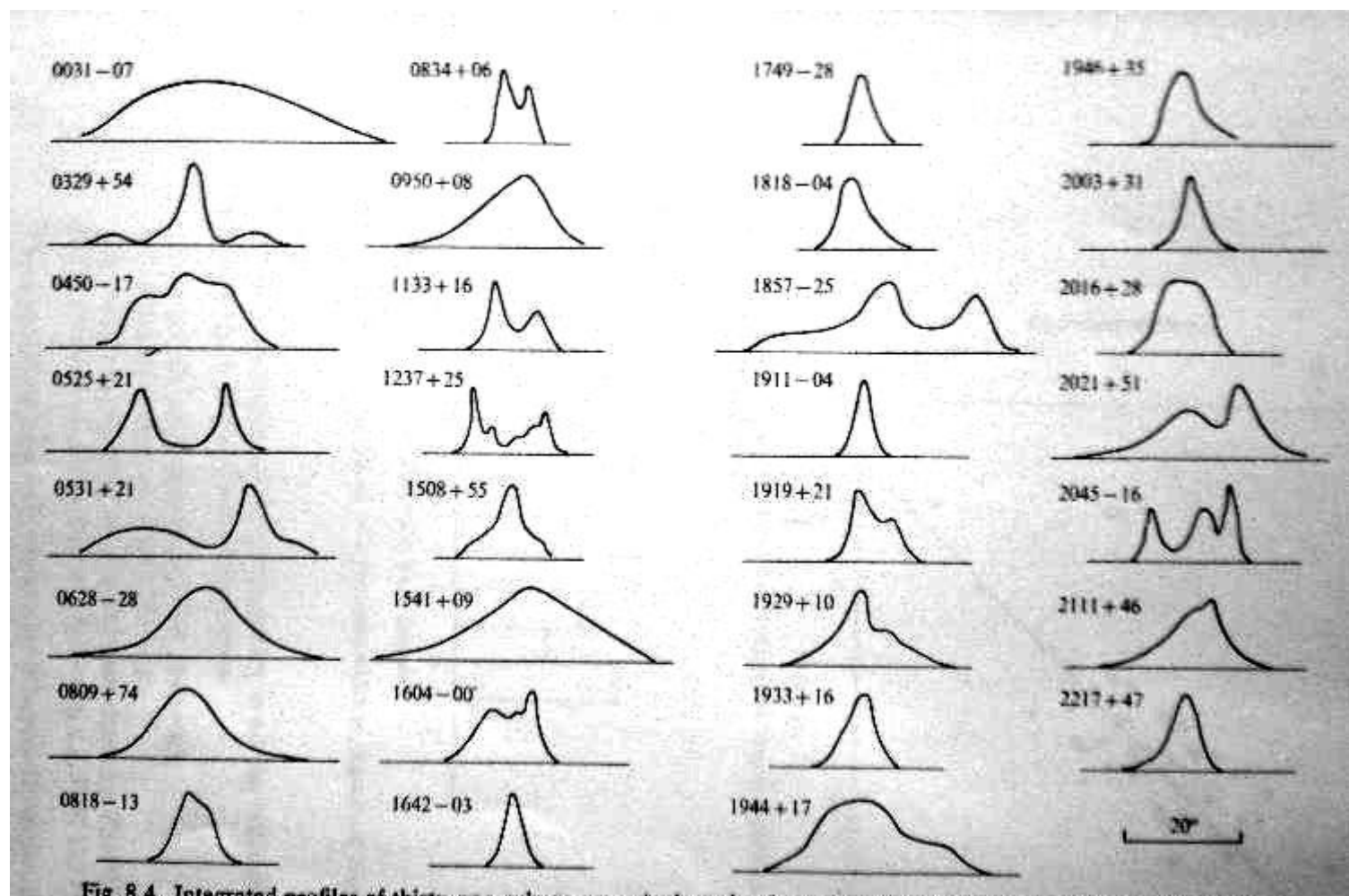


**Fig. 8.4.** Integrated profiles of thirty-one pulsars, on a single scale of rotational longitude. (Jodrell Bank; 408 MHz.)

*Figure 4: Intergrated profiles of thirty-one pulsars, on a single scale of rotational longitude. (Jodrell Bank; 408 MHz.)*

*Between the pulses there is a remarkably low intensity, usually below the detection level. For some pulsars a second component, known as 'interpulse', appears somewhere near but not exactly at the halfway point between the main pulses.*

## (ii) Individual Radio Pulses

*The well organized and characteristic behaviour of the integrated pulse profiles becomes more surprising as one examines in greater detail the complexity and variety of the individual pulses that add to make the integrated profiles. The intensity and shape of the pulses varies from pulse to pulse on a very short time scale. A sequence of a few pulses may present such chaotic variations that is hard to believe that the sum of any sequence of only a few hundred pulses can yield the characteristic integrated profile. Such a sequence of PSR 0525+21 (Scan 7827) can be seen below.*

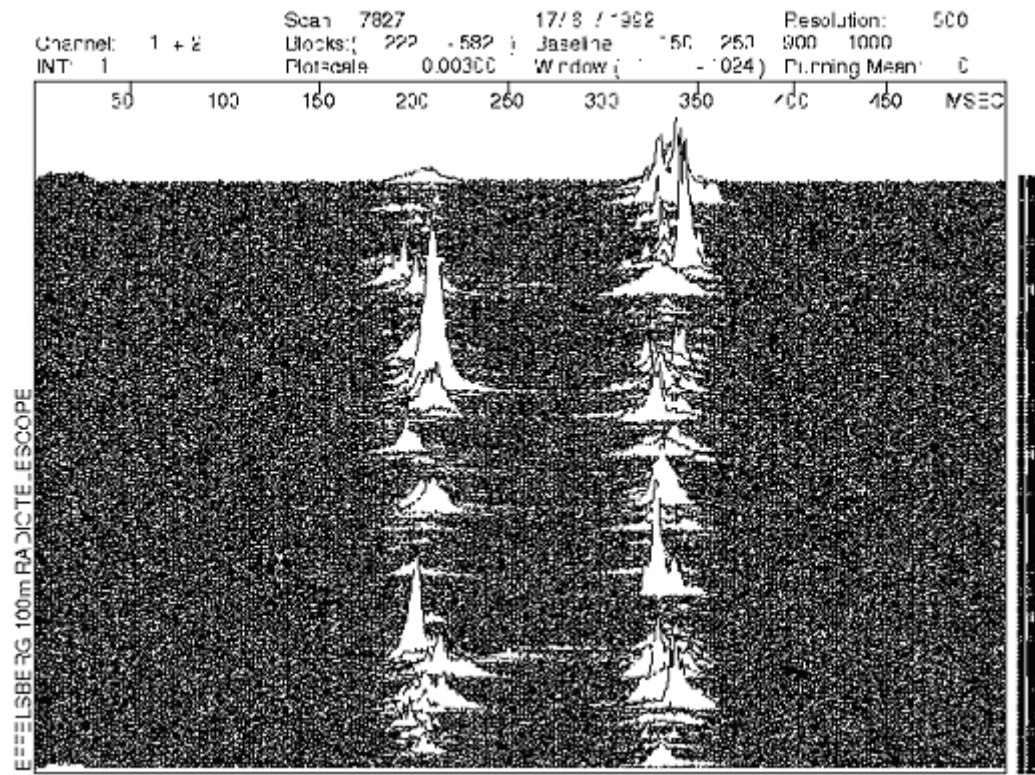


*Figure 5: Sequence of pulses for PSR 0525+21*

*But there is often a quite simple statistical description of the pulse behaviour, and there are precise rules governing much of the apparent chaos. For example the energy in a single pulse, as measured at a particular part of radio spectrum, follows a typical statistical distribution, which is near Poissonian for some pulsars and quite different from others; furthermore this distribution is usually well established from a sequence of only a few hundred pulses.*

*Individual pulses commonly have a width of only one-tenth or less of the width of the integrated profile; they may appear almost at random at any part (or 'phase') of the profile. Their occurrence is not completely random. Often successive pulses will appear as narrow pulses at nearly the same phase, and in some pulsars a sequence of several pulses will be related in this way. A slow 'drift' of phase is often seen, usually towards the earlier part of the profile. Some pulsars radiate pulses with two or more such narrow components. The consistency of these narrow components together with a characteristic polarization observed within the narrow component, has led to their isolation as a basic component of pulsar radiation. They are known as 'sub-pulses'.*

More rapid fluctuations of intensity occur, usually in the pulsars with shorter periods. These fluctuations are known as the ‘microstructure’. They include some remarkably short and intense pulse components in the Crab Pulsar: a single one of these ‘giant’ pulses may last only 10  $\mu$ s, but during that time the intensity can exceed the radio intensity from the whole Crab Nebula. The microstructure does not have a continuity from pulse to pulse.

Individual pulses from a given pulsar vary greatly in intensity, shape and polarization from one period to the next. In general, they do not have the same form as the integrated profile. Variations are often random in character but periodic changes are also observed, particularly in the pulse intensity.

### (a) Beam components, core and cone

The symmetry displayed in the profiles of many pulsars leads naturally to a classification in which a central component is called the core while the outer components are regarded as part of a hollow cone. There is a gradation in properties with radial distance from the beam center: the core components have larger widths and steeper spectra.

The angular radiated width of the individual components within the beam may be found using the same statistical method as for the whole beamwidth.

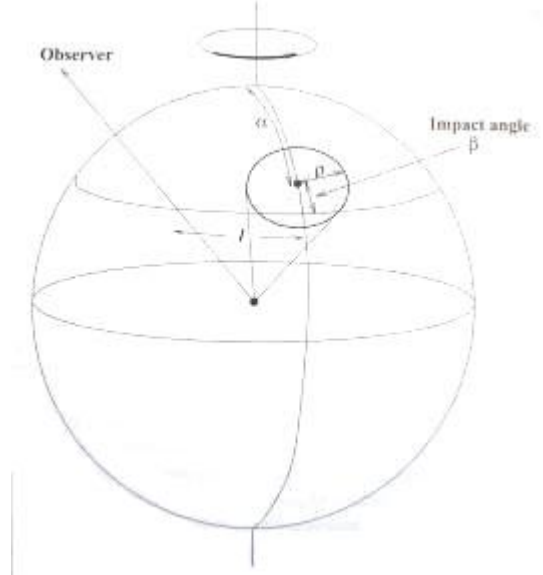


**Figure 6:** The relation of the overall profile width to the beam geometry. The radiation beam is shown as a symmetrical cone, angular width  $2\rho$ , at inclination angle  $\alpha$ , cut by a line of sight with impact parameter  $\beta$ .

The distribution of widths again shows a well-defined lower bound, both for the core and conal components, which may be taken as the width for pulsars where the viewing angle  $\alpha$  is near 90°; the scatter of points above this lower limit corresponds to pulsars with smaller values of  $\alpha$ . From this lower bound, the half-power widths  $w_{50}$  (in degrees) of conal and core components are found to be

$$w_{50,conal} = 1.75P^{-1/2} / \sin \alpha$$

$$w_{50,core} = 2.5P^{-1/2} / \sin \alpha$$

The marked difference in width between the core and the conal components is confirmed in practically all individual pulsars.

As already mentioned, the apparent symmetry of many integrated profiles with two or more components led to the suggestion that they might be arranged as a central core surrounded by a hollow cone of emission (Komesaroff et al, 1970). This model was developed by Rankin (1993), who made the further suggestion that the occurrence of five-component profiles indicated an arrangement in a double hollow cone. The cones are regarded as a preferred arrangement for component beams, rather than an unbroken ring, since there are no wide component observed that would correspond to tangential cuts across a hollow cone as in Figure 6.

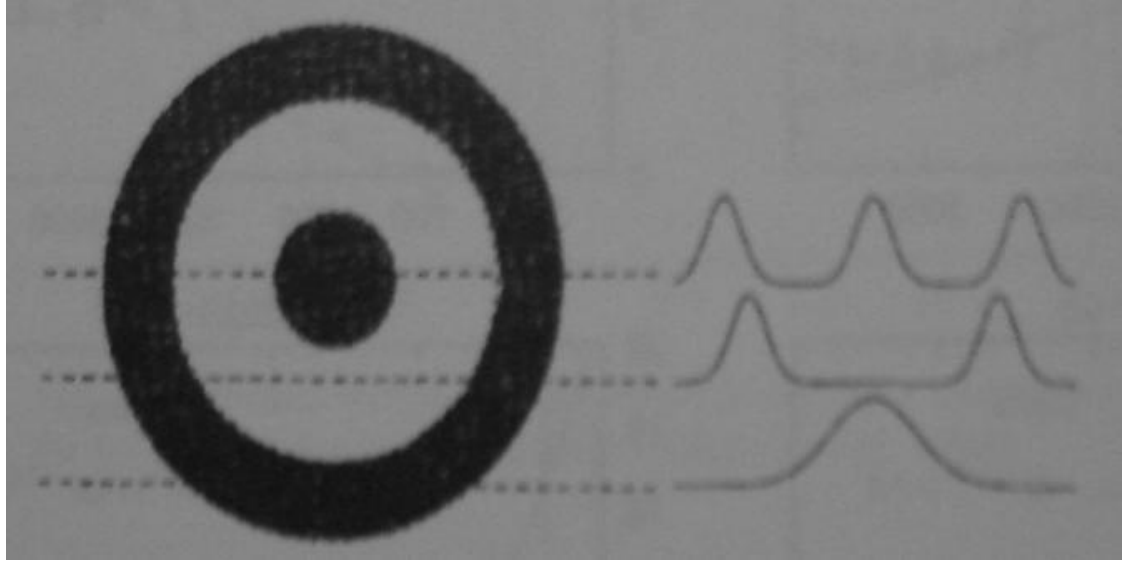


**Figure 7:** A model of the core and conal beams, with various types of symmetrical profiles generated at different impact parameters

Locating the component beams within an overall beam requires some knowledge of the impact parameter  $\beta$ , and preferably also the inclination angle  $\alpha$ , for each pulsar. Lyne & Manchester (1988) used estimated of these angles for some hundreds of pulsars, and found no preference for components to be located within discrete cones. The distinction between conal and core emission is evidently not clear cut. However, Han & Manchester (2001) followed the same geometric procedure to construct a two dimensional image of the mean radio beam shape for 87 pulsars. They again found a smooth distribution over the polar cap, but with some enhanced emission at the core and at around 0.7 of the polar cap radius.

### (b) Subpulses

Individual pulses normally consist of one or more subpulses. These subpulses, which appear to be basic units of emission, typically have a rather simple, almost Gaussian shape and width between 3 and 10 degrees of longitude. Subpulses occur at various longitudes within the integrated profile, and often overlap when two or more subpulses are present in an individual pulse. Components or peaks are formed in the integrated profile when subpulses are stronger and/or occur more frequently at a given longitude. Longitude-time diagrams of the intensity variations in sequences of individual pulses from three pulsars are shown in Figure 6. These diagrams show that subpulses are generally narrow compared to the integrated profile and that they occur

preferentially at certain longitudes. This is especially true for multiple-component pulsars, such as PSR 1133+16 and PSR 1237+25.

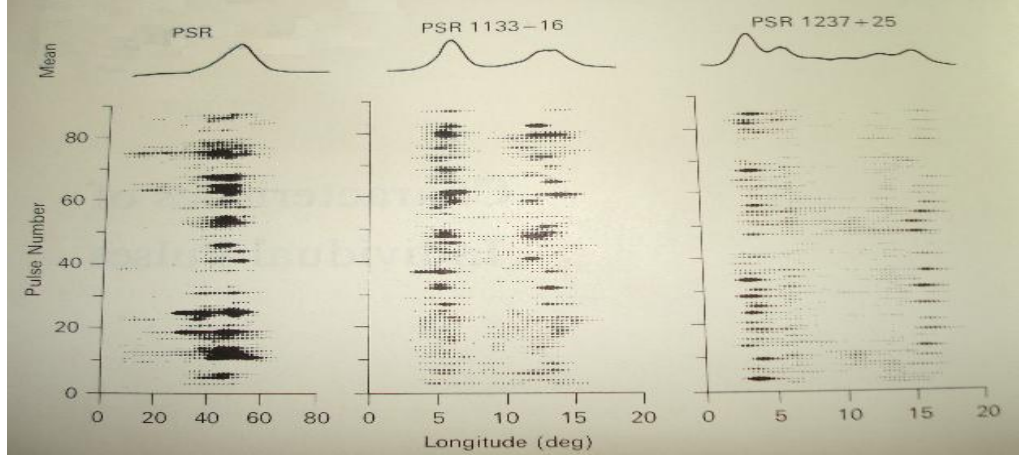


**Figure 8:** Longitude-time diagrams for three pulsars showing the variations in shape and intensity of a series of individual pulses. Each horizontal series of dots represents one pulse; the size of the dots indicates intensity. Successive pulses are plotted upwards on the diagram; integrated profiles are shown at the top. Subpulses, or bursts of enhanced emission covering 3-10 degrees of longitude, can be seen in most pulses.

Subpulse widths are comparable to the integrated-profile widths, only for pulsars with integrated profiles, dominated by a single component, e.g PSR 0329+54 and PSR 1642-03. The width is smaller for pulsars with periods greater than 0.75 seconds. The mean subpulse widths plotted against the widths of the integrated profiles of a number of pulsars can be seen in Figure 7.

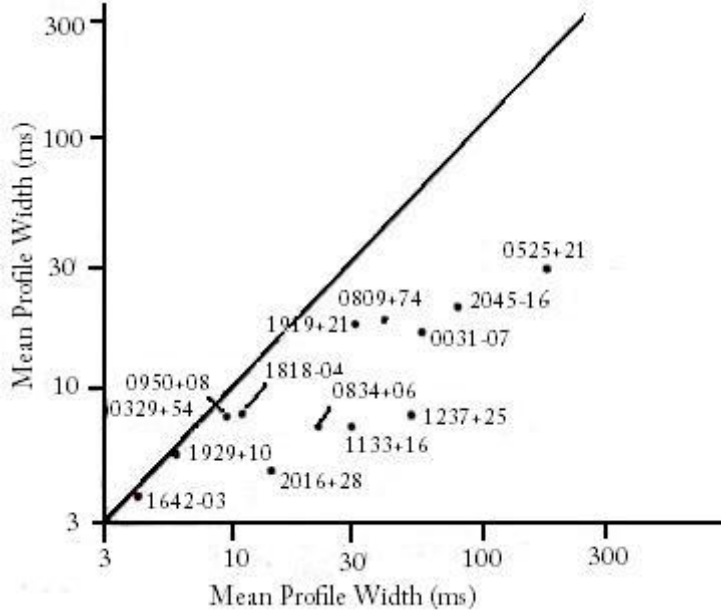


**Figure 9:** Mean half-power width of subpulses plotted against the half-power width of the integrated profile for 14 pulsars. Near the diagonal line, all subpulses have widths similar to that of the integrated profile. [After Taylor et al., 1975.]

The widths are approximately proportional to  $P^{1/2}$ , although there is a large scatter. On the other hand the equivalent widths of integrated profiles, are proportional to period. This suggests that the subpulse profile may represent a time variation in intensity rather than a beam profile. Figure 9 could be interpreted as showing that the subpulse widths represent a time scale for emission that is independent of period. The observed subpulse widths are of course restricted by

*the beaming process that produces the integrated profile. This cutoff (represented by the diagonal line in Figure 9) is especially significant for the shorter-period pulsars.*

*Subpulse widths are not strongly dependent on either frequency or pulse longitude within the integrated profile, however subpulses that occur between the various components of multiple-component profiles tend to be wider than average. There is some correlation between the subpulse intensity and width, as the stronger subpulses tend to be narrower than the weaker ones. Observations at widely spaced frequencies show that subpulse intensities are very well correlated over wide frequency intervals. It can be concluded that the subpulse emission process is broadband, with bandwidths typically exceeding 200 MHz. Robinson & co-workers (1968) showed that the spectra of most individual pulses from PSR 1919+21 were similar with one another and therefore similar to that of the integrated profile. This is true probably true from most pulsars. For those with multiple-component profiles the observed frequency dependence of component separation, together with, high correlation of intensities at different frequencies implies that the longitude interval between a given subpulse and the profile centre is greater at low frequencies than at high frequencies, with a dependence of approximately  $v^{-0.25}$ .*

### **(c) Intensity fluctuations**

*A study of Figure 8 shows that subpulse intensities vary very much from one pulse to the next. There are two characteristic types of fluctuation, Pulse Nulling and Periodic Intensity variations.*

*Pulse nulling is a relatively common phenomenon in which the pulse intensity suddenly drops to a low value for a few pulses and then abruptly returns to normal. In multiple-component profiles all components drop in intensity. Ritchings (1976) found that the intensity of null pulses is less than 1% that of the normal pulse intensity. Short nulls of one or two missing pulses occur in many pulsars but are prominent in PSR 0834+06 and PSR 1929+10. In a sequence of 5000 pulses from PSR 1929+10, Backer (1970b) found about 50 nulls, in each of which one or two pulses were missing. Longer nulls of 3-10 pulse periods are common. PSR 0031-07 (a pulsar with highly organised drifting subpulse), is in a null state for about 50% of the time, with pulse bursts of 10 – 100 pulses separated by nulls of similar duration. PSR 1944+17, (a pulsar that shows drifting subpulses) is in a null state for more than 75% of the time. The fraction of time that a pulsar is in null state is related to the pulsar period and period derivative, as shown by Ritchings (1976).*

*The occurrence of these longer nulls appears to be random – no significant periodicities have been observed. Power-spectral analysis of sequences of pulse energies show, that periodic fluctuations in pulse intensity do exist in a number of pulsars. In some pulsars these fluctuations appear to be related to the nulling phenomenon, whereas in others they are related to drifting subpulses. Fluctuation spectra show that narrow line features, (which represent strongly periodic fluctuations) are rather common, especially for the longer-period Type C and type D pulsars. Below the separately computed fluctuation spectra for different longitudes in the profile and the corresponding integrated profile of PSR 1237+25 can be seen.*

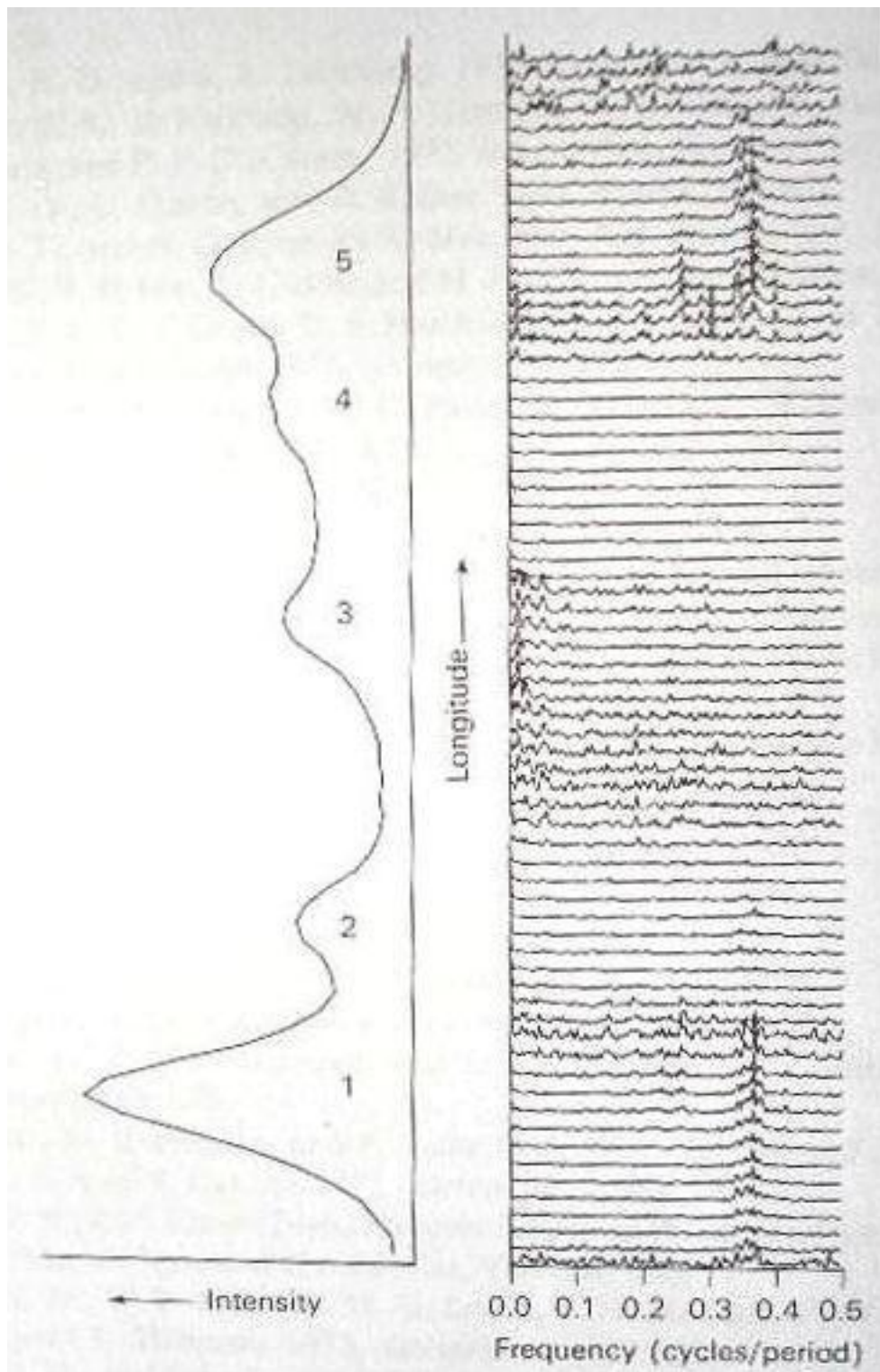


**Figure 10:** Separately computed fluctuation spectra for different longitudes in the profile of PSR 1237+25 and the corresponding integrated profile showing the five distinct components

A series of spectra was computed separately for different longitudes throughout the profile. The feature at 0.35 cycles/period is clearly confined to components 1 & 5, whereas the spectra for components 2 & 4 are essentially featureless. For the region about the profile center including component 3, the spectra are dominated by low-frequency features; this component tends to occur in clumps of 5-10 subpulses every 20-50 periods. The high degree of symmetry of the fluctuation

characteristics about the profile center in this pulsar is striking. Similar symmetries are also seen in other multiple-component pulsars, such as PSR 1133+16 and PSR 2045-16.

A relationship between these periodic modulations and mode changing was found for PSR 1237+25 by Taylor, Manchester and Huguenin (1975). The strong period modulation in component 1 is present only when the pulsar is in its normal mode; in the other mode there may be a weak feature at about 0.24 cycles/period, but the 0.35 cycle/period modulation is completely absent.

The degree of modulation of pulse intensities is best represented by the modulation index,  $m$ , defined by

$$m = \frac{\sigma_{on}^2 - \sigma_{off}^2}{\langle I \rangle}$$

where  $\sigma_{on}$  is the r.m.s variation of pulse intensities about the mean value  $\langle I \rangle$  and  $\sigma_{off}$  is the r.m.s value of the random noise off the pulse. Observed values of the modulation index (after removing the effects of interstellar scintillation) range between about 0.5 and 2.5 for different pulsars. The modulation is almost is almost invariably deeper at lower radio frequencies. For example, at 147 MHz the modulation index for PSR 0329+54 is 2.3, whereas at 400 MHz it is only 1.0. Like the fluctuation spectra, the modulation indexes are different for different longitudes in a given pulsar. Modulation indexes are different for different longitudes in a given pulsar. For PSR 1237+25 the modulation indexes for the different components are different, and the mirror symmetry is seen in the fluctuation spectra. For other pulsars changes in modulation index occur within apparently single components. For example, for PSR 1642-03 the index is high for the leading half of the profile and low for the trailing half. The modulation index is often higher in the wings of a profile than in the center; examples of this are PSR 1133+16, PSR 1929+10 and PSR 2016+28.

For the highly modulated pulsars, histograms of the pulse intensity have an approximately exponential form, with a maximum at zero and a few pulses with intensity as much as ten times the mean value. For the less modulated sources, histograms usually peak just below the mean value and high-intensity tails do not extend significantly beyond four times the mean energy. Pulsars with extended nulls often have a bimodal distribution with one of the peaks at zero intensity (Hesse and Wielebinski, 1974; Ritchings, 1976).

Although the sub-pulses may well be a basic entity, around which interpretations have naturally centered, they only provide a complete description of the whole radiation from a very few pulsars. A study of PSR 1919+21 by Cordes (1975) shows that the intensity ratio between the subpulse and other components varies through the pulse profile. In Figure 11 sequence of pulses from PSR 1919+21 recorded simultaneously at 111 MHz and 318 MHz shows that the subpulse structure is most prominent in the early part of the integrated profile and also that it is more prominent at the lower radio frequency. These subpulses seem to be cut up by the rapid fluctuations of microstructure, but they nevertheless show the characteristic drifting.

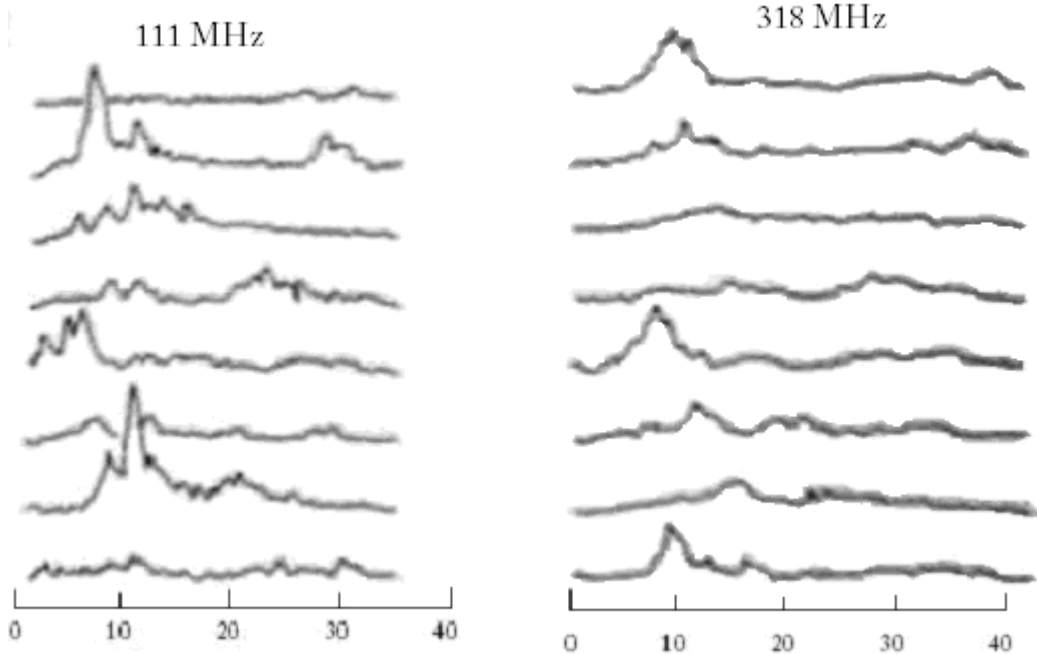


**Figure 11:** Sequence of pulses from PSR 1919+21 recorded simultaneously at 111MHz and 318 MHz. A time resolution is achieved by the use of 'de-dispersion'. (After Cordes, 1975)

#### (d) Polarization

A very important characteristic of the subpulses is their very high degree of polarization. It was discovered by Clark & Smith (1969) in PSR 0329+54, which has easily distinguishable subpulses. It is common to find polarization in excess of 95% in individual subpulses. The polarization is in general elliptical, changing in form throughout a subpulse as, for example, by the smooth change from elliptical through linear to elliptical in the opposite hand. Completely circular, or completely linear, polarization may occur during a subpulse. As far as is known, all clearly defined subpulses follow a similar pattern of polarization, in which there is a smooth, simple sweep of polarization characteristics through a single subpulse.

The identification of the subpulses as a basic entity depends on their appearance (as discrete, symmetrical components), on their coherence and drifting between successive pulses and on their very high polarization with its typical swing of characteristics. The separate components of an integrated profile, on the other hand do not generally show symmetry or very high polarization, and the microstructure appears as a modulation of intensity in which the polarization remains unchanged.

### **(e) Nulling and Moding**

*There is a tendency for pulses to appear in groups, which accounts for the enhancements of the low-frequency end of some fluctuation spectra. These groups are often marked off by nulls, sometimes lasting several periods, which tend to occur at intervals. Those time intervals are characteristic of individual pulsars.*

*In PSR 0031-07, whose behaviour is in many ways similar to that of PSR 0809+74, the nulls occur at typical intervals of 100 rotation periods, i.e about 2 minutes. The nulls last as long as the active periods. The switching on or off, occurs within the time of a single rotation of the pulsar.*

*There distinction between the random variations of energy from pulse to pulse during the ‘on’ state and the switch from ‘on’ to ‘off’ states can easily be distinguished. So pulse nulling can be compared with the phenomenon of moding, (which was described in the previous paragraph) as a variation in the integrated profile. The difference is that moding represents a switch between two configurations of coherent particle motions, while nulling represents a complete stop to the radiation. The causes of the two phenomena may be related, but we have no understanding of the changes occurring in the magnetosphere that act as the trigger between the two stable states in either phenomenon. Furthermore, the time scales involved are very hard to understand. The reason is that oscillations and relaxation processes in a neutron start or in its magnetosphere have a time scale of less than a millisecond rather than some hundreds of seconds. It has been observed that the nulling phenomenon is commoner in the long-period pulsar and therefore might be a sign of old age.*

### **(f) Mode changing**

*During the phenomenon of mode changing or switching, the integrated profile switches between two different forms. Both forms are stable for a long time sequence of individual pulses. Individual components of the two profiles may occur in both modes, but with different intensities. Mode changing and nulling appear to be closely related; they occur in the same population of older pulsars and on similar time scales. A null may be regarded as a mode change in which all components have disappeared to switched to a very low intensity. Pulsar PSR 0525+21 is known to exhibit two modes.*

## **(B) Experimental Data:**

### *I. Pulsars used in the study*

The observational data of the five pulsars that were used in this study, were recorded by Professor John-Hugh Seiradakis, with the 100 m Effelsberg Radiotelescope of the Max-Planck Institute located near the city of Bonn, in Germany.

#### (1.1) Pulsar PSR 0525+21:

- Constellation: Taurus
- Period  $P = 3745,5\text{ms}$
- Age  $1,48 \times 10^6 \text{ yrs}$

A radio map of the area can be seen below, the circled source is 0525+21:

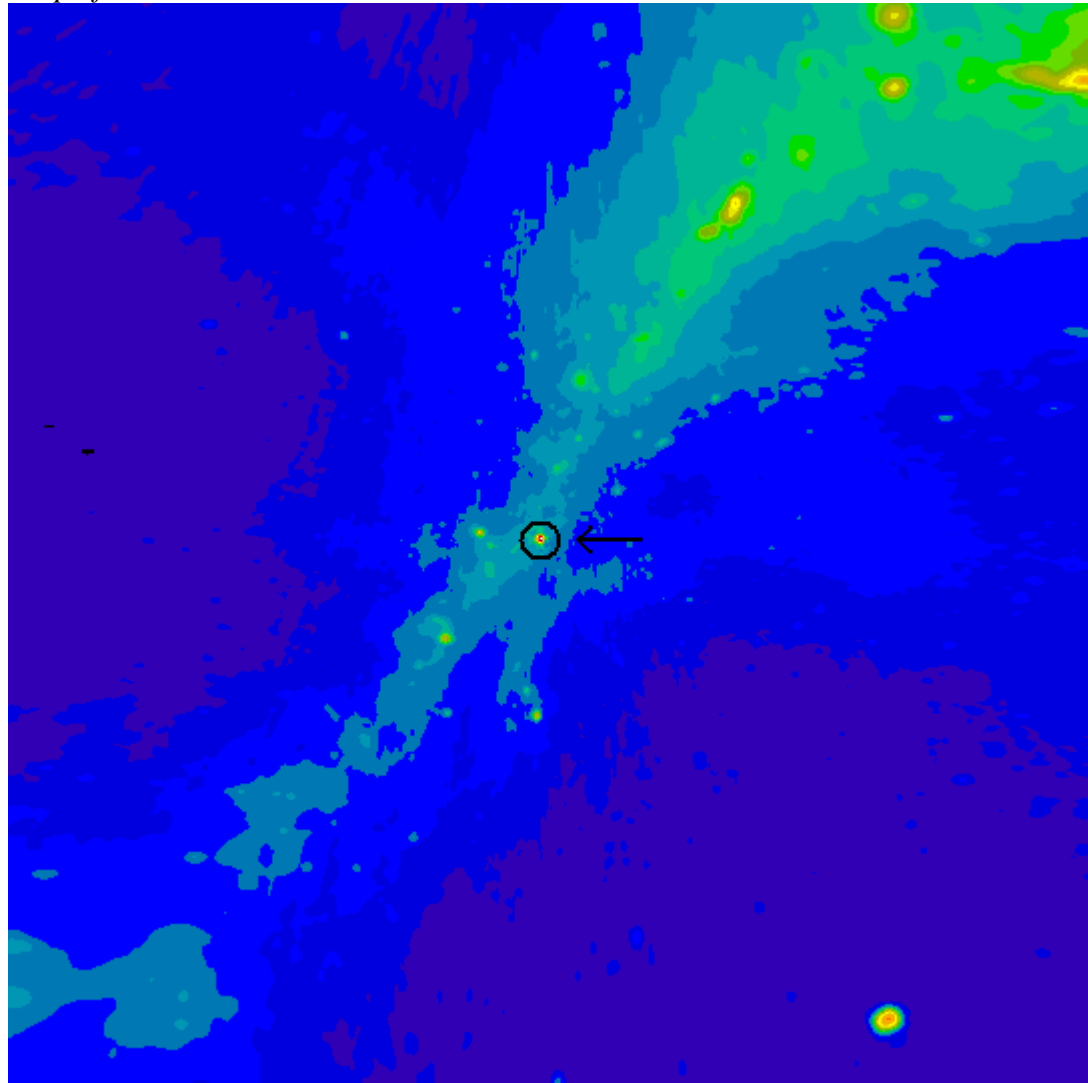


*Figure 12: Radio map of the area around PSR 0525+21*

In this study we used different scans. Their integrated profiles differ and can be seen bellow.

(Scan 7699)

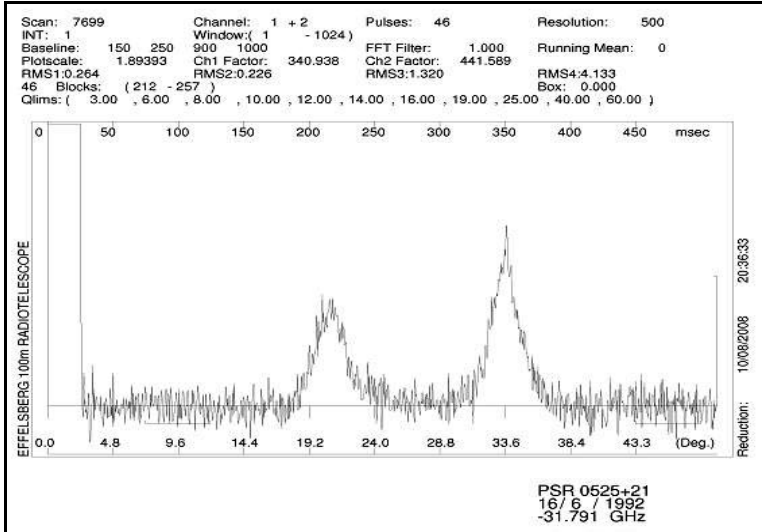


Figure 13: Integrated Profile of PSR 0525+21

(Scan 7700)

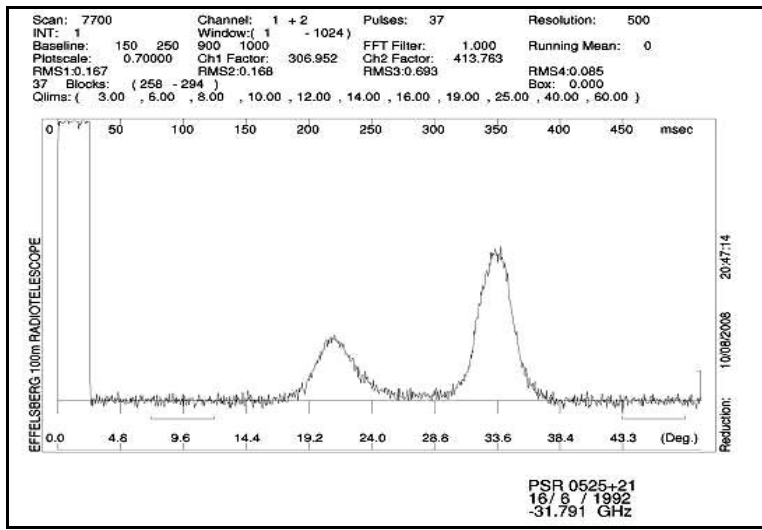


Figure 14: Integrated Profile of PSR 0525+21

(Scan 7702)

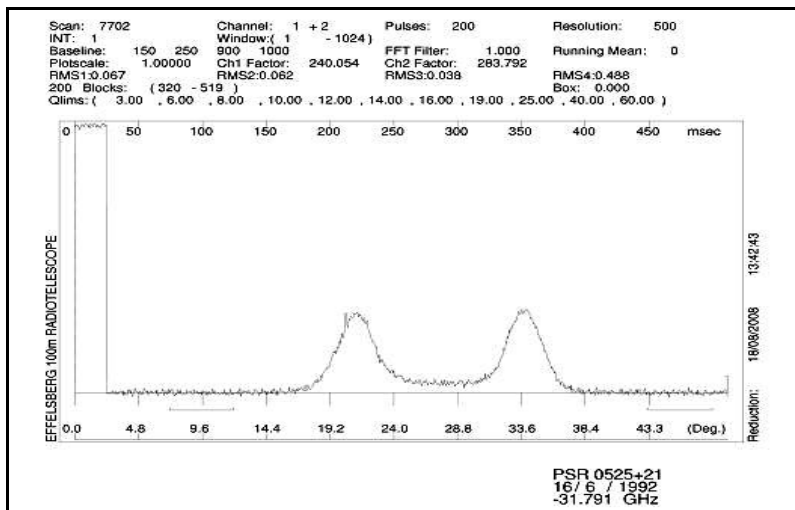
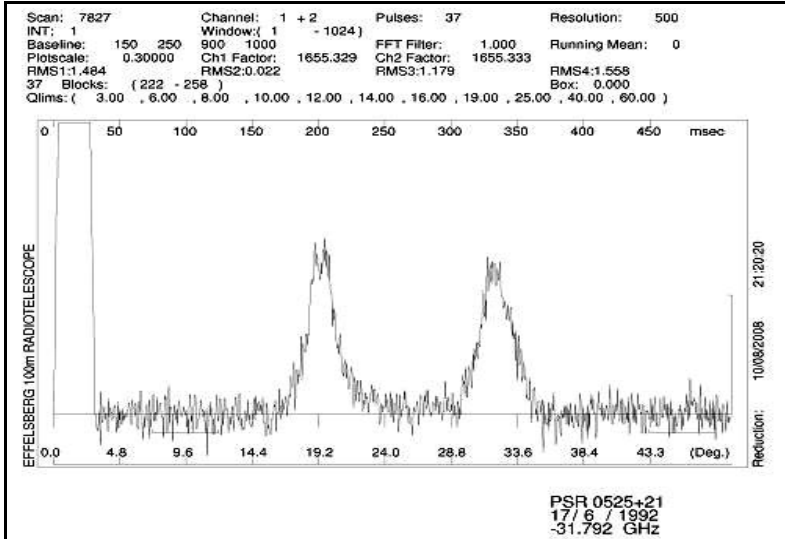


Figure 15: Integrated Profile of PSR 0525+21

(Scan 7827)



**Figure 16: Integrated Profile of PSR 0525+21**

(Scan 7833)

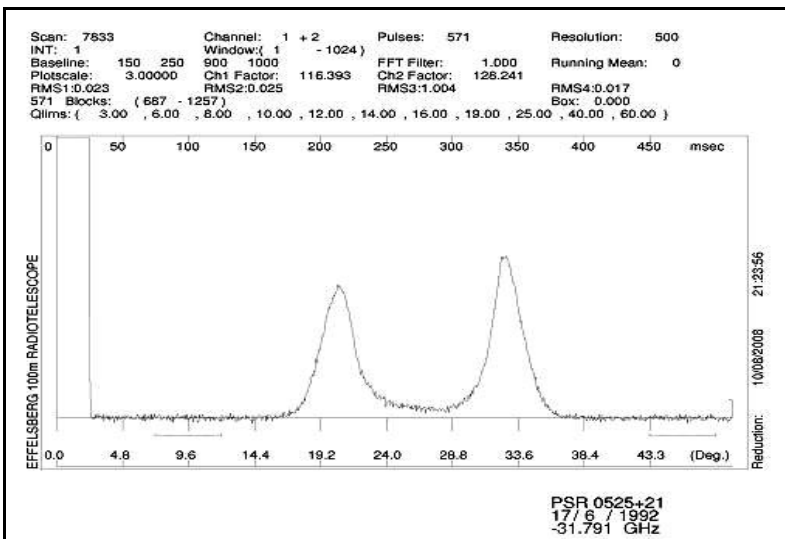


**Figure 17: Integrated Profile of PSR 0525+21**

(Scan 9008)

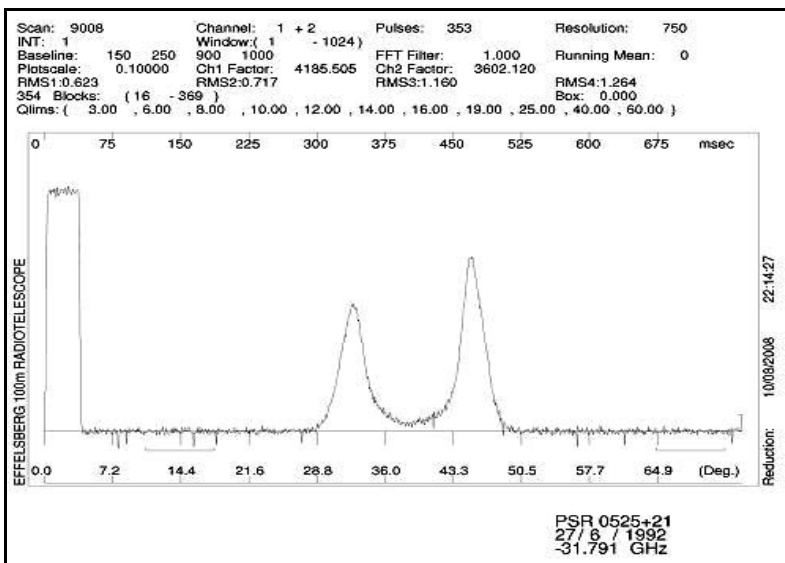


**Figure 18: Integrated Profile of PSR 0525+21**

### (1.2) Pulsar PSR 0329+54:

- Constellation: Camelopardalis
- Period  $P = 714,5\text{ms}$
- Age  $5,53 \times 10^6 \text{ yrs}$

A series of radio maps of the area can be seen below, the first image shows PSR 0329+54:

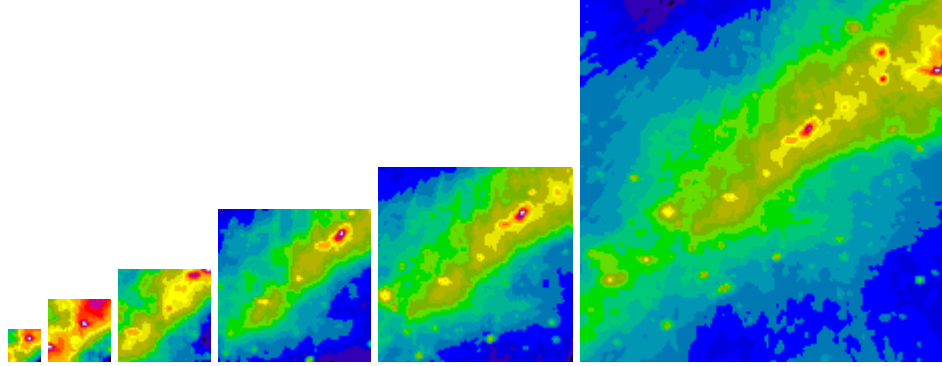


Figure 19: Series of radio maps of the area around PSR 0329+54

In this study we used different scans. Their integrated profiles differ and can be seen bellow.

### (Scan 8653)

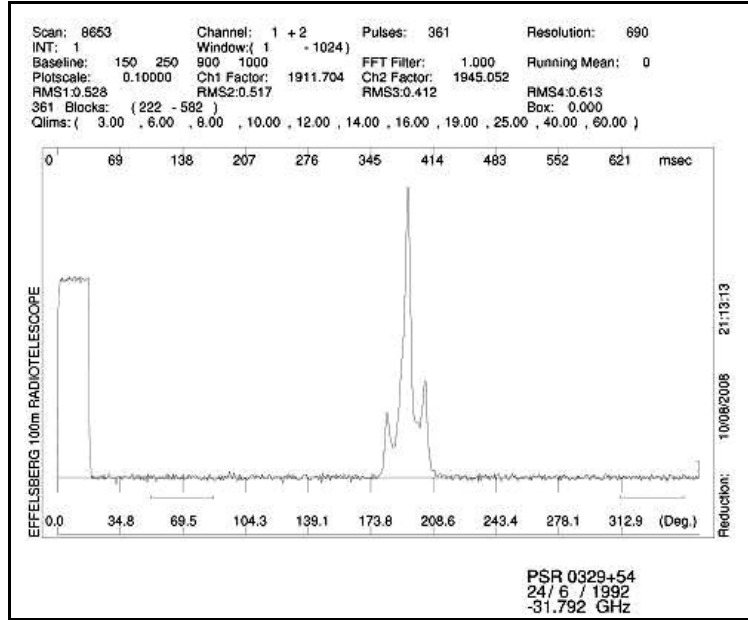
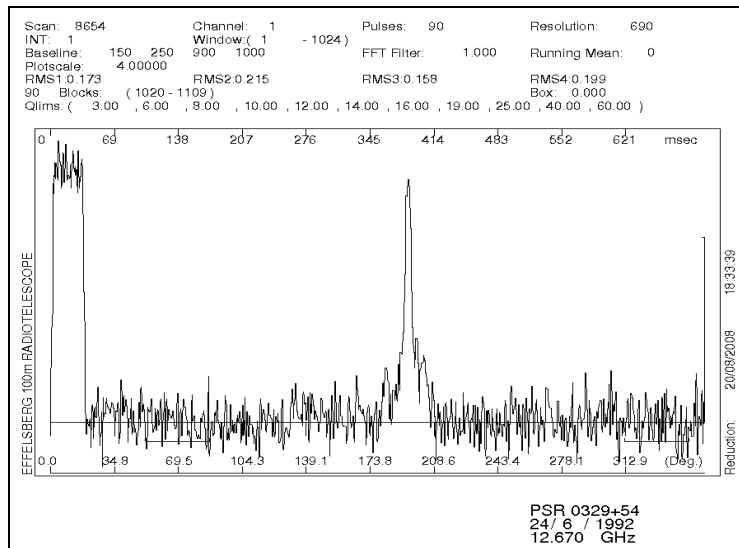


Figure 20: Integrated Profile of PSR 0329+54

*(Scan 8654)*



**Figure 21: Integrated Profile of PSR 0329+54**

*(Scan 8656)*

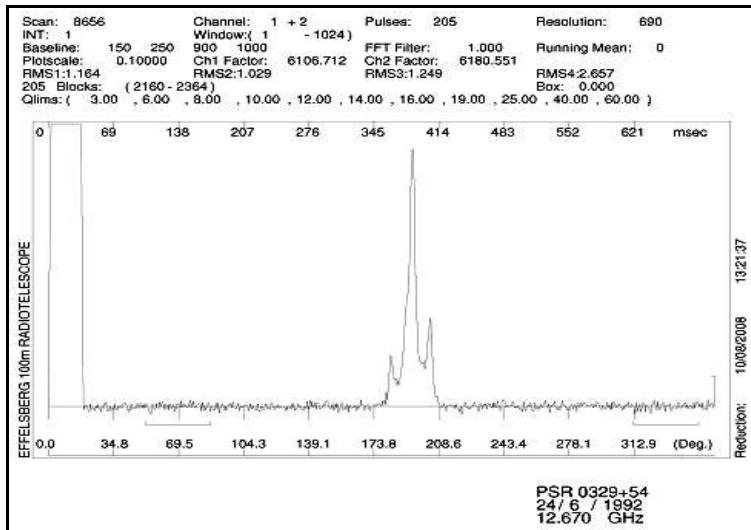


**Figure 22: Integrated Profile of PSR 0329+54**

*(Scan 8657)*

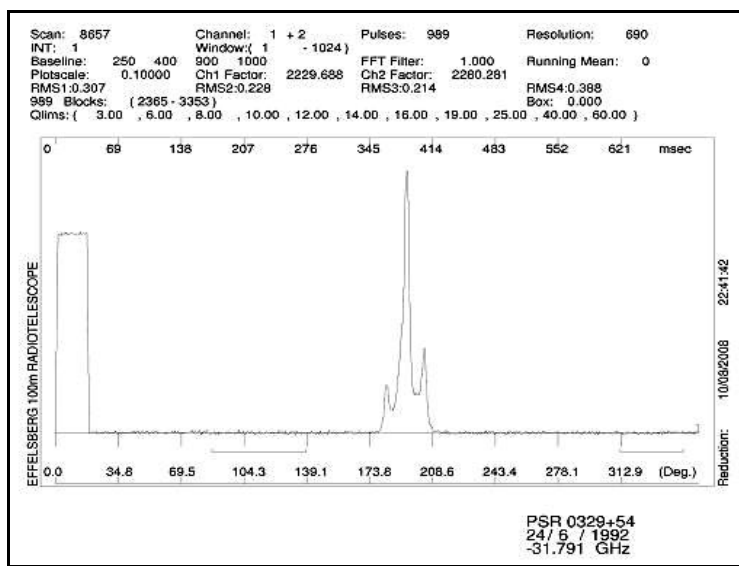


**Figure 23: Integrated Profile of PSR 0329+54**

(Scan 8660)

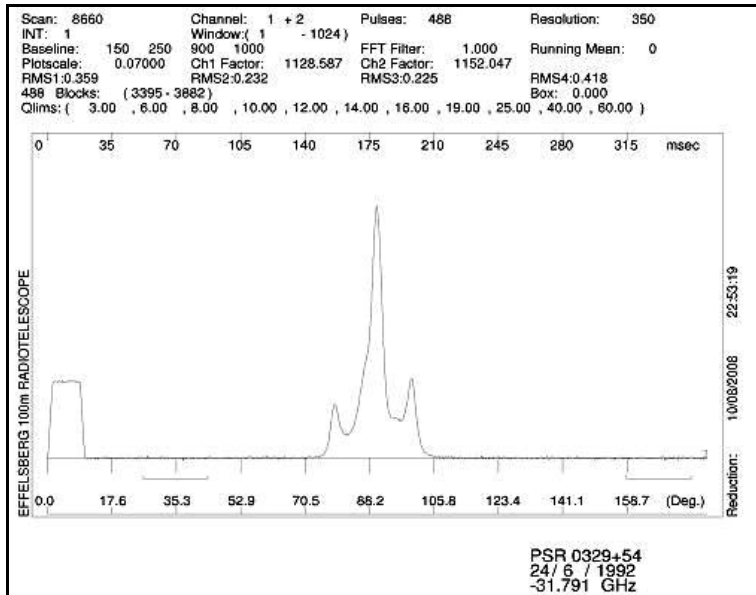
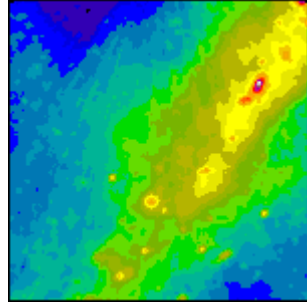


Figure 24: Integrated Profile of PSR 0329+54

(1.3) Pulsar PSR 0450+55:

- Constellation: Camelopardalis
- Period  $P = 340.7\text{ms}$
- Age  $2.28 \times 10^5 \text{ yrs}$

A series of radio maps of the area can be seen below, the first image shows PSR 0329+54:



**Figure 25:** A radio map of the area around PSR 0450+55

We studied one scan, which can be seen below:

Scan 9038

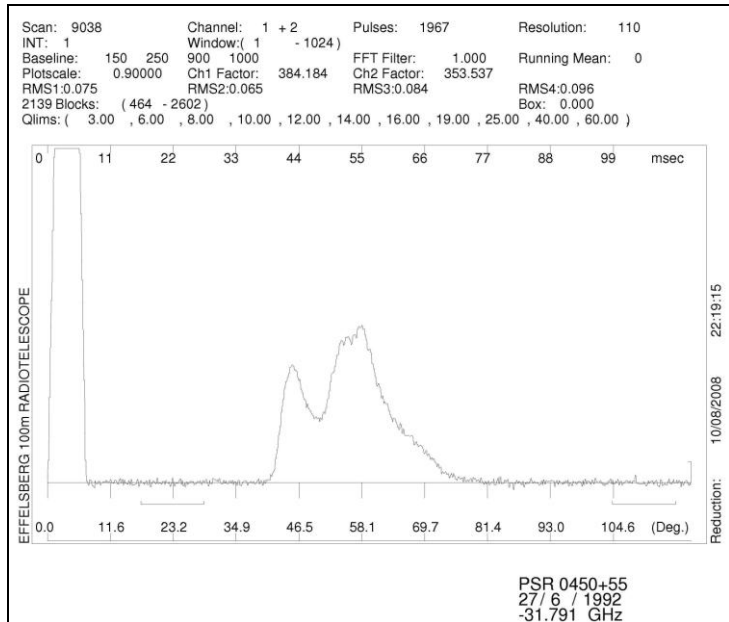


**Figure 26:** Integrated Profile of PSR 0450+55

(1.4) Pulsar PSR 1822-09:

- Constellation: Scutum
- Period  $P = 768.9\text{ms}$
- Age  $2.33 \times 10^5 \text{ yrs}$

A series of radio maps of the area can be seen below, the first image shows PSR 1822-09:

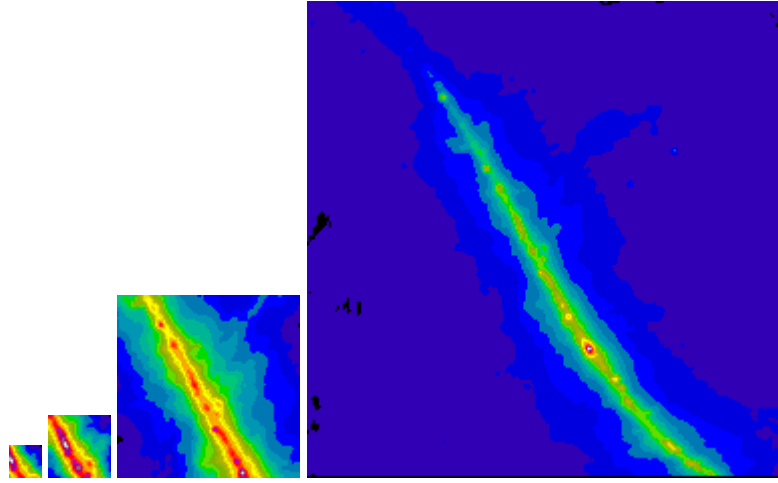


Figure 27: Series of radio maps of the area around PSR 1822-09

In this study we used different scans. Their integrated profiles differ and can be seen below.

(Scan 9118)

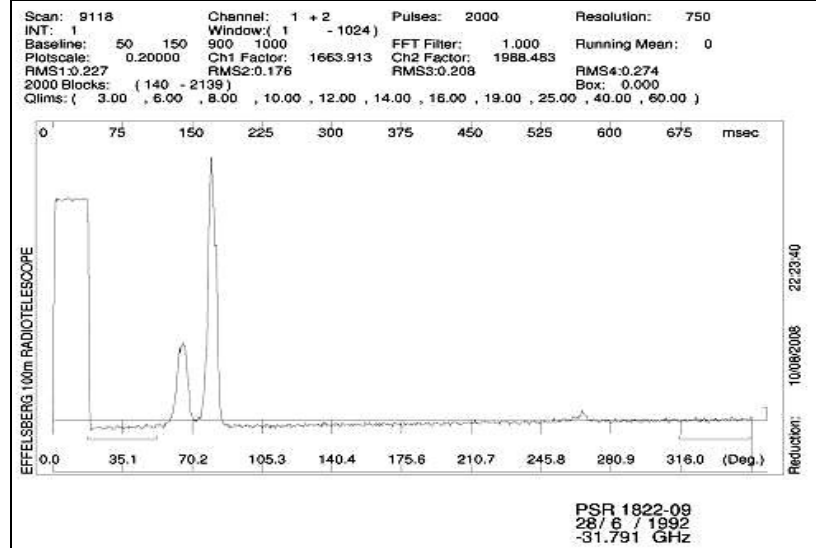


Figure 28: Integrated Profile of PSR 1822-09

(Scan 9119)

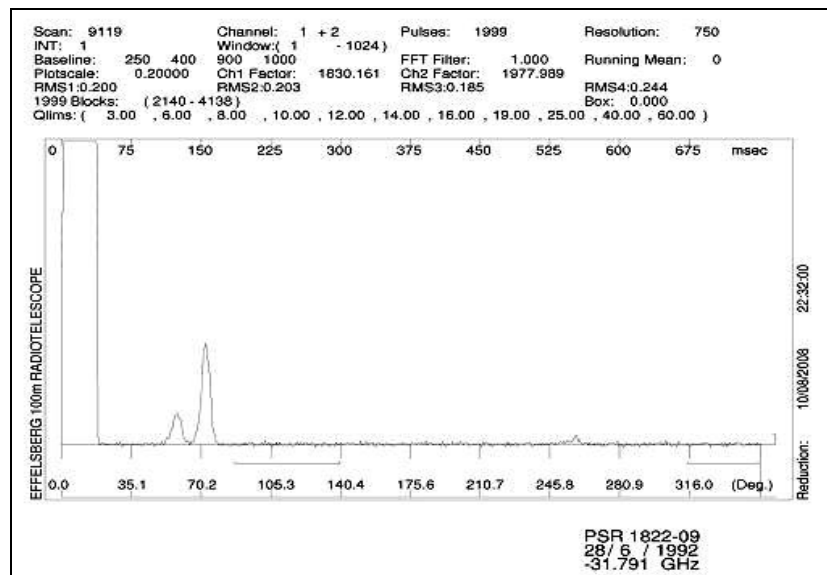
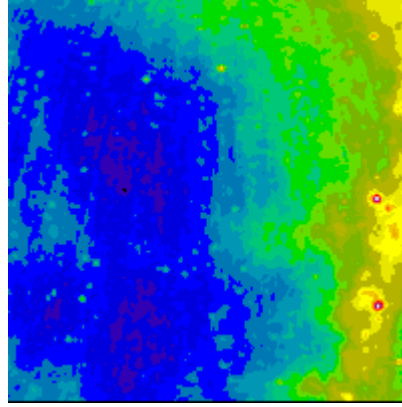


Figure 29: Integrated Profile of PSR 1822-09

(1.5) Pulsar PSR 0823+26:

- Constellation: Cancer
- Period  $P = 530.6\text{ms}$
- Age  $4.30 \times 10^6 \text{ yrs}$

A radio map of the area can be seen below:



**Figure 30:** A radio map of the area around PSR 1822-09

We studied one scan, which can be seen below:

(Scan 9175)

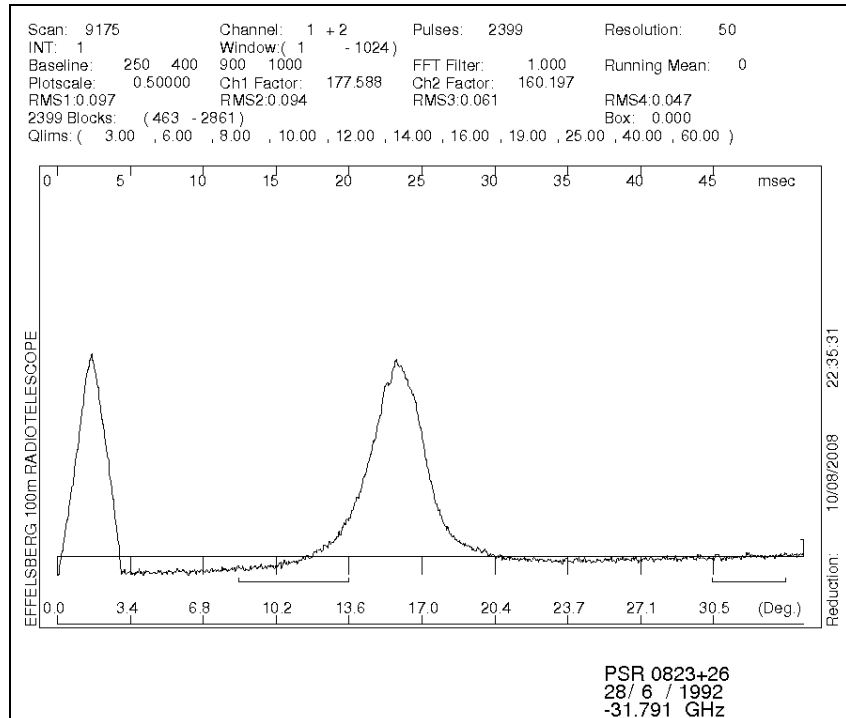


**Figure 31:** Integrated Profile of PSR 1822-09

### (1.6)Pulsar PSR 1133+73

- Constellation: Taurus
- Period  $P = ms$
- Age yrs

A radio map of the area can be seen below, the circled source is 1133+73:

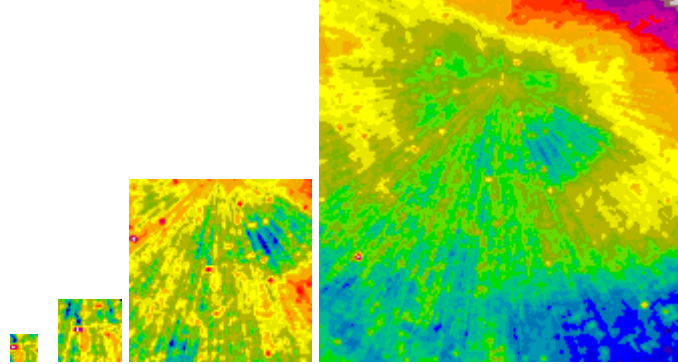


Figure 32: Radio map of the area around PSR 1133+73

### (Scan 6160)

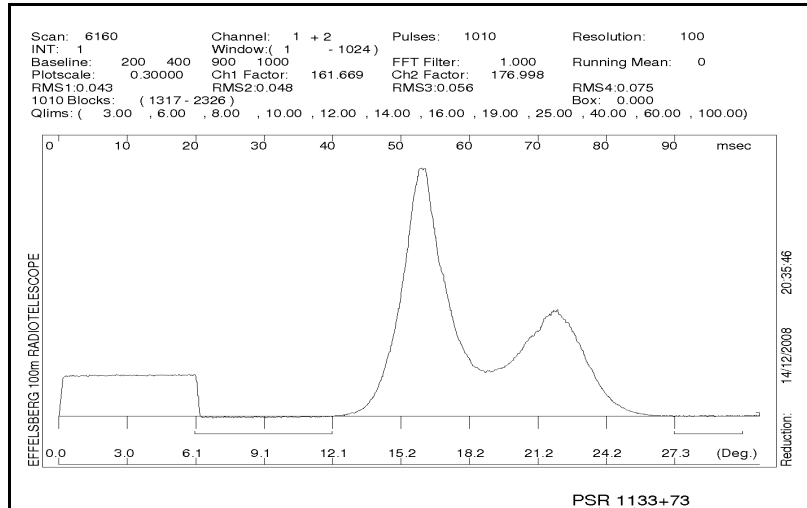


Figure 33: Integrated Profile of PSR 1133+73

## *II. Data Processing Program*

### **(2.1) Main Menu:**

The name of the Data Processing Program is jhsmnull. When the program is run a list of the main command options appears on the screen, as show bellow:

```
| PULSAR ANALYSIS: MAIN MENUE 1.0 |
|-----|
(help) list of options
(exit) program end
(addata) add data
(ad12) add channel 1 and 2. (ad34) add channel 3 and 4
(base) subtract baseline (data overwritten) [ 150- 250- 900-1000]
(fast) fast plot of successive blocks
(filt) smooth data with FFT (data overwritten) [1.0000]
(head) print header
(look) quick look (lineprinter mode) of successive pulses
(mean) compute mean,rms over baseline range and ratio max/sigma
(flux) compute pulse energy and flux
(tsys) evaluate calibration and tsys
(plot) plot the profile
(print) print current data
(read) read and integrate blocks
(radd) read data from .ADD or .ASC file
(scan) read and integrate a whole scan
(shift) read & shift blocks in time & write to new file
(sequ) plot sequence of successive blocks
(show) show contents of file
(smooth) smooth data with running mean (data overwritten) [ 0 ]
(succ) succession of fluxes
(peak) compute ratios of the peaks
(wadd) write data to .ADD and/or .ASC file
(freq) set observation frequency
(file) choose input file, default= ./pul9999.dat
(quality) classify data according to their quality
(path) choose input path, default= /
(call) read commands from file
(retu) return from macro execution
(exec) execute an OS command
(quit) exit program
```

*Figure 34: The main command options list of the program*

*The use of the most important of them are explained bellow:*

*(1.1) (file): chooses and opens the file we wish to study*

*(1.2) (show): prints on the screen the contents of the file we wish to study*

*(1.3)(read): reads the data in the file we have chosen.*

*We need to type in the number of the initial and the final block we wish to read.*

(1.4) (ad12)

*adds channels 1 and 2 essentially resulting in the elimination of the calibration block at the beginning of integrated profile plot of the channel 2. The length of the calibration block must be provided.*

(1.5) (plot)

*opens the submenu plot that allows the plotting of the pulses.*

(1.6) (quality)

*opens the quality submenu that allows the classification of the pulses in 12 categories according to their intensity*

(1.7) (exit)

*exits the program*

## **(2.2) Submenu Quality:**

The Quality subprogram is responsible for classifying the pulses to twelve categories according to their intensity. The ( $\sigma$ ) “sigma” is assigned as the unit of the intensity of the pulse and it is equal to the maximum intensity of the pulse divided by the mean deviation of the noise of the signal.

A value of  $\sigma=1$  means that the maximum intensity of the pulse is equal to the mean deviation of the noise of the signal, therefore no pulse can be observed. We must have a value of  $\sigma>1$  and preferably over 1,5 for the results to be of any use.

After the limits are set, the pulses are plotted in a graph called the “Quality Graph” with the Plot subprogram. When the submenu Quality is accessed the following command list appears:

```
|-----| PULSAR ANALYSIS: MENU 2.4 (Quality) |-----|
|-----|
|(exit)  exit program
|(wind)   start - end sample    [ 1-1024]
|(base)   choose baseline range [ 150- 250- 900-1000]
|(blocks) choose records to work with [ 1- 1]
|(ad12)  add channel 1 and 2. (ad34) add channel 3 and 4
|(filt)   smooth data with FFT (data overwritten) [1.0000]
|(channel) channel number      [ 1]
|(limits) set quality limits
|(plot)   plot the profile
|(help)   show options
|(back)   go back to main program
|(start)  start the distribution of pulses
```

**Figure 35:** The command options of the Quality submenu

The use of the most important of them are explained below:

- |                |   |
|----------------|---|
| (2.1) (blocks) | determines the initial and final block of the record used.  |
| (2.2) (ad12)   | adds channels 1 and 2. It acts exactly like command ad12 on the main menu, with the difference that one needs to know the values beforehand (they are provided by the command ad12 on the main menu). |
| (2.3) (wind)   | determines the window the span of the pulse(the pulse by default spans 1–1024). If we type 1, 1042 we will get the whole period the pulse spans in.   |
| (2.4) baseline | sets the baseline for the plotting  |
| (2.5) limits   | sets the limits for the classification of the   |

*pulse. The limits are based on the intensity of the pulses.*

(2.6) *start*

*begins the process of classification of the pulses according to their intensity by separating them in windows.*

(2.7) *plot*

*it opens the Plot submenu and allows the printing of the quality graph.*

*To print the quality graph we need to use the Plot submenu with the use of the command plot.*

### **(2.3) Submenu Plot:**

When the submenu *Plot* is accessed the following list of commands appears:

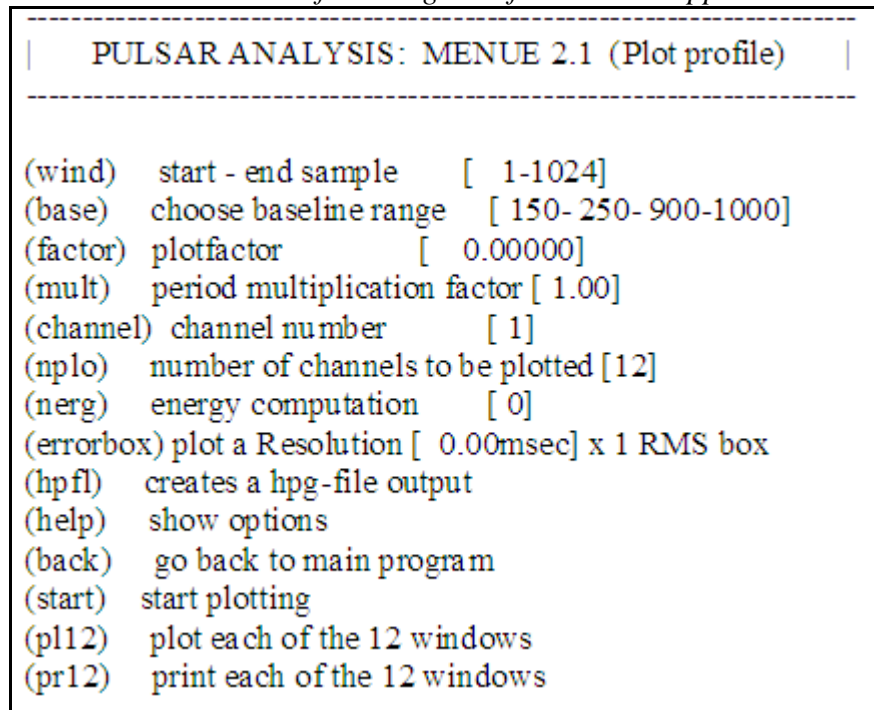


*Figure 36: The command options of the Plot submenu*

The use of the most important of them are explained bellow:

(3.1) (wind)

*determines the window the pulse spans in (it spans 1 – 1024). If we type 1 - 1024 we will get the whole period the pulse spans in.*

(3.2) (fact4)

*provides the scale of the plot*

(3.3) (start)

*begins the plotting of the integrated profile and the quality profile*

(3.4)(channel)

*provides the number of the channel plotted*

(3.5)(nplo)

*provides the number of windows plotted*

(3.6)(pl12)

*allows the plotting of each of the 12 windows separately*

(3.7)(pr12)

*allows the printing of the values of the pulses for each of the 12 windows*

### III. Data Analysis and Results

The diagram consists of twelve windows. Starting with the lower intensity to the highest intensity the pulses are distributed into twelve windows. On the upper left corner of each window the number of the window is displayed, on the upper right corner is the number of the pulses in the window. Above the twelve windows the values of the limits set is displayed.

First we use the commands (1.1) - (1.5) and then (3.3) to create the integrated profile. Then by restarting the program and using commands (1.1) - (1.4), (1.6), (2.1) - (2.7) and (3.3) in this order we produce the quality plots for each of the scans.

Then using the pr12 command in the plot menu we calculate the values of the pulses. The maximum values of the components are then plotted in a diagram, and conclusions are drawn from its shape.

#### (3.1) Pulsar PSR 0525+21

##### Scan 7699

The sequence of pulses and the integrated profile of the scan can be seen below. A study of the sequence of pulses and the integrated profile reveal that they are rather well defined.

A closer study of the sequence as well as the quality graph reveals that the intensity-noise ratio has a rather low value and therefore no accurate results can be drawn from its study. The very low limit values in the quality graph confirm those observations. The limits value (the sigma) must be over one for the results to be of any use.

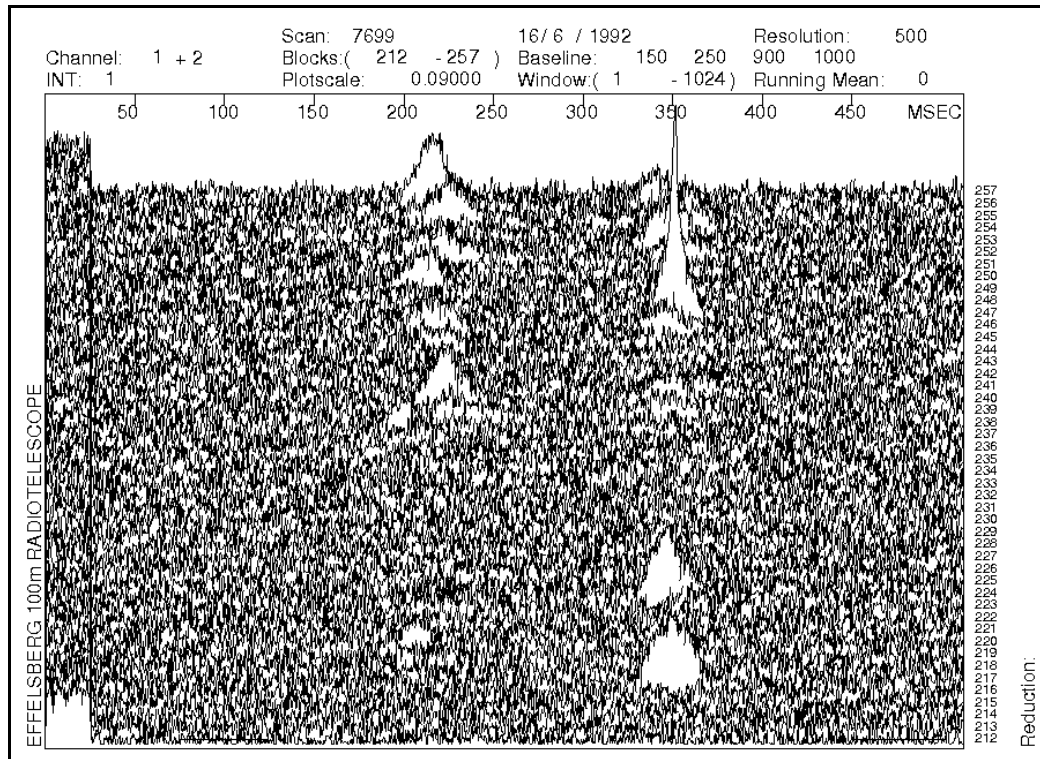
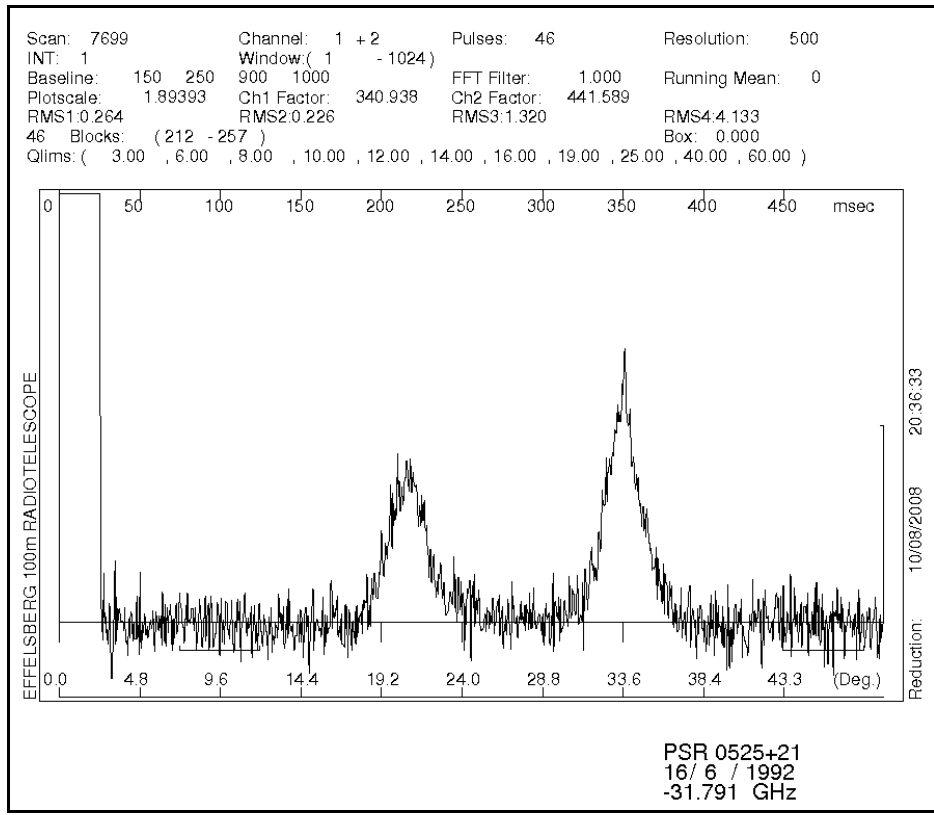
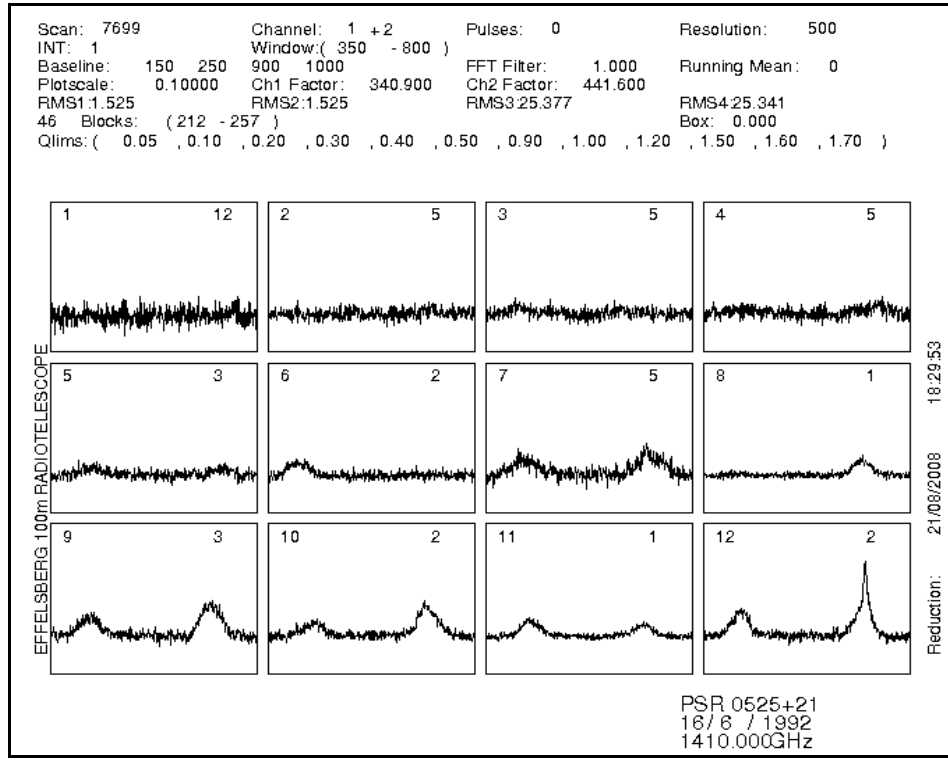


Figure 37: Sequence of pulses of Scan 7699



**Figure 38: Integrated Profile of Scan 7699**

As we see in the graph below, there are not enough pulses with sigma greater than 1. More than six or more pulses in each window are needed for the results to be accurate and of any scientific value.



**Figure 39: Quality Profile of Scan 7699**

### Scan 7700

The sequence of pulses and the integrated profile of the scan can be seen below. A study of the sequence of pulses and the integrated profile reveal that they are rather well defined. A closer study of the sequence as well as the quality graph reveals that the intensity-noise ratio has a rather low value for the majority of the pulses and therefore no accurate results can be drawn from its study. The very low limit values in the quality graph confirm those observations. The limits value (the sigma) must be over one for the results to be of any use.

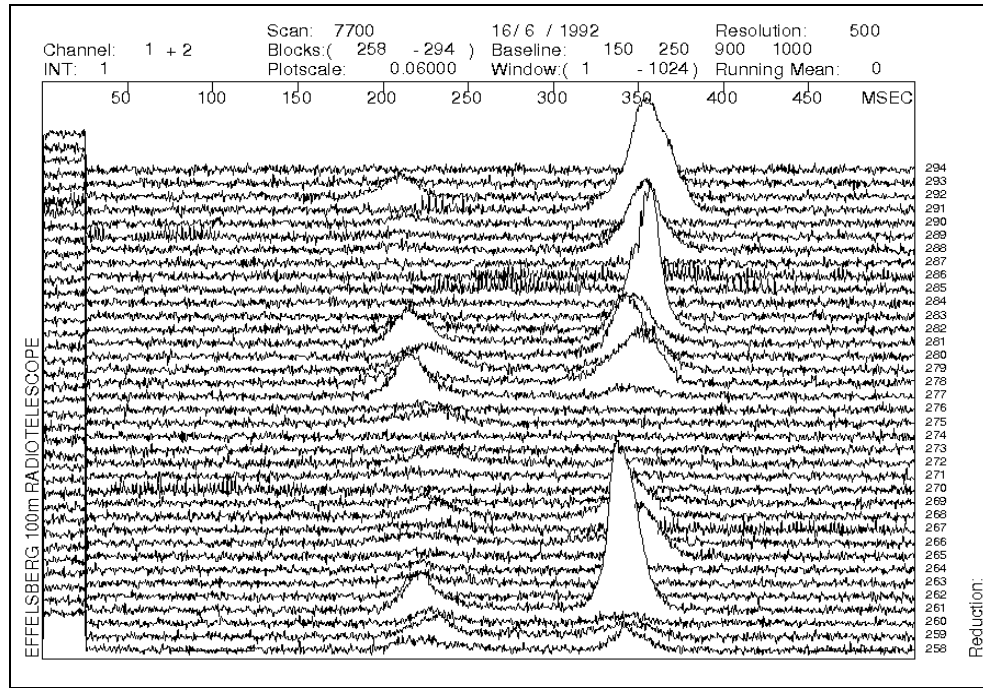


**Figure 40:** Sequence of pulses of Scan 7700

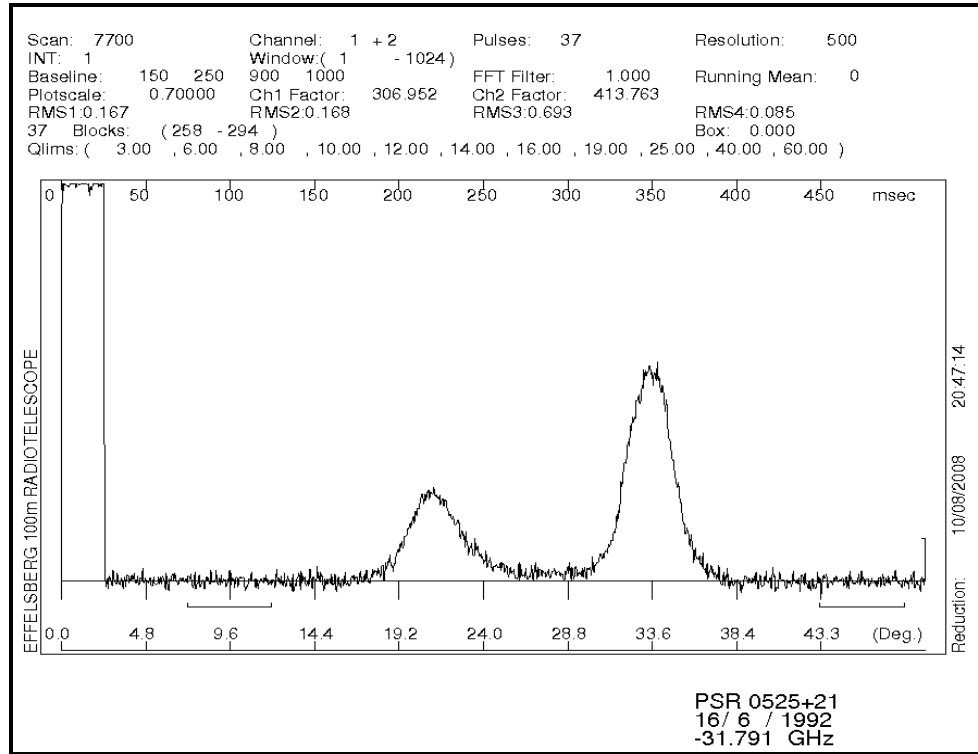


**Figure 41:** Integrated Profile of Scan 7700

As we see in the graph below, there are not enough pulses with sigma greater than 1.

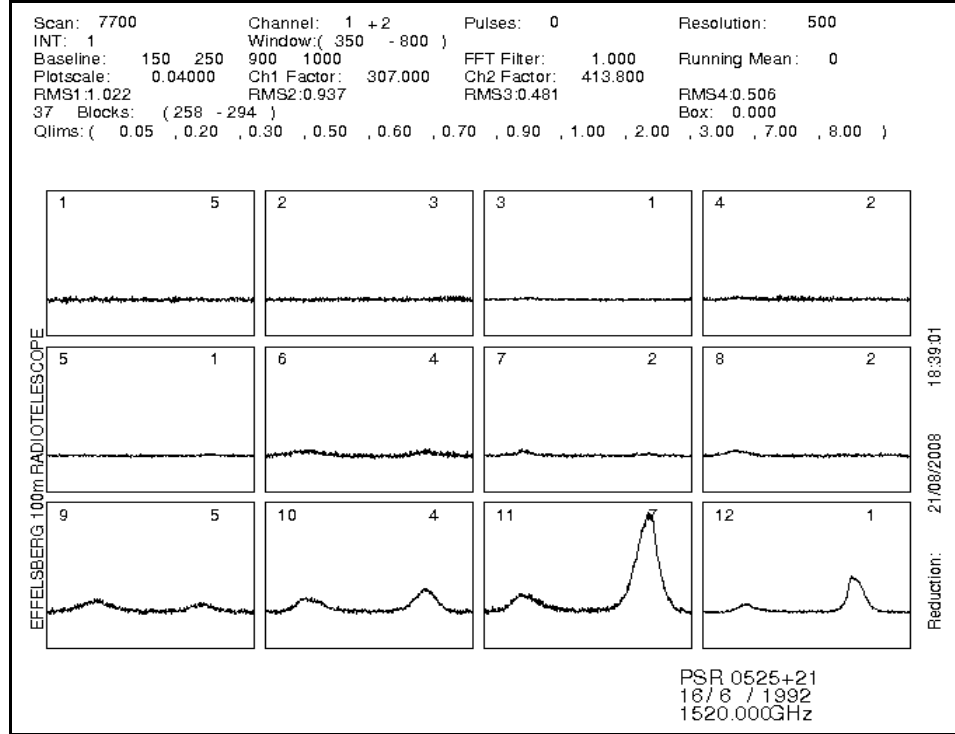


Figure 42: Quality Graph of Scan 7700

### Scan 7702

The sequence of pulses and the integrated profile of the scan can be seen below. A study of the sequence of pulses and the integrated profile reveal that they are rather well defined. A closer study of the sequence as well as the quality graph reveals that the intensity-noise ratio has a rather high value. That allows for accurate results to be drawn from its study. The main component is the pulse component with the highest values. So we assume that the main component (core component) is the second pulse in the integrated profile.

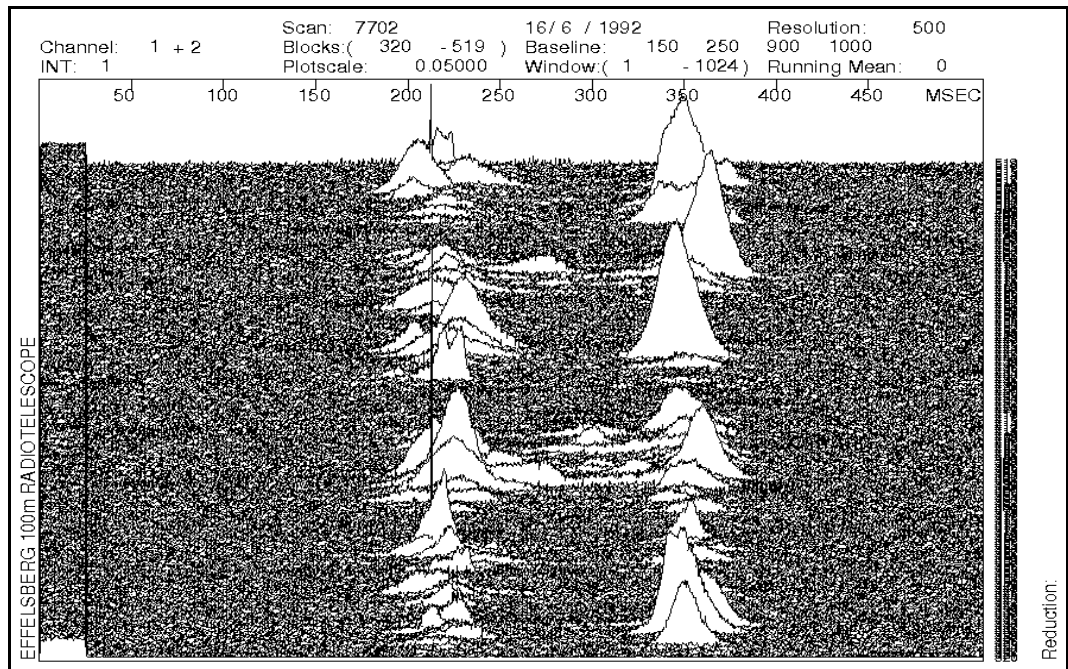
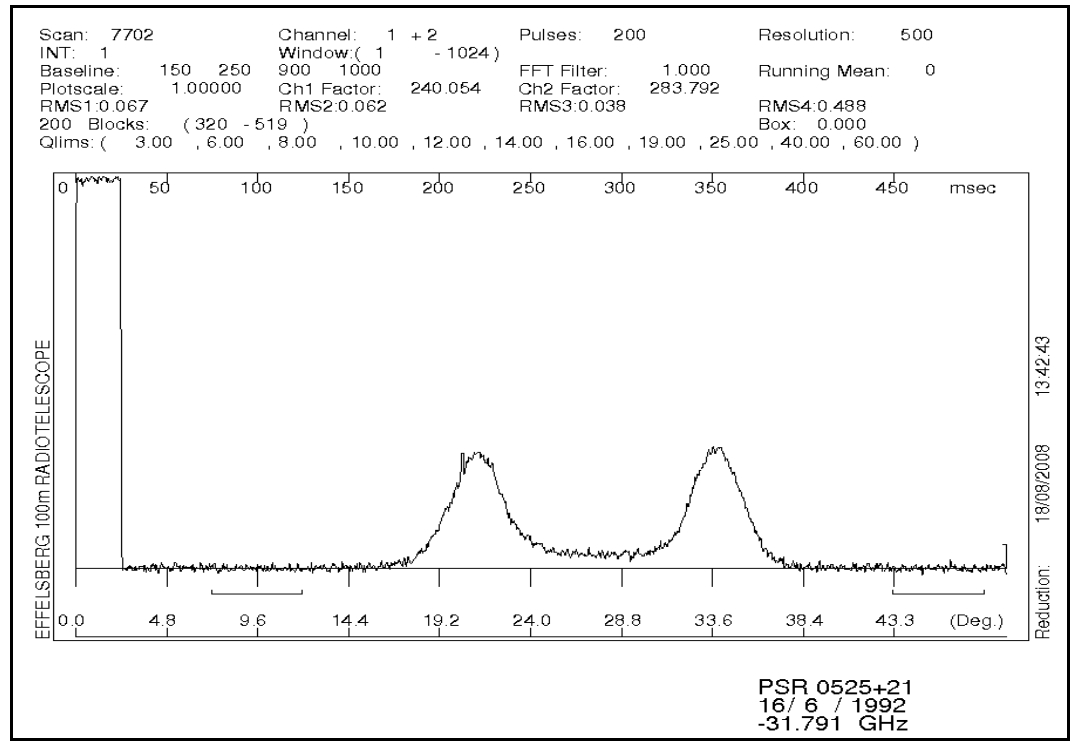
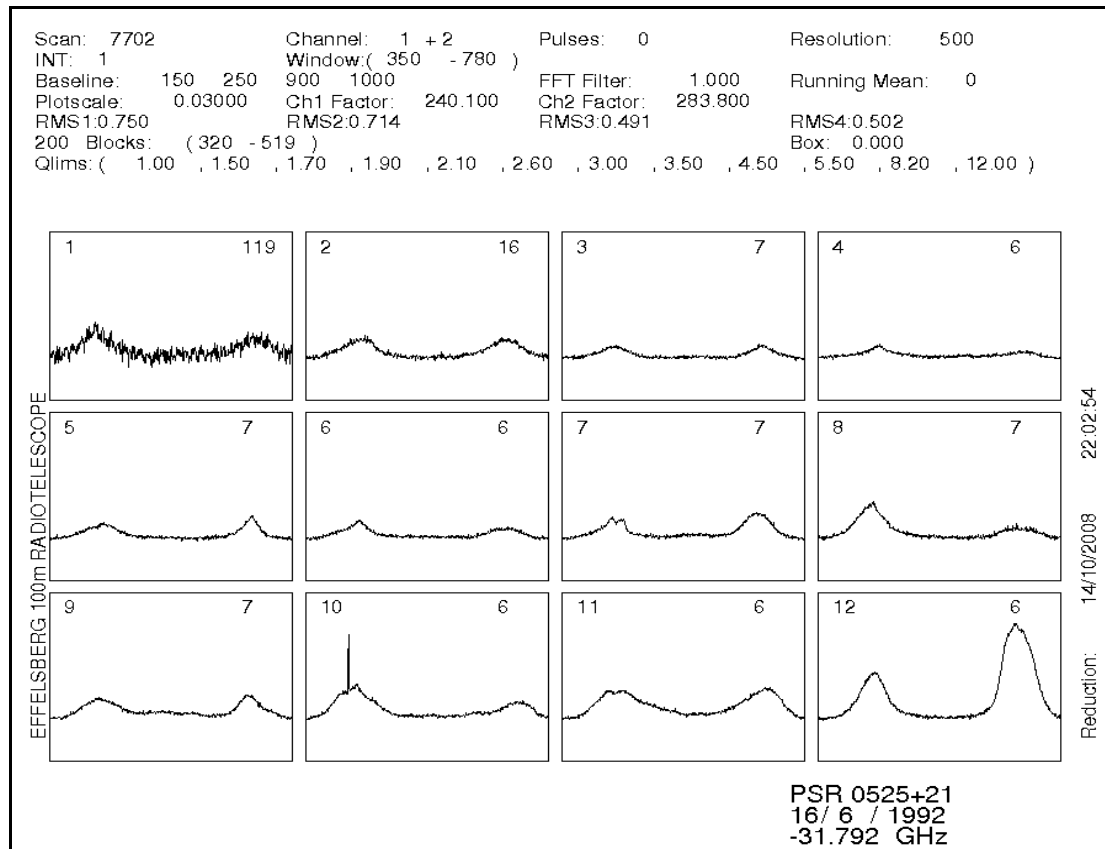


Figure 43: Sequence of pulses of Scan 7702



**Figure 44:** Integrated Profile of Scan 7702

The first window depicts noise mostly since sigma equals 1. We see that, while for small values of sigma the maximum pulse intensity of the main component is either higher or equal to that of the maximum value of the first component, for the highest sigma it is the opposite.



**Figure 45:** Quality Graph for Scan 7702

We can see the maximum values of each component for each window in the following table.

Table 3: Scan 7702

Channel	1	2	3	4	5	6
<b>Main Component</b>	6,42423E+01	5,11077E+01	3,31740E+01	1,89508E+01	5,48953E+01	2,75729E+01
<b>Component 1</b>	8,79558E+01	5,50596E+01	3,04267E+01	3,42236E+01	3,94471E+01	4,39975E+01
<b>Main/Comp.1</b>	<b>1,36912595</b>	<b>1,077324943</b>	<b>0,917185145</b>	<b>1,805918484</b>	<b>0,71858793</b>	<b>1,595679091</b>
Channel	7	8	9	10	11	12
<b>Main Component</b>	6,43737E+01	3,17826E+01	5,78139E+01	8,46954E+07	7,58969E+01	2,28837E+02
<b>Component 1</b>	4,86955E+01	8,96570E+01	5,18995E+01	4,33142E+01	6,92767E+01	1,12412E+02
<b>Main/Comp.1</b>	<b>0,756450227</b>	<b>2,820946052</b>	<b>0,897699342</b>	<b>5,11411E-07</b>	<b>0,912773776</b>	<b>0,49123175</b>

From the tables above we get the following diagram:

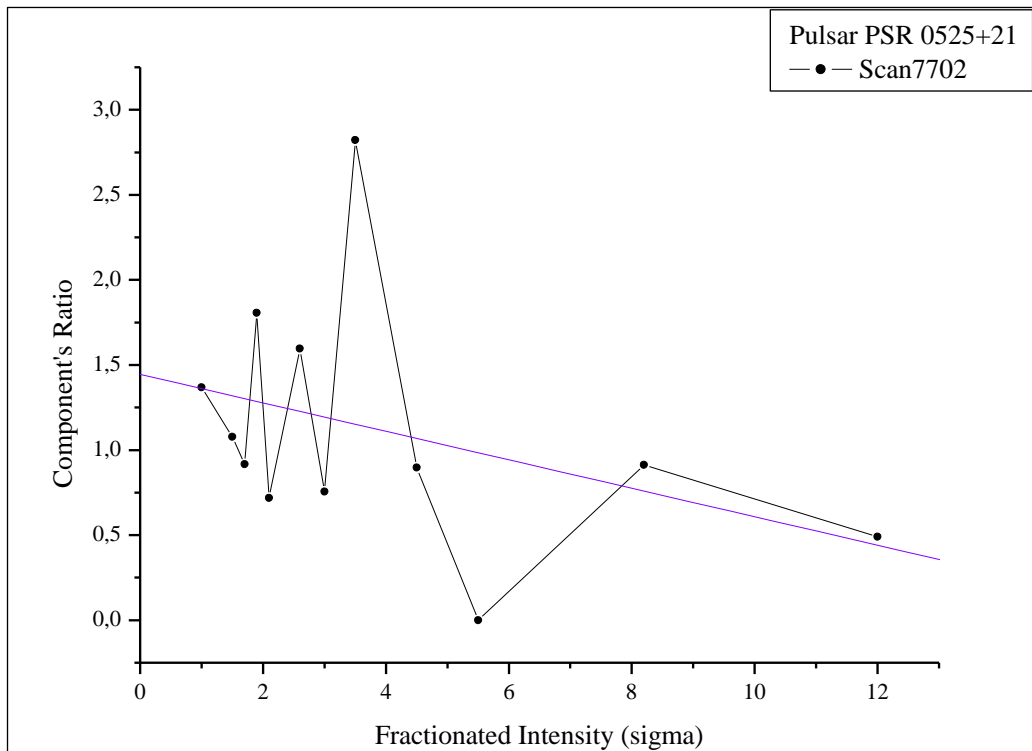


**Figure 46: First to Main component ratio of Scan 7702**

The linear fit gives us a descending line with the following equation:

$$y = 1,44488 - 0,0837x$$

A descending line means that the ratio of the main and first component decreases as the fractionated intensity (sigma) increases.

### Scan 7827

The sequence of pulses and the integrated profile of the scan can be seen below. A study of the sequence of pulses and the integrated profile reveal that they are rather well defined. A closer study of the sequence as well as the quality graph reveals that the intensity-noise ratio has a rather high value. That allows for accurate results to be drawn from its study. The main component is the pulse component with the highest values. So we assume that the main component (core component) is the first in the integrated profile.

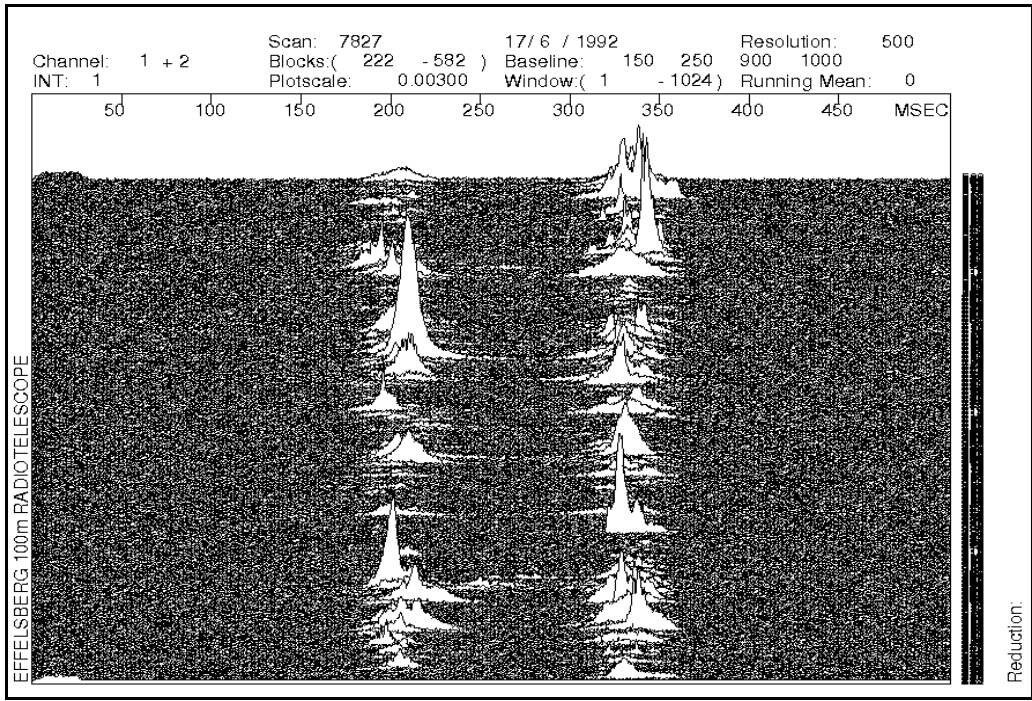


**Figure 47:** Sequence of pulses of Scan 7827

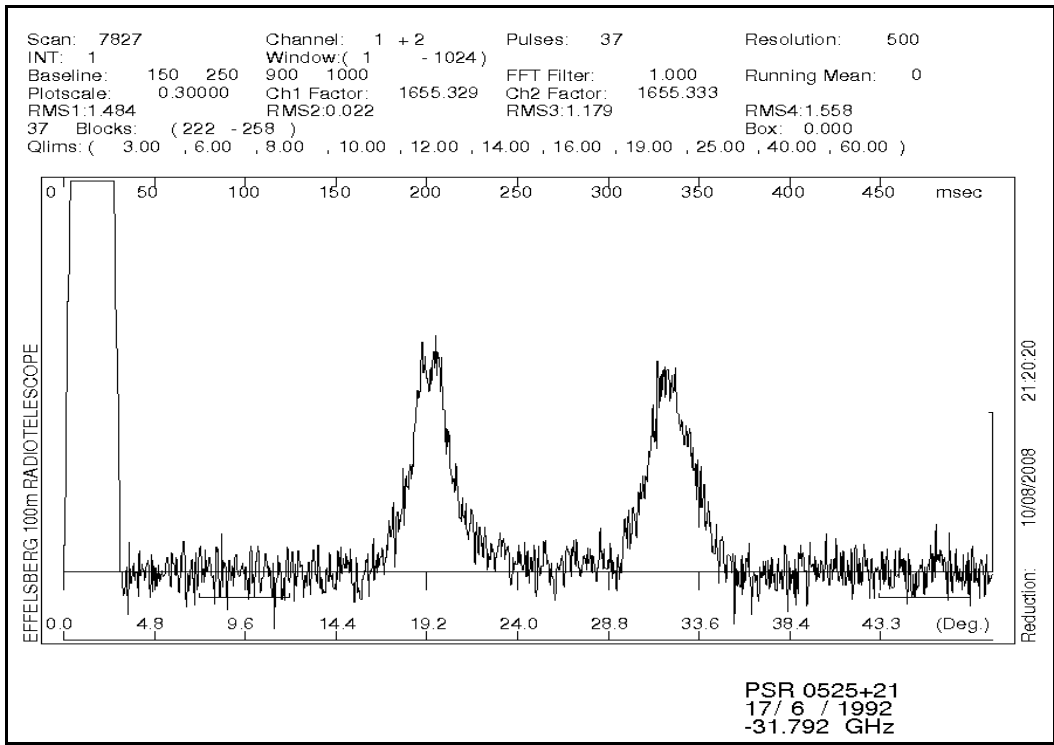


**Figure 48:** Integrated Profile of Scan 7827

The first window depicts mostly noise, with a weak pulse since sigma equals 1.5. We see that, while for small values of sigma the maximum pulse intensity of the main component is either lower or equal to that of the maximum value of the first component, for the highest sigma it is the opposite.

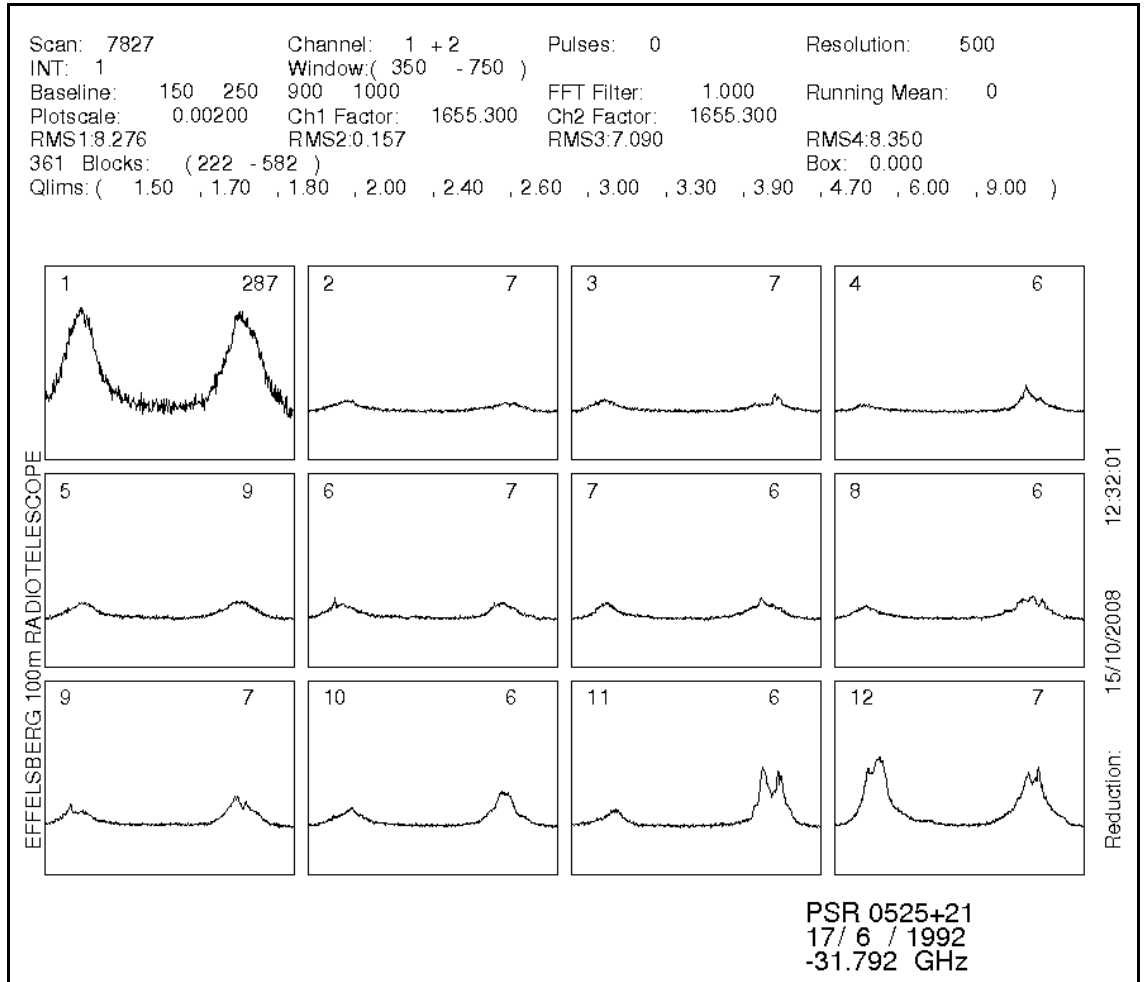


*Figure 49: Quality Graph for Scan 7827*

We can see the maximum values of each component for each window in the following table.

*Table 4: Scan 7827*

Channel	1	2	3	4	5	6
Main Component	3,14263E+03	2,83329E+02	5,60928E+02	8,20638E+02	5,64945E+02	5,24957E+02
Component 1	3,26651E+03	3,53359E+02	3,78862E+02	2,39296E+02	5,27821E+02	6,54857E+02
Main/Comp.1	<b>1,03942E+00</b>	<b>1,24717E+00</b>	<b>6,75420E-01</b>	<b>2,91598E-01</b>	<b>9,34287E-01</b>	<b>1,24745E+00</b>
Channel	7	8	9	10	11	12
Main Component	6,57147E+02	7,22625E+02	9,35910E+02	1,11774E+03	1,84866E+03	1,84178E+03
Component 1	5,05865E+02	4,19593E+02	7,03410E+02	6,00092E+02	5,59656E+02	2,15844E+03
Main/Comp.1	<b>7,69790E-01</b>	<b>5,80651E-01</b>	<b>7,51579E-01</b>	<b>5,36880E-01</b>	<b>3,02736E-01</b>	<b>1,17193E+00</b>

From the tables above we get the following diagram:

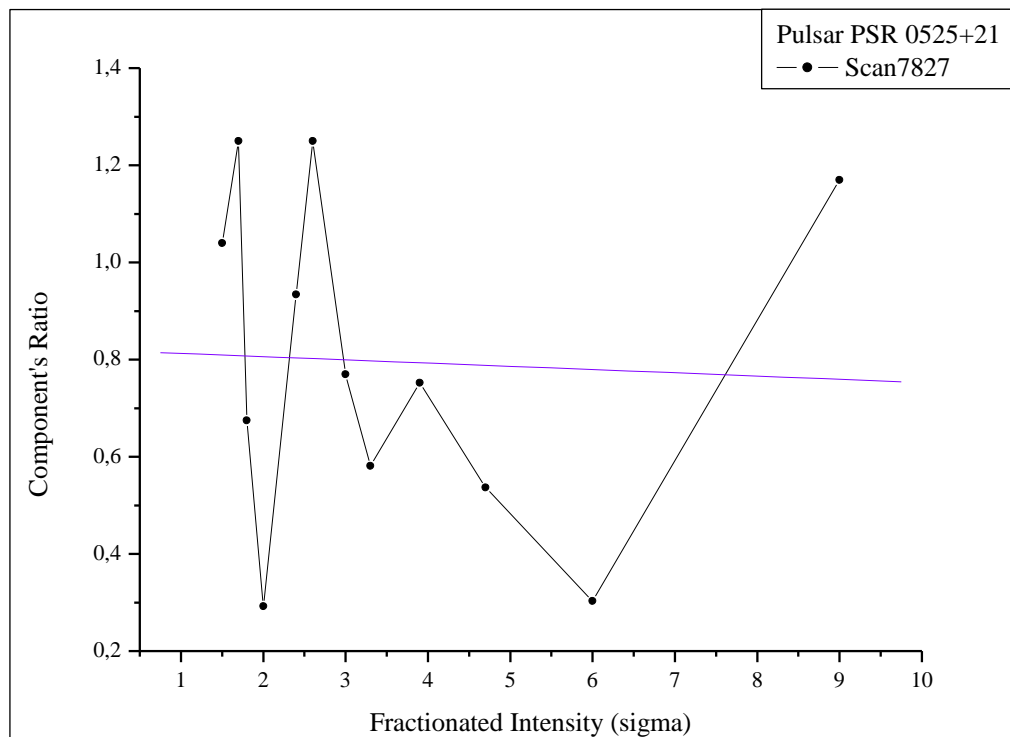


**Figure 50:** First to Main component ratio of Scan 7827

The linear fit gives us a descending line with the following equation:

$$y = 0,81943 - 0,0066x$$

A descending line means that the ratio of the main and first component decreases as the fractionated intensity (sigma) increases. We observe that the slope in this scan is lower than in the scan 7702.

### Scan 7833

The sequence of pulses and the integrated profile of the scan can be seen below. A study of the sequence of pulses and the integrated profile reveal that they are rather well defined. A closer study of the sequence as well as the quality graph reveals that the intensity-noise ratio has a rather high value. That allows for accurate results to be drawn from its study. The main component is the pulse component with the highest values. So we assume that the main component (core component) is the second in the integrated profile.

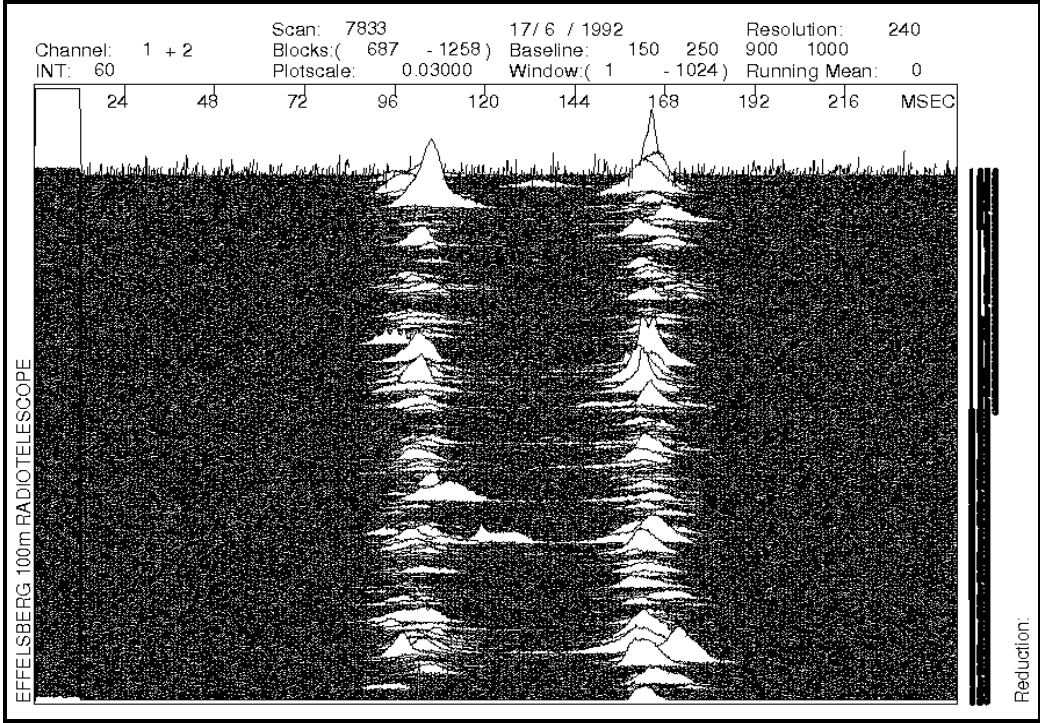


**Figure 51:** Sequence of pulses of Scan 7833

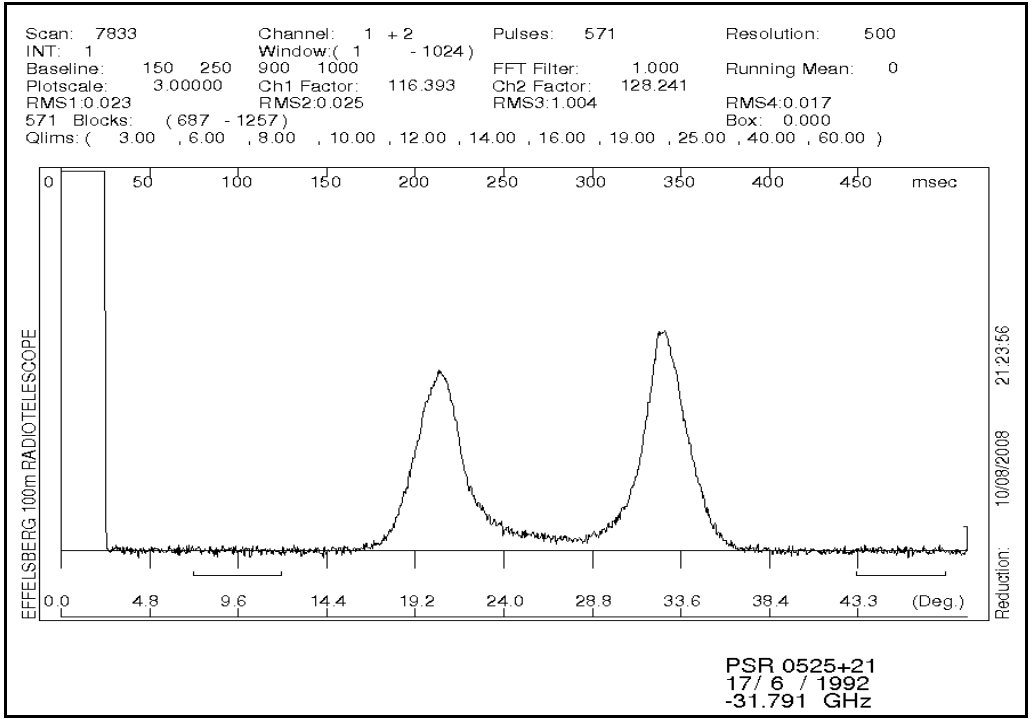


**Figure 52:** Integrated Profile of Scan 7833

The first window depicts mostly noise, with a weak pulse since sigma equals 1.5. We see that, while for small values of sigma the maximum pulse intensity of the main component is either lower or equal to that of the maximum value of the first component, for the two highest sigma it's the opposite.

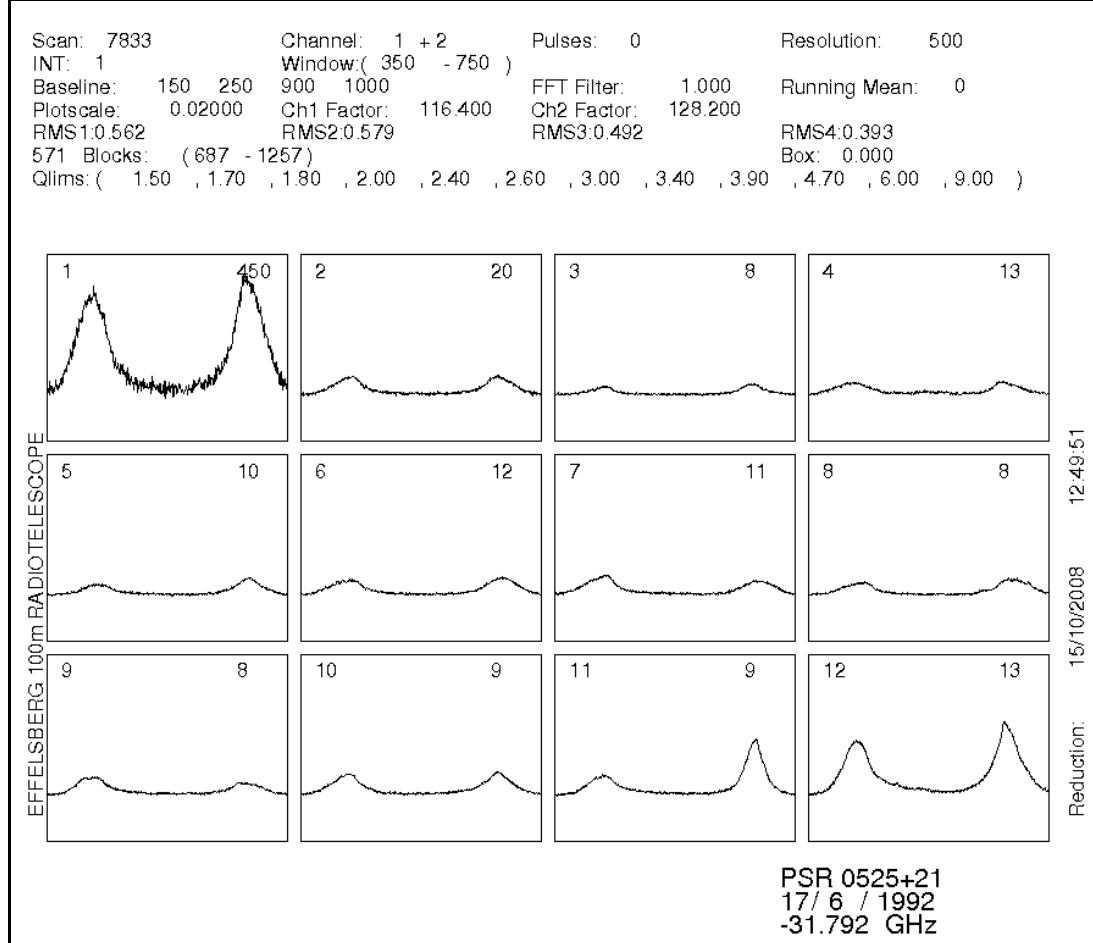


Figure 53: Quality Graph of Scan 7833

We can see the maximum values of each component for each window in the following table.

Table 5: Scan 7833

Channel	1	2	3	4	5	6
Main Component	3,86701E+02	6,35501E+01	3,44812E+01	4,27509E+01	5,62271E+01	5,83766E+01
Component 1	3,53781E+02	6,00491E+01	2,79682E+01	4,10224E+01	3,54950E+01	5,03094E+01
Main/Comp.1	<b>9,14870E-01</b>	<b>9,44910E-01</b>	<b>8,11114E-01</b>	<b>9,59568E-01</b>	<b>6,31279E-01</b>	<b>8,61808E-01</b>
Channel	7	8	9	10	11	12
Main Component	4,59277E+01	5,35281E+01	4,04546E+01	7,55540E+01	1,81534E+02	2,36303E+02
Component 1	6,48841E+01	4,16590E+01	5,87473E+01	6,85591E+01	6,56274E+01	1,76648E+02
Main/Comp.1	<b>1,41274E+00</b>	<b>7,78264E-01</b>	<b>1,45218E+00</b>	<b>9,07419E-01</b>	<b>3,61516E-01</b>	<b>7,47549E-01</b>

From the tables above we get the following diagram:

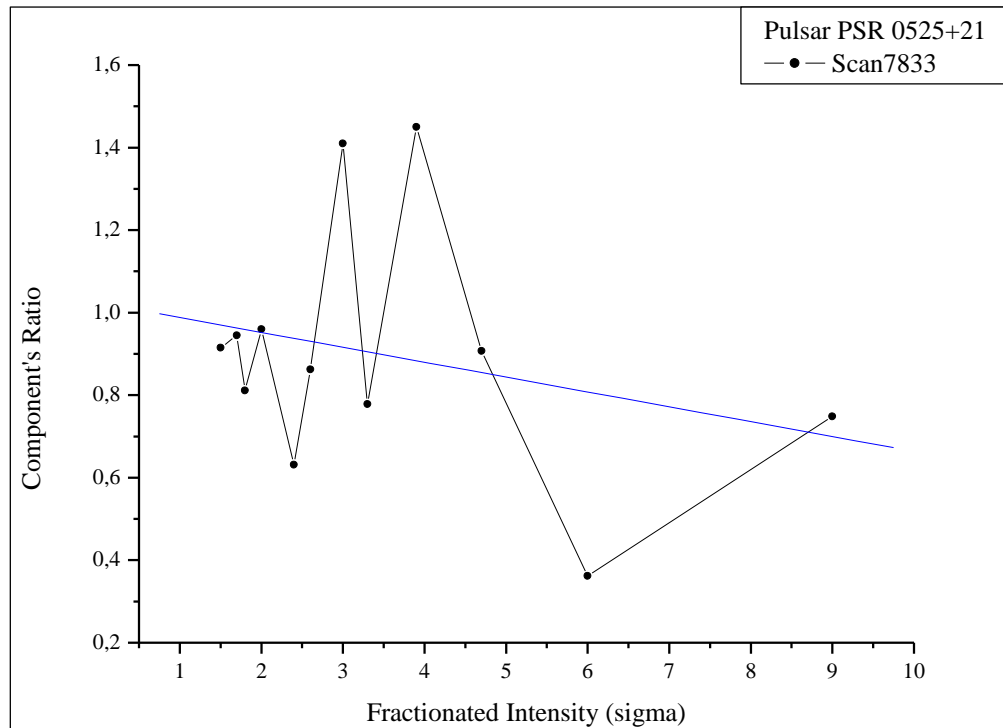


**Figure 54:** First to Main component ratio of Scan 7833

The linear fit gives us a descending line with the following equation:

$$y = 1,02412 - 0,03605x$$

A descending line means that the ratio of the main and first component decreases as the fractionated intensity (sigma) increases. We observe that the slope in this scan is higher than in the scan 7833.

### Scan 9008

The sequence of pulses and the integrated profile of the scan can be seen below. A study on the sequence of pulses and the integrated profile reveal that they are rather well defined. A spike can be seen during one pulse, in the sequence of pulses. It was caused by the accidental rebooting of the amplifier. A closer study of the sequence as well as the quality graph reveals that the intensity-noise ratio has a rather high value. That allows for accurate results to be drawn from its study. The main component is the pulse component with the highest values. So we assume that the main component (core component) is the second in the integrated profile.

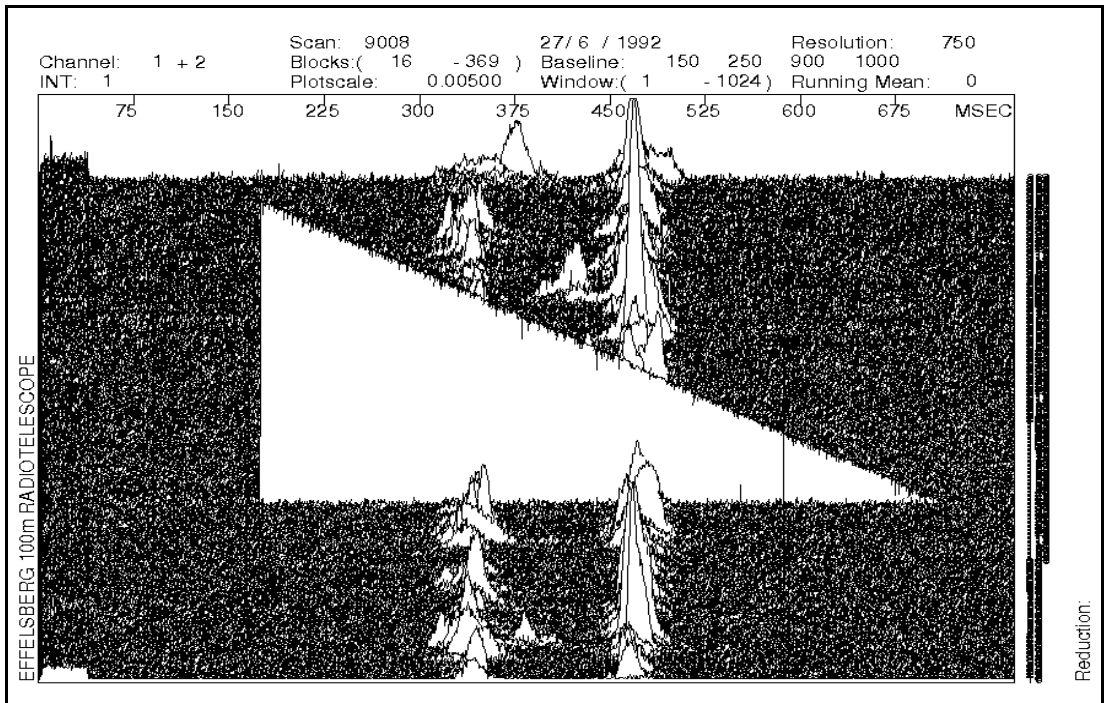


**Figure 55:** Sequence of pulses of Scan 9008

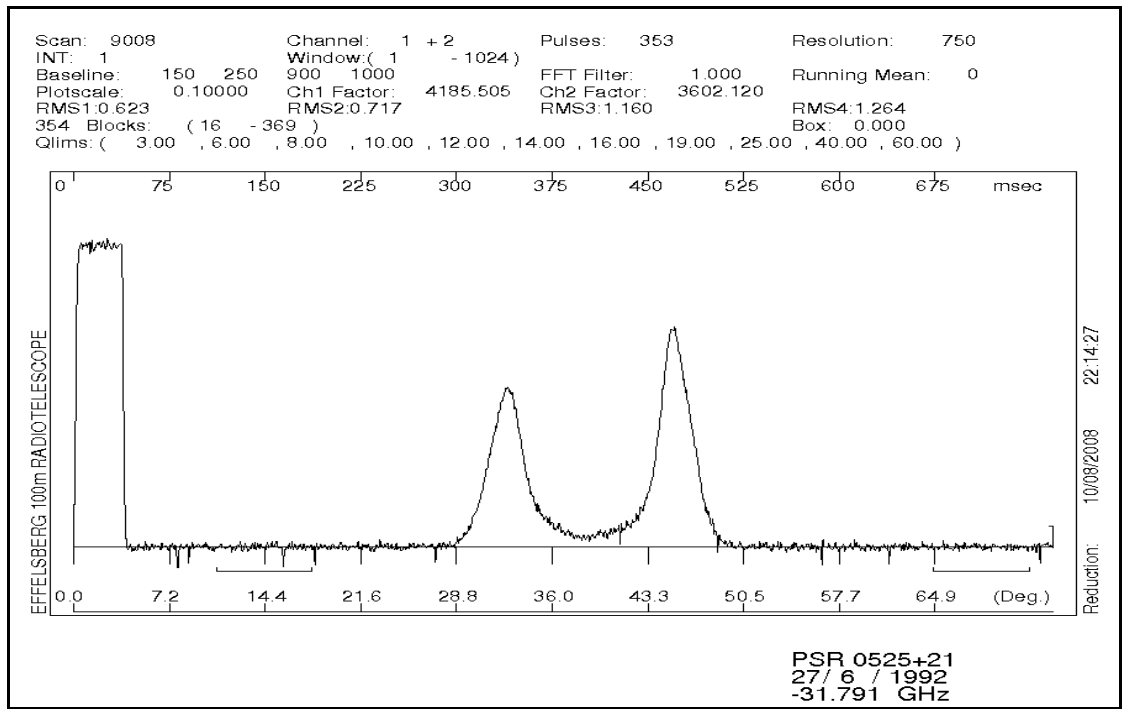


**Figure 56:** Integrated Profile of Scan 9008

The first window depicts mostly noise, with a weak pulse since sigma equals 1.5. We see that, while for small values of sigma the maximum pulse intensity of the main component is either lower or equal to that of the maximum value of the first component, for the two highest sigma it is the opposite. There are more pulses with considerable intensity in this scan than in the previous scans.

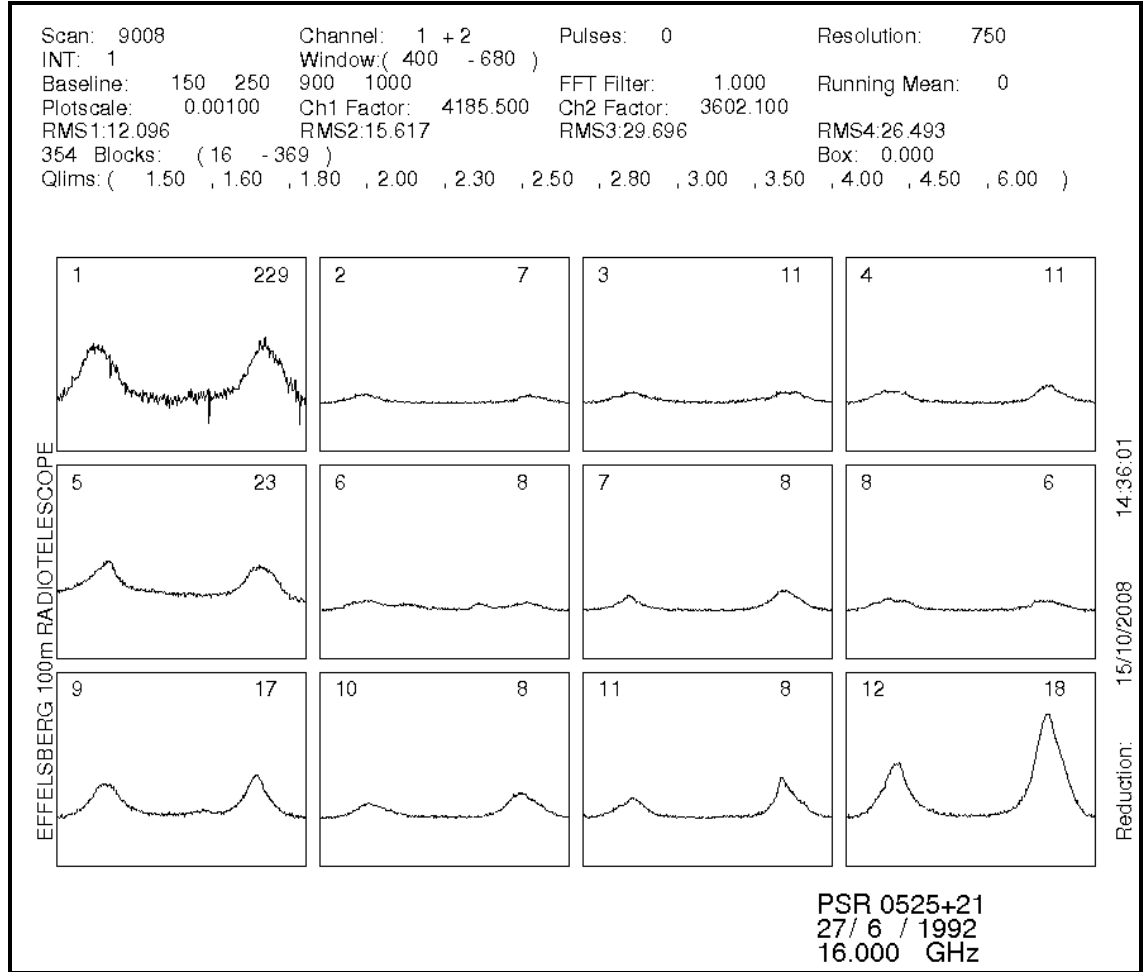


Figure 57: Quality Graph of Scan 9008

We can see the maximum values of each component for each window in the following table.

Table 6: (Scan 9008)

Channel	1	2	3	4	5	6
Main Component	4,09432E+03	5,66879E+02	7,24650E+02	1,14222E+03	2,82512E+03	5,27774E+02
Component 1	3,77499E+03	5,66135E+02	7,02633E+02	7,98146E+02	3,10997E+03	6,62089E+02
Main/Comp.1	<b>0,922006585</b>	<b>0,998687551</b>	<b>0,969617057</b>	<b>0,698767313</b>	<b>1,100827575</b>	<b>1,254493401</b>
Channel	7	8	9	10	11	12
Main Component	1,28773E+03	6,40781E+02	2,71765E+03	1,60748E+03	2,55585E+03	6,54702E+03
Component 1	9,37580E+02	8,21818E+02	2,17775E+03	9,81575E+02	1,25515E+03	3,47113E+03
Main Comp. 1	<b>0,72808741</b>	<b>1,282525543</b>	<b>0,801335713</b>	<b>0,610629681</b>	<b>0,49108907</b>	<b>0,530184725</b>

From the tables above we get the following diagram:

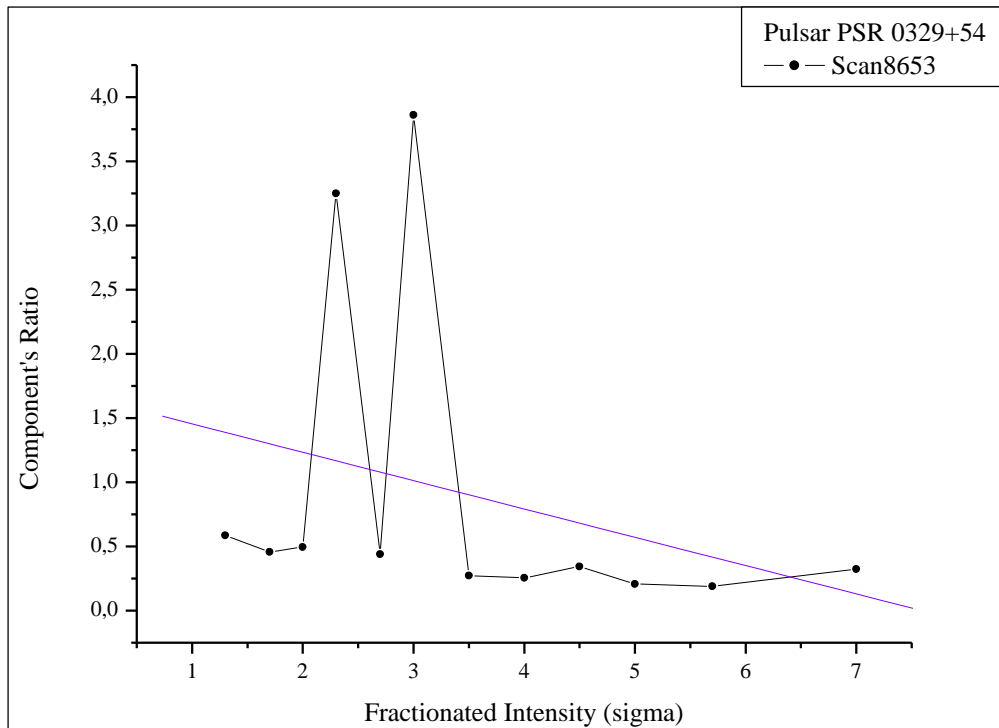


**Figure 58:** First to Main component ratio of Scan 9008

The linear fit gives us a descending line with the following equation:

$$y = 1,22462 - 0,12133x$$

A descending line means that the ratio of the main and first component decreases as the fractionated intensity (sigma) increases. We observe that the slope in this scan is higher than in the scan 7833.

### (3.2)Pulsar PSR 0329+54

#### Scan 8653

The sequence of pulses and the integrated profile of the scan can be seen below. A study of the sequence of pulses and the integrated profile reveal that they are not well defined. It is obvious from the sequence of pulses that there is quite a lot of noise present. A closer study of the sequence as well as the quality graph reveals that the intensity-noise ratio has a rather high value. That allows for accurate results to be drawn from its study. The main component is the pulse component with the highest values. So the main component (core component) is the central pulse in the integrated profile. The first component is the second pulse and the third the first.

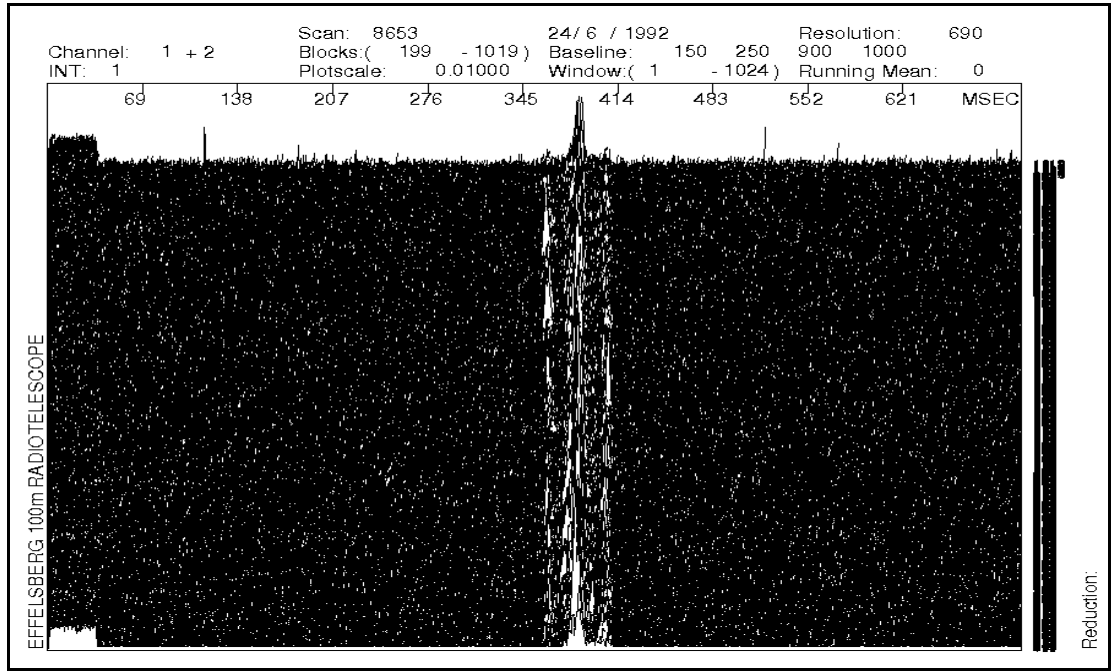


**Figure 59:** Sequence of pulses of Scan 8653

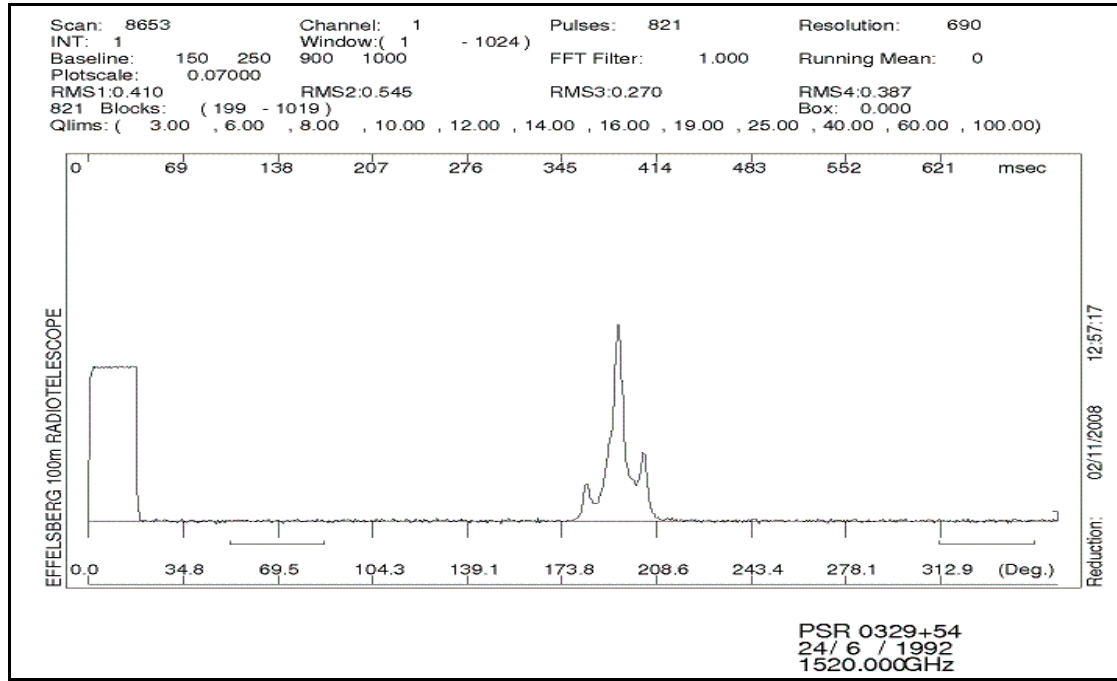


**Figure 60:** Sequence of pulses of Scan 8653

The first window depicts mostly noise, with a weak pulse since sigma equals 1,3. We see that, while for small values of sigma the maximum pulse intensity of the main component is either lower or equal to that of the maximum value of the first component, for the two highest sigma it is the opposite. There are more pulses with considerable intensity in this scan than in the previous scans.

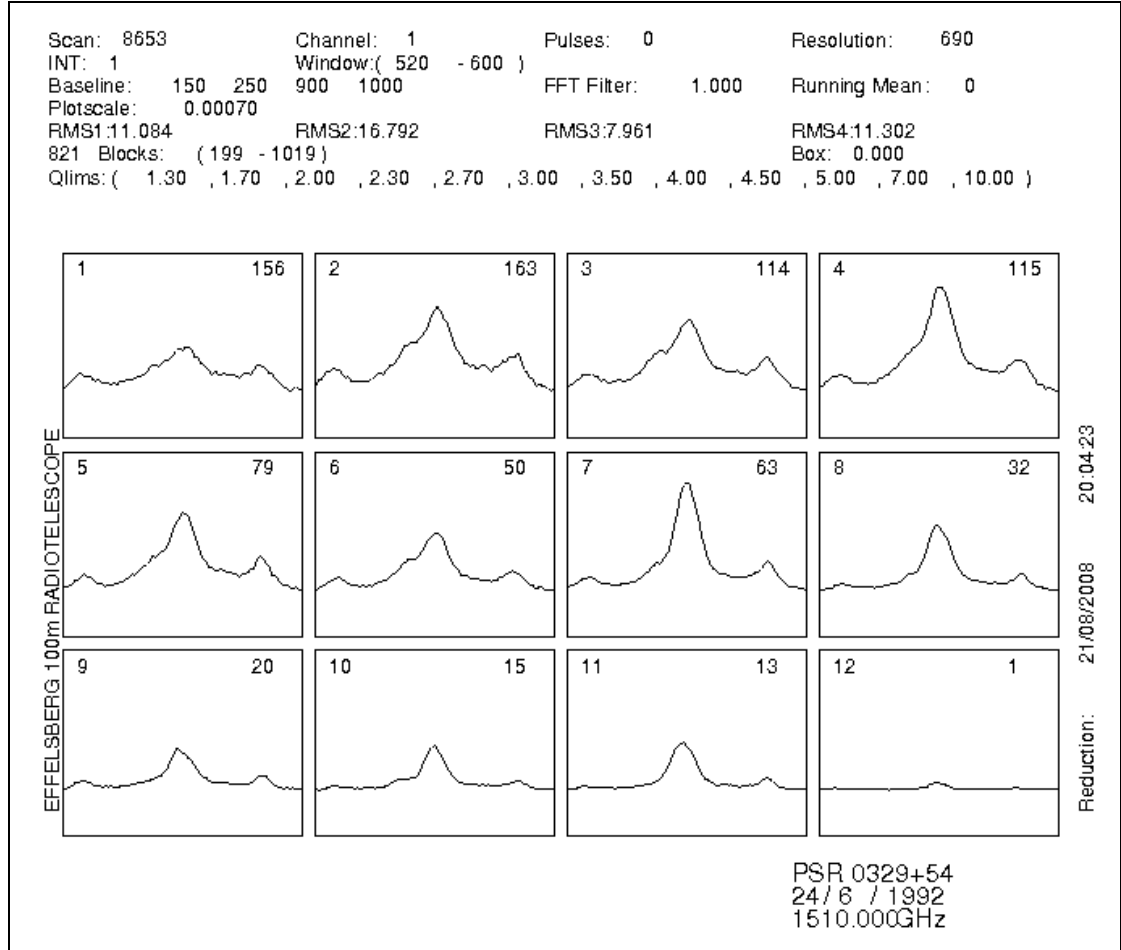


*Figure 61: Quality Graph of Scan 8653*

We can see the maximum values of each component for each window in the following table.

*Table 7: Scan 8653*

Channel	1	2	3	4	5	6
<b>Main Component</b>	4,23175E+03	7,98990E+03	6,79306E+03	3,01236E+03	7,35451E+03	1,38183E+03
<b>Component 1</b>	2,47774E+03	3,65244E+03	3,35836E+03	9,78191E+03	3,23932E+03	5,33750E+03
<b>Component 2</b>	1,78297E+03	2,20450E+03	1,71994E+03	1,61362E+03	1,56176E+03	1,83100E+03
<b>Main/Comp. 1</b>	<b>5,85512E-01</b>	<b>4,57132E-01</b>	<b>4,94381E-01</b>	<b>3,24726E+00</b>	<b>4,40454E-01</b>	<b>3,86263E+00</b>
<b>Main/Comp. 2</b>	<b>4,21332E-01</b>	<b>2,75911E-01</b>	<b>2,53191E-01</b>	<b>5,35666E-01</b>	<b>2,12354E-01</b>	<b>1,32505E+00</b>
<b>Comp.2/Comp.1</b>	<b>7,19595E-01</b>	<b>6,03569E-01</b>	<b>5,12137E-01</b>	<b>1,64960E-01</b>	<b>4,82126E-01</b>	<b>3,43044E-01</b>
Channel	7	8	9	10	11	12
<b>Main Component</b>	1,01158E+04	6,20241E+03	3,85373E+03	4,15354E+03	2,41188E+03	2,61364E+03
<b>Component 1</b>	2,75045E+03	1,58479E+03	1,32381E+03	8,54605E+02	4,57116E+02	8,40341E+02
<b>Component 2</b>	1,30040E+03	6,57105E+02	8,33542E+02	3,31461E+02	1,81588E+02	3,43992E+02
<b>Main/Comp. 1</b>	<b>2,71896E-01</b>	<b>2,55512E-01</b>	<b>3,43514E-01</b>	<b>2,05753E-01</b>	<b>1,89527E-01</b>	<b>3,21521E-01</b>

Main/Comp. 2	<b>1,28551E-01</b>	<b>1,05943E-01</b>	<b>2,16295E-01</b>	<b>7,98020E-02</b>	<b>7,52890E-02</b>	<b>1,31614E-01</b>
Comp.2/Comp.1	<b>4,72795E-01</b>	<b>4,14632E-01</b>	<b>6,29654E-01</b>	<b>3,87853E-01</b>	<b>3,97247E-01</b>	<b>4,09348E-01</b>

From the tables above we get the following diagrams:

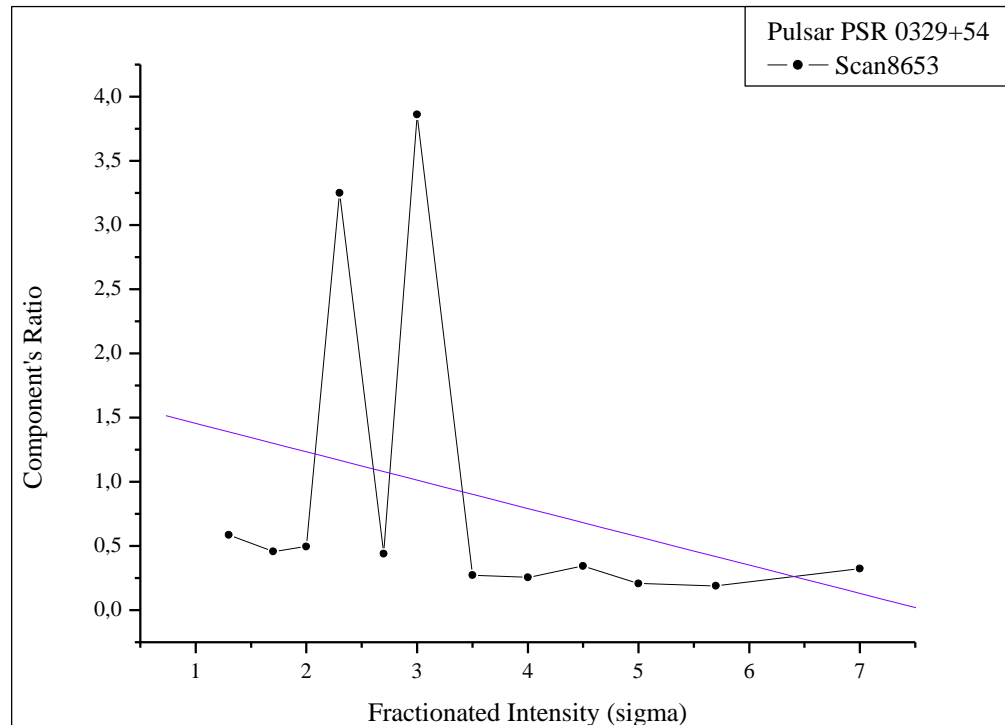


**Figure 62:** First to Main component ratio of Scan 8653

The linear fit gives us a descending line with the following equation:

$$y = 1,67533 - 0,22077x$$

A descending line means that the ratio of the main and first component decreases as the fractionated intensity (sigma) increases.

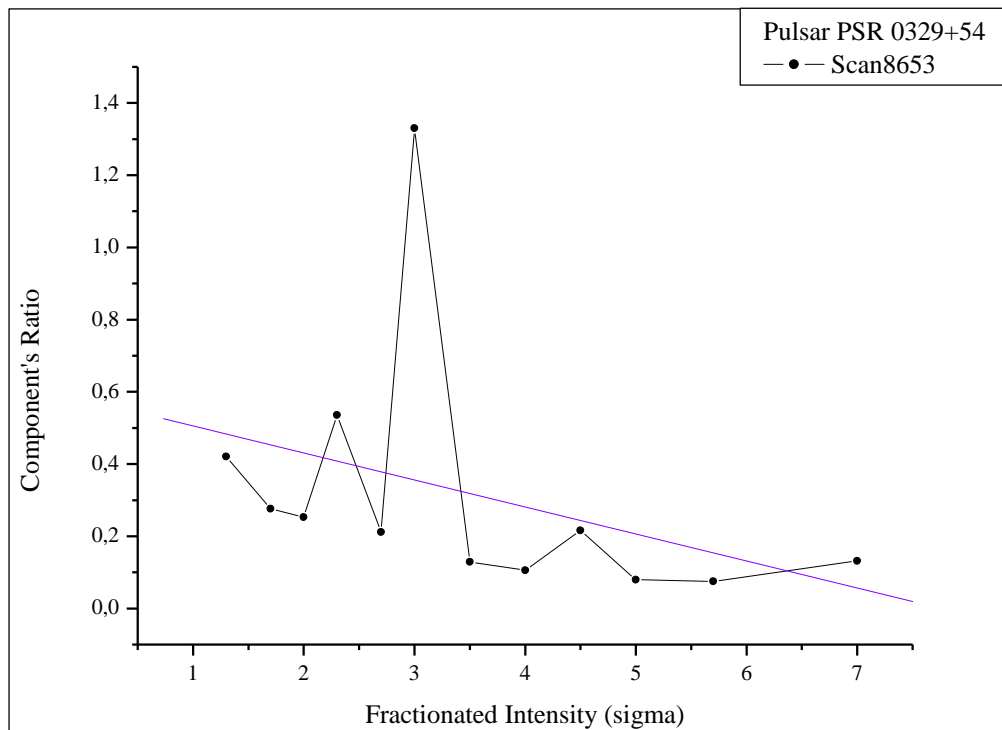


**Figure 63:** Second to Main component ratio of Scan 8653

The linear fit gives us a descending line with the following equation:

$$y = 0,57996 - 0,07479x$$

A descending line means that the ratio of the main and first component decreases as the fractionated intensity (sigma) increases.

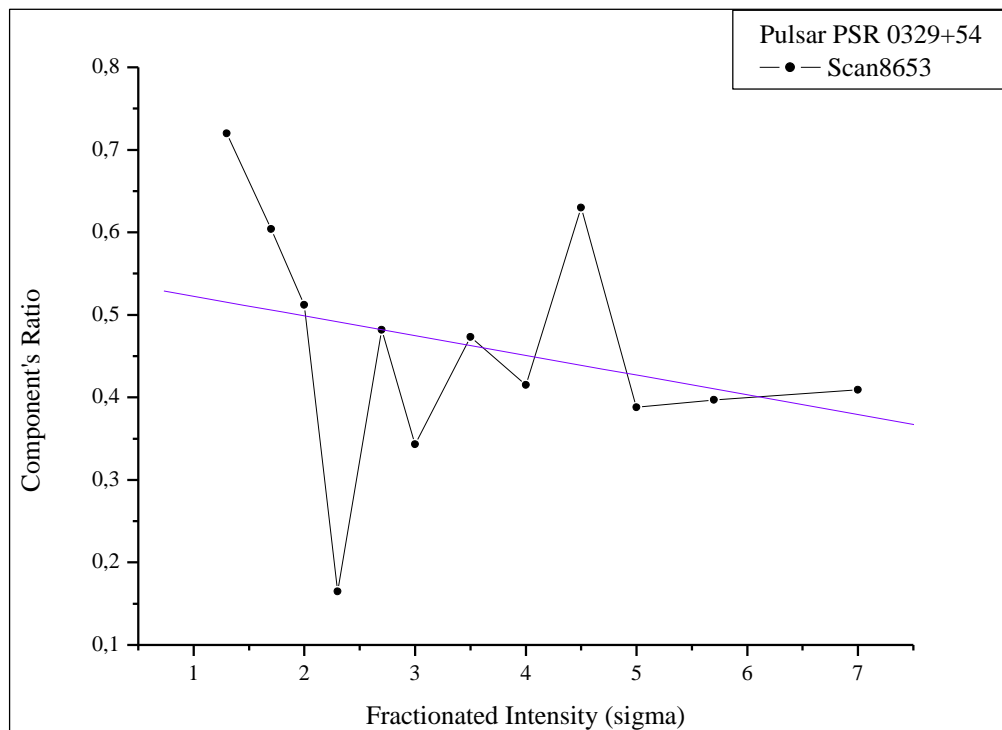


**Figure 64:** Second to First component Ratio for scans 8653

The linear fit gives us a descending line with the following equation:

$$y = 0,54646 - 0,02388x$$

A descending line means that the ratio of the main and first component decreases as the fractionated intensity (sigma) increases.

### Scan 8654

The sequence of pulses and the integrated profile of the scan can be seen below. A study of the sequence of pulses and the integrated profile reveal that they are not at all well defined. It is obvious from the sequence of pulses that there is a lot of noise present. A closer study of the sequence as well as the quality graph reveals that the intensity-noise ratio has a rather low value. That does not allow for accurate results to be drawn from its study. A study of the integrated profile reveals that only the main pulse is clearly defined.

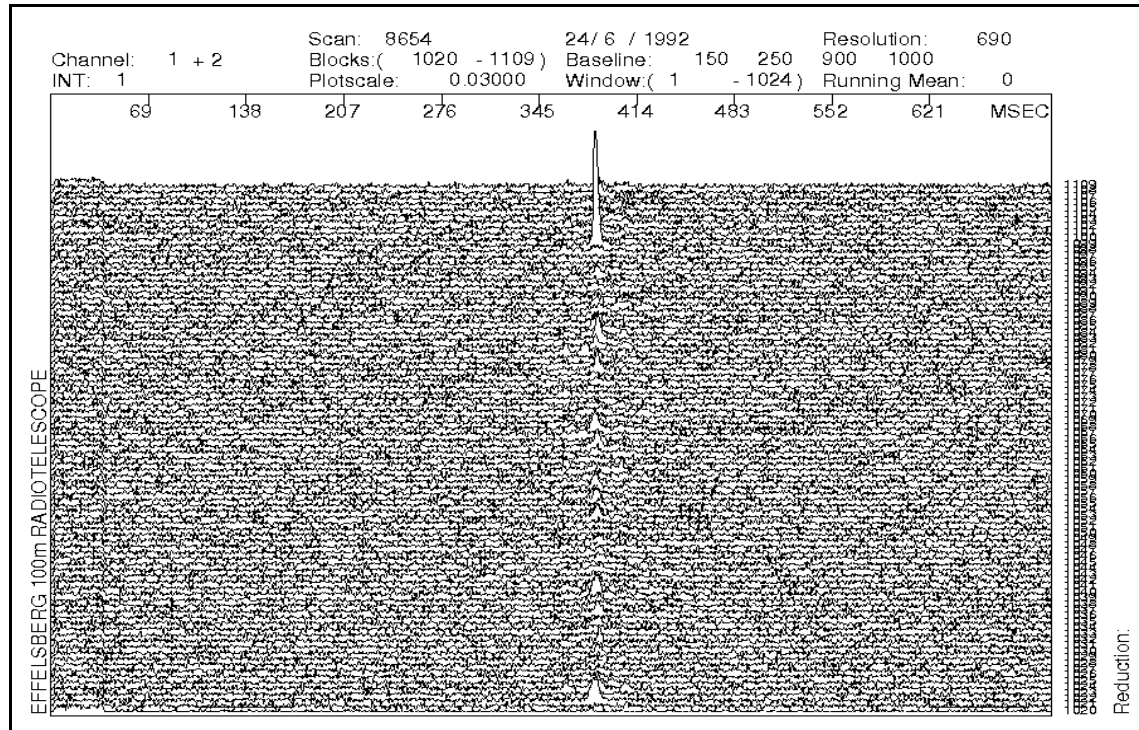


Figure 65: Sequence of pulses of Scan 8654

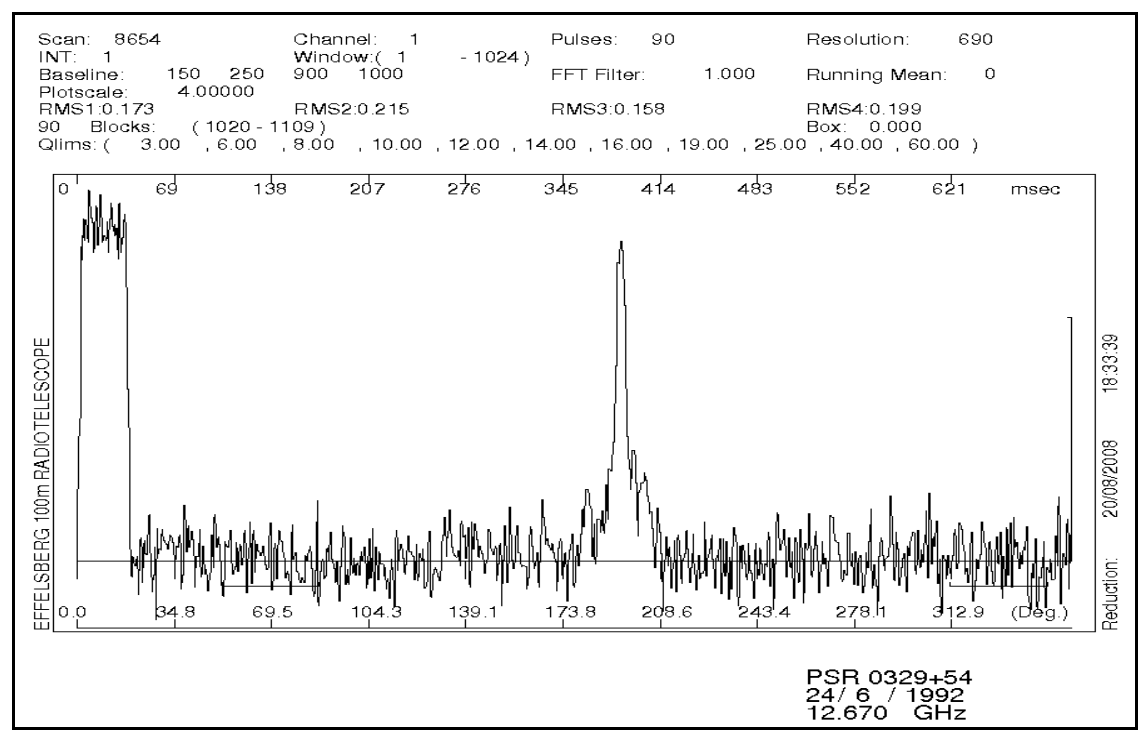
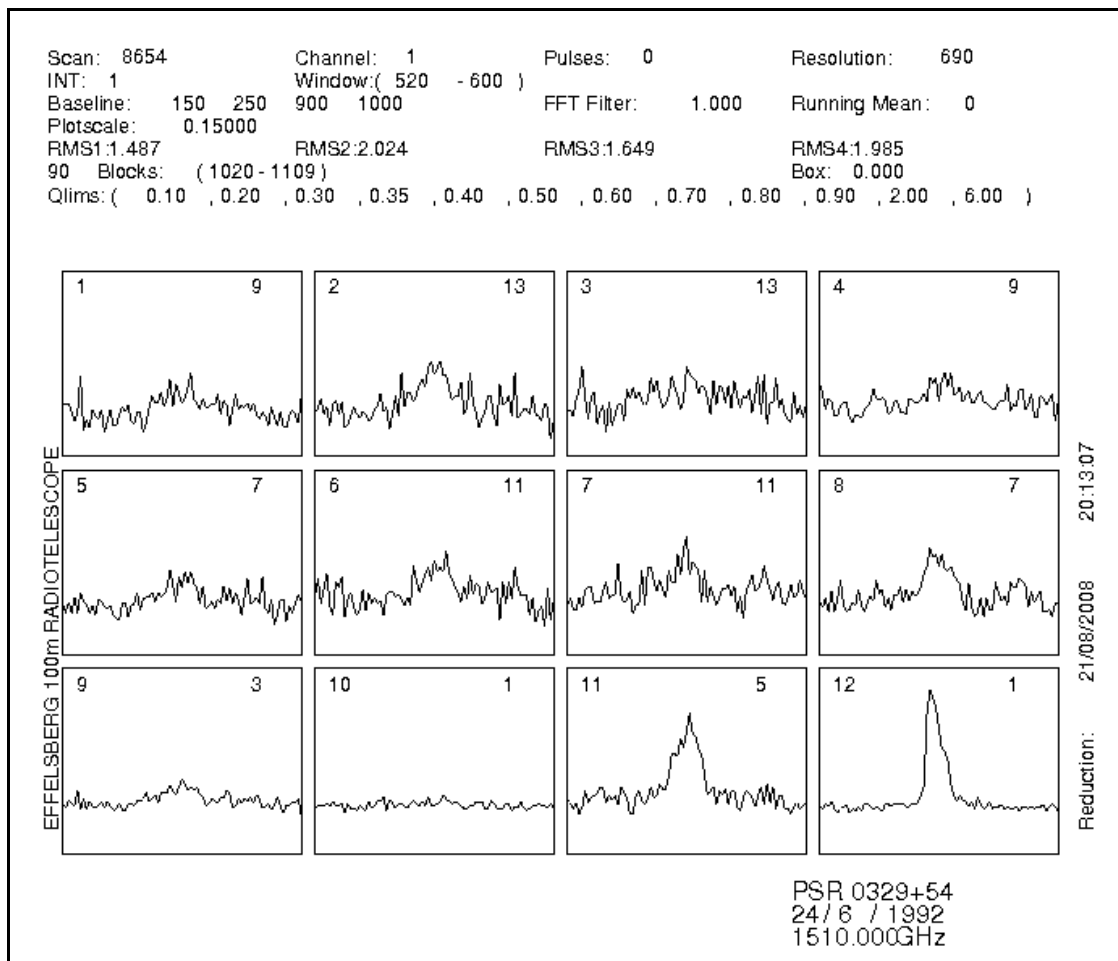


Figure 66: Integrated Profile of Scan 8654



*Figure 67: Quality Graph of Scan 8654*

### Scan 8656

The sequence of pulses and the integrated profile of the scan can be seen below. A study of the sequence of pulses and the integrated profile reveal that they are not well defined. It is obvious from the sequence of pulses that there is quite a lot of noise present. A closer study of the sequence as well as the quality graph reveals that the intensity-noise ratio has a rather low value. That does not allow for accurate results to be drawn from its study.

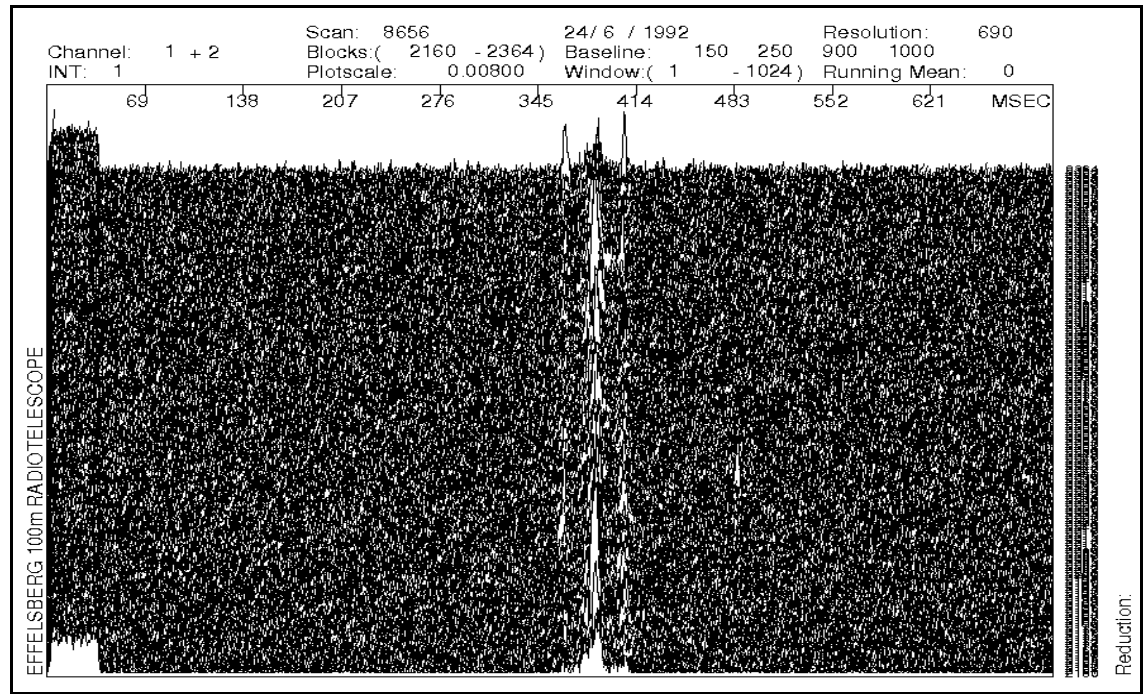


Figure 68: Sequence of pulses of Scan 8656

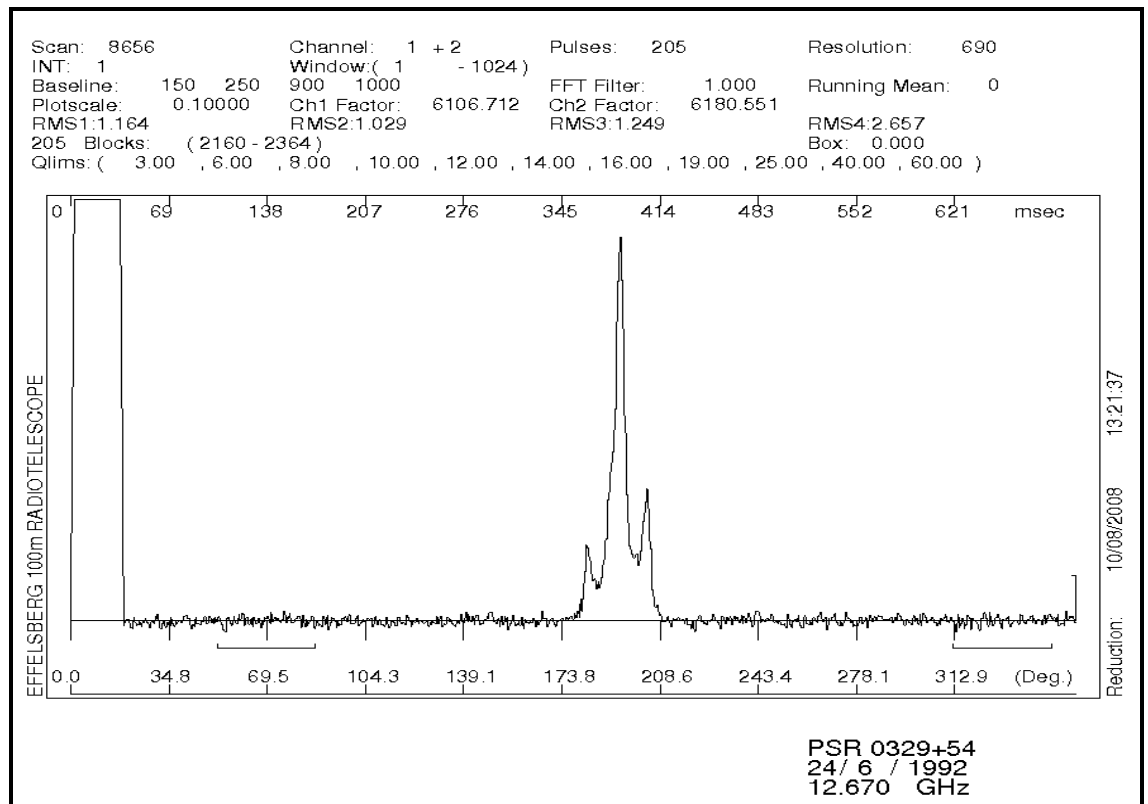
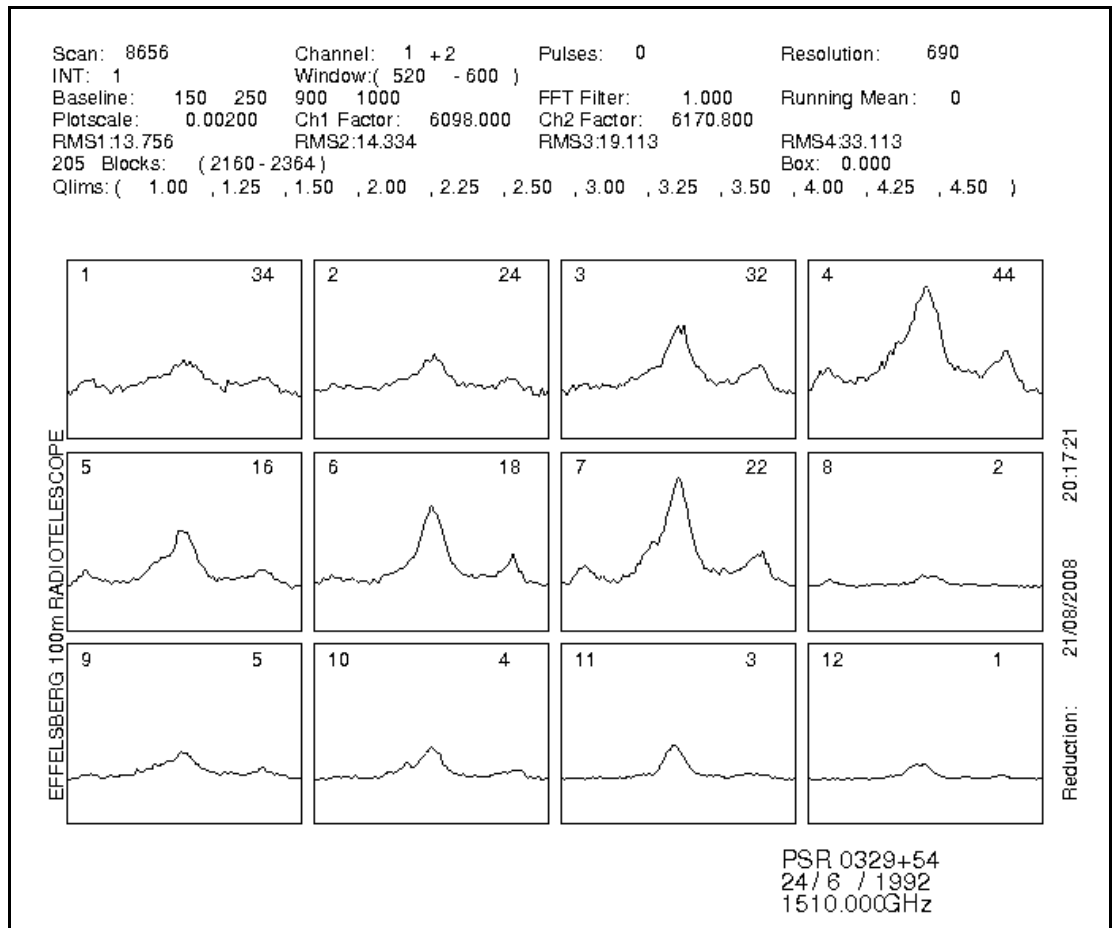


Figure 69: Integrated Profile of Scan 8656

As we can see below the sigma has very low values and the pulses with intensity greater than 2 sigma are few and not enough for a successful analysis.



**Figure 70:** Quality Graph of Scan 8656

### Scan 8657

The sequence of pulses and the integrated profile of the scan can be seen below. A study of the sequence of pulses and the integrated profile reveal that they are well defined. A closer study of the sequence as well as the quality graph reveals that the intensity-noise ratio has a rather high value. That allows for accurate results to be drawn from its study. The main component is the pulse component with the highest values. So we assume that the main component (core component) is the central pulse, the first component the second “pulse” and the third component the first “pulse” in the integrated profile.

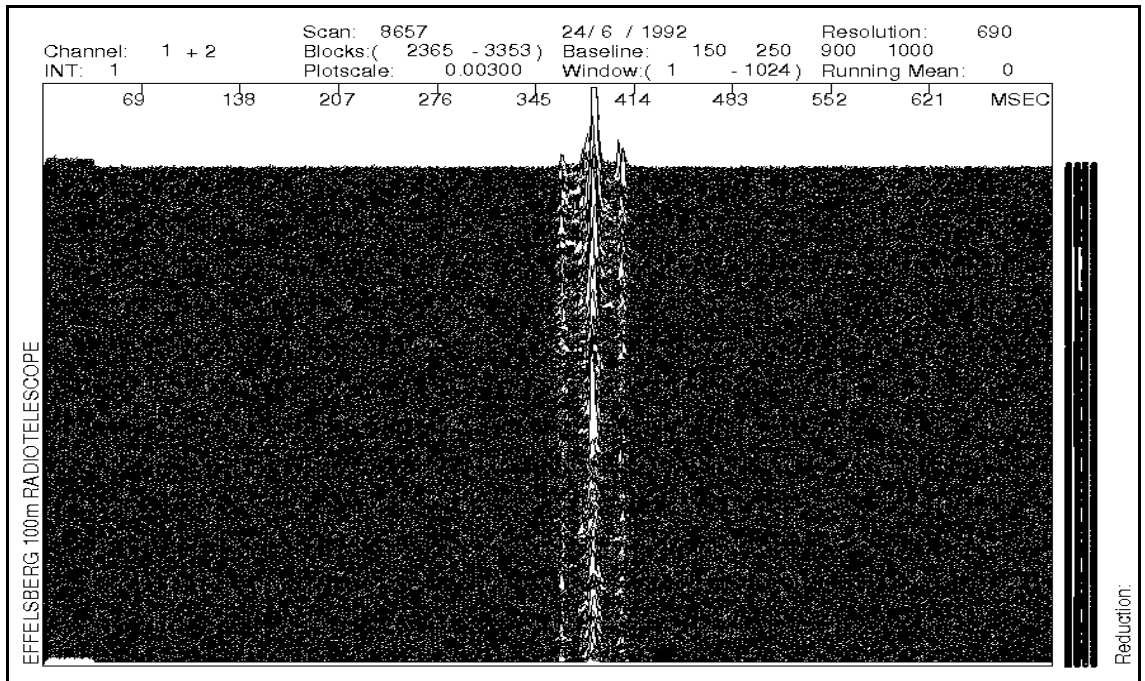


**Figure 71:** Sequence of pulses of Scan 8657

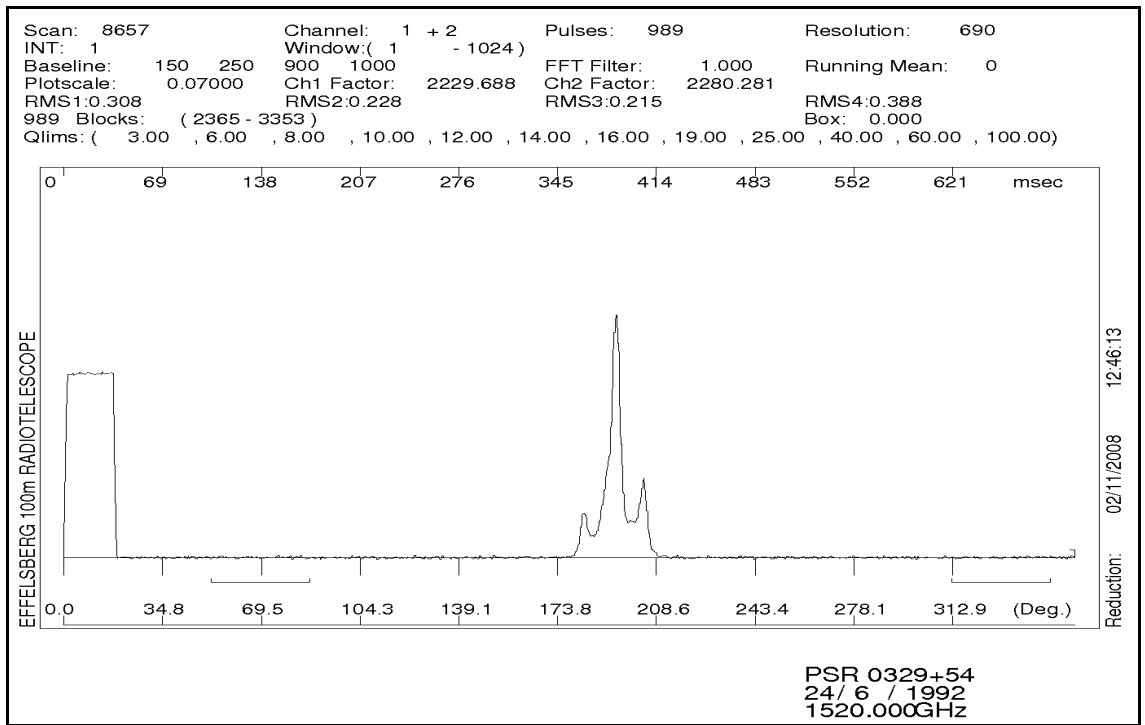


**Figure 72:** Integrated Profile of Scan 8657

The first window depicts mostly noise, with a weak pulse since sigma equals 1.3. We see that, the intensity of all the components drops with the increase of the sigma. Only in the 12<sup>th</sup> window (the one with the largest sigma) do we see a significant increase in the maximum value of the main component.

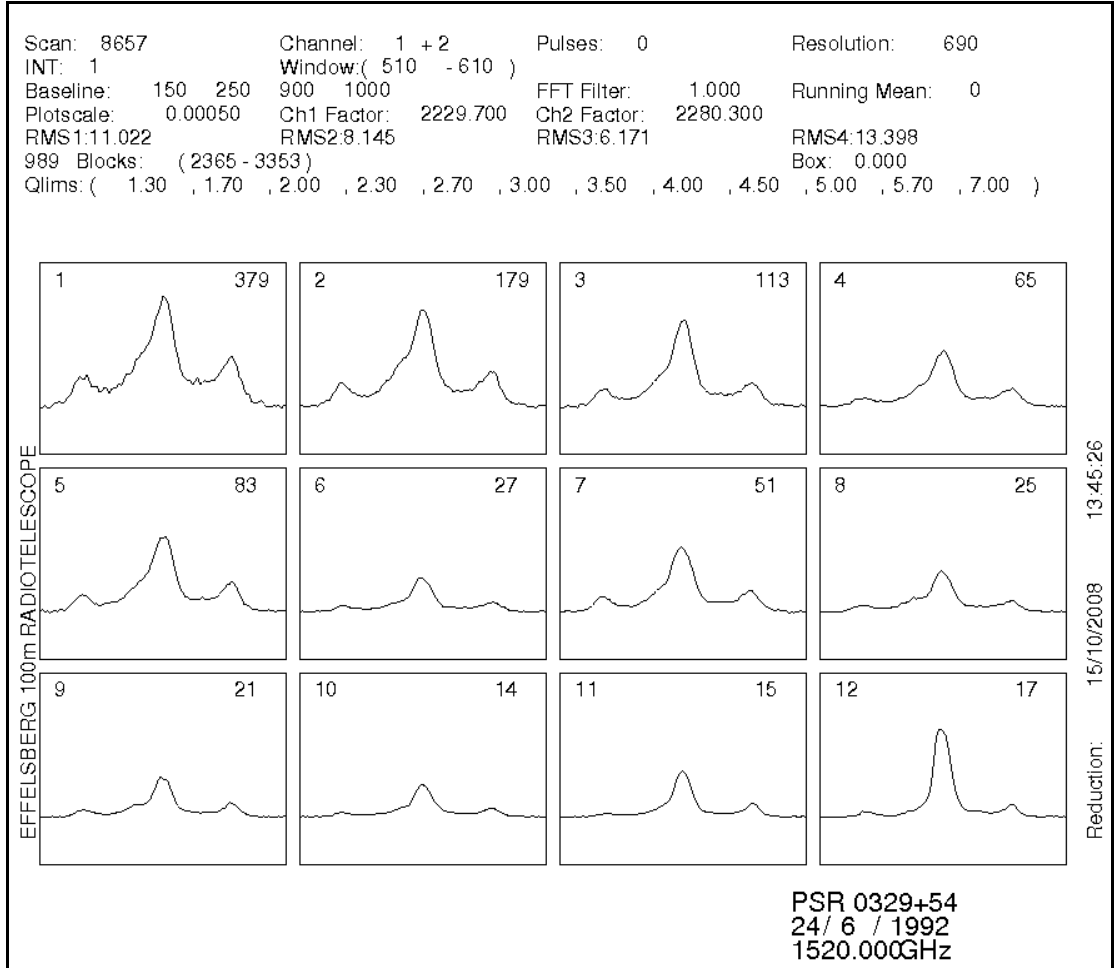


Figure 73: Quality Graph of Scan 8657

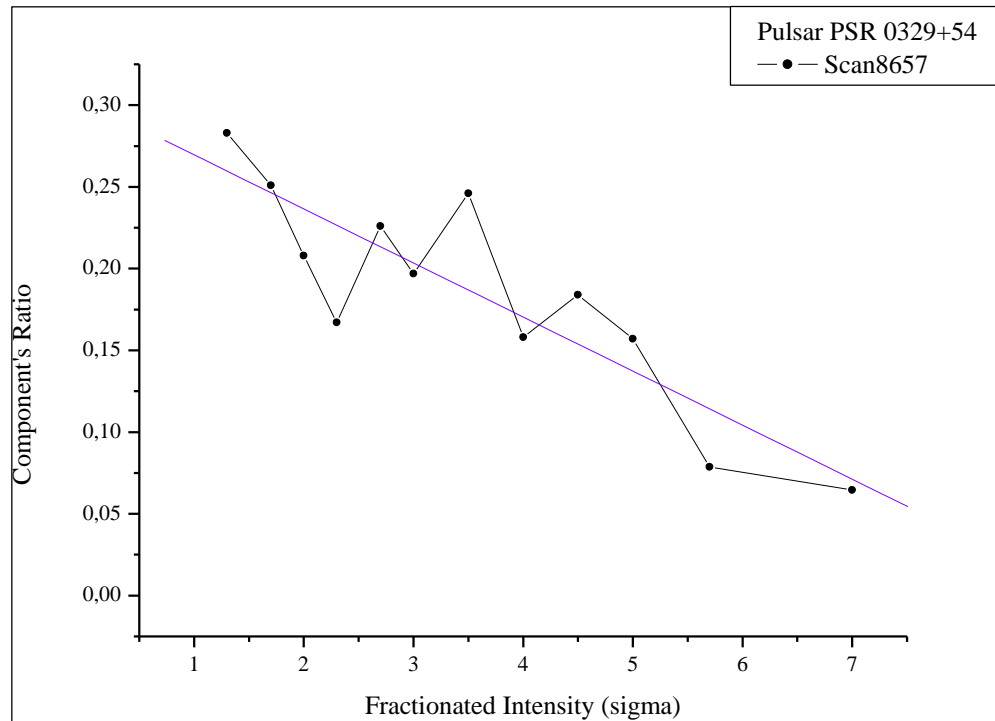
We can see the maximum values of each component for each window in the following table.

Table 10: Scan 8657

Channel	1	2	3	4	5	6
<b>Main Component</b>	1,41081E+04	1,23051E+04	1,09211E+04	7,17012E+03	9,54365E+03	4,32741E+03
<b>Component 1</b>	3,99775E+03	3,08415E+03	2,26895E+03	1,19761E+03	2,15992E+03	8,53691E+02
<b>Component 2</b>	6,37136E+03	4,46727E+03	3,16114E+03	2,32681E+03	3,85348E+03	1,22877E+03
<b>Main/Comp. 1</b>	<b>2,83366E-01</b>	<b>2,50640E-01</b>	<b>2,07758E-01</b>	<b>1,67028E-01</b>	<b>2,26320E-01</b>	<b>1,97275E-01</b>
<b>Main/Comp. 2</b>	<b>4,51610E-01</b>	<b>3,63042E-01</b>	<b>2,89453E-01</b>	<b>3,24515E-01</b>	<b>4,03774E-01</b>	<b>2,83950E-01</b>
<b>Comp.2/Comp.1</b>	<b>1,59374E+00</b>	<b>1,44846E+00</b>	<b>1,39322E+00</b>	<b>1,94288E+00</b>	<b>1,78408E+00</b>	<b>1,43936E+00</b>
Channel	7	8	9	10	11	12
<b>Main Component</b>	8,18941E+03	5,17353E+03	5,13310E+03	4,05827E+03	5,77428E+03	1,11835E+04
<b>Component 1</b>	2,01782E+03	8,19115E+02	9,44893E+02	6,38348E+02	4,54254E+02	7,21531E+02
<b>Component 2</b>	2,68893E+03	1,48678E+03	1,82800E+03	1,12596E+03	1,77013E+03	1,52112E+03

<b>Main/Comp. 1</b>	<b>2,46394E-01</b>	<b>1,58328E-01</b>	<b>1,84078E-01</b>	<b>1,57296E-01</b>	<b>7,86685E-02</b>	<b>6,45175E-02</b>
<b>Main/Comp. 2</b>	<b>3,28342E-01</b>	<b>2,87382E-01</b>	<b>3,56120E-01</b>	<b>2,77448E-01</b>	<b>3,06554E-01</b>	<b>1,36015E-01</b>
<b>Comp.2/Comp.1</b>	<b>1,33259E+00</b>	<b>1,81511E+00</b>	<b>1,93461E+00</b>	<b>1,76387E+00</b>	<b>3,89678E+00</b>	<b>2,10818E+00</b>

From the tables above we get the following diagram:



**Figure 74:** First to Main component ratio of scans 8657

The linear fit gives us a descending line with the following equation:

$$y = 0,30269 - 0,03307x$$

A descending line means that the ratio of the main and first component decreases as the fractionated intensity (sigma) increases.

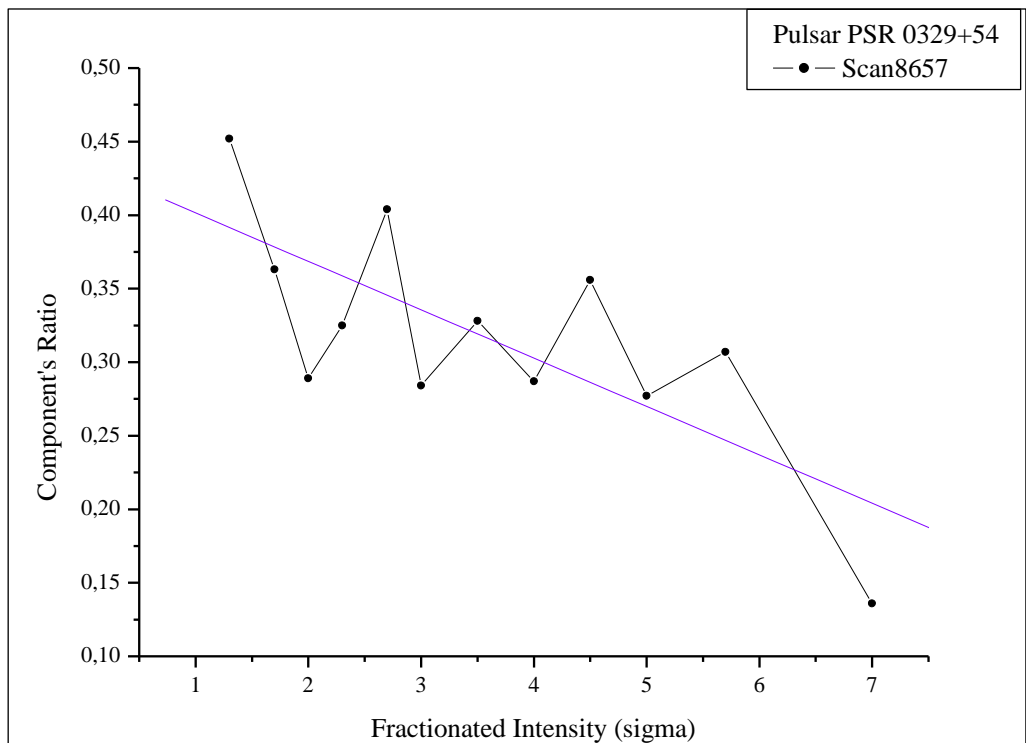


**Figure 75:** Second to Main component Ratio of scans 8657

The linear fit gives us a descending line with the following equation:

$$y = 0,43437 - 0,03289x$$

A descending line means that the ratio of the main and first component decreases as the fractionated intensity (sigma) increases. We observe that the slope is similar with in the main/first component diagram.

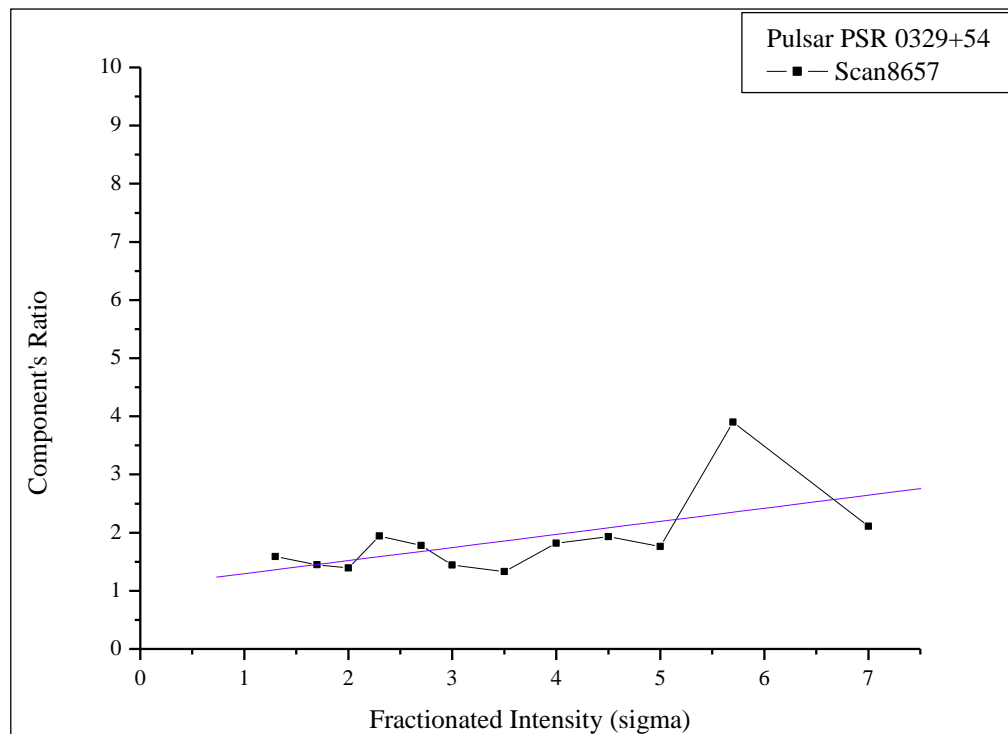


**Figure 76:** Second to First component Ratio of Scan 8657

The linear fit gives us an ascending line with the following equation:

$$y = 1,06949 + 0,22497x$$

A decreasing line means that the ratio of the main and first component decreases as the fractionated intensity (sigma) increases. So far in all the above diagrams we show descending lines, but this one is ascending.

### Scan 8658

The sequence of pulses and the integrated profile of the scan can be seen below. A study of the sequence of pulses and the integrated profile reveal that they are well defined. Although the quality of the scan is good, there are too few pulses for an analysis to be made possible.

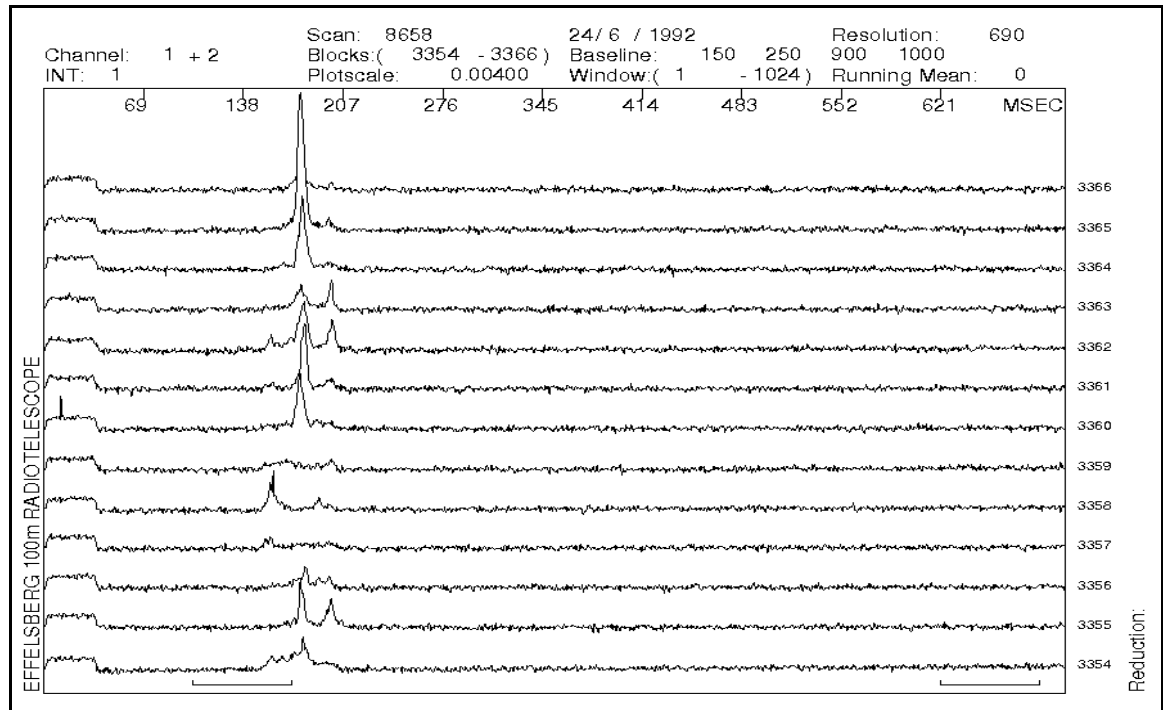


**Figure 78:** Sequence of pulses of Scan 8658

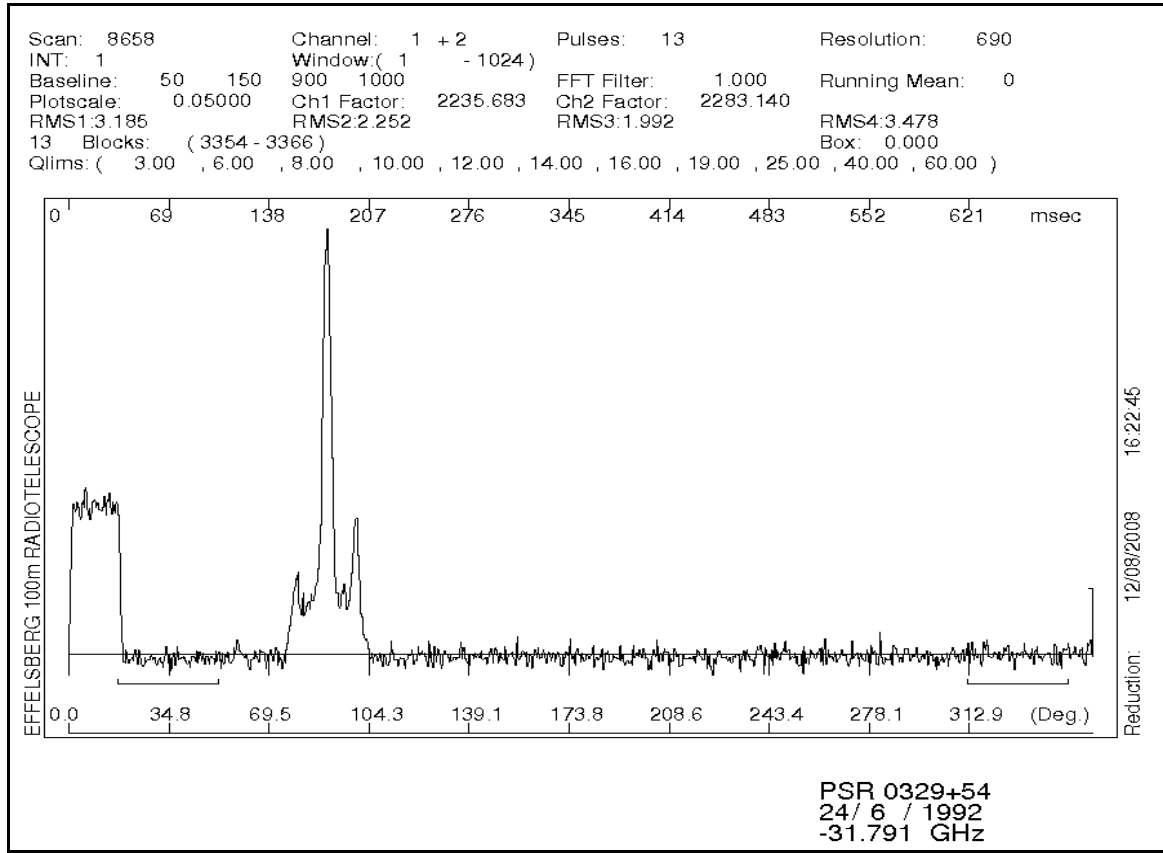


**Figure 79:** Integrated Profile of Scan 8658

A study of the quality graph shows that indeed there are too few pulses, since no more than 2 pulse per window can be seen in the graph below.

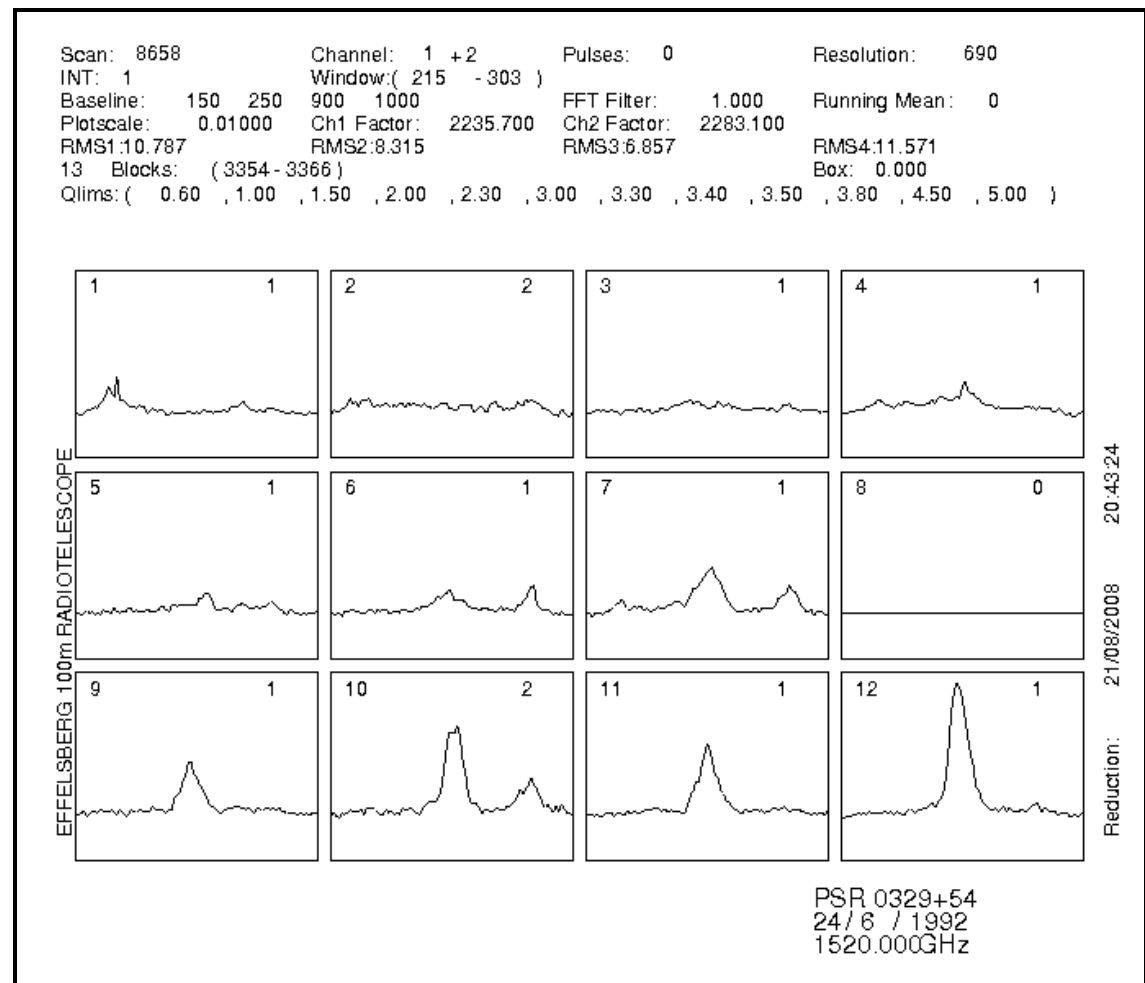


*Figure 80: Quality Graph of Scan 8658*

### Scan 8659

The sequence of pulses and the integrated profile of the scan can be seen below. A study of the sequence of pulses and the integrated profile reveal that they are well defined. Although the quality of the scan is good, there are too few pulses for an analysis to be made possible.

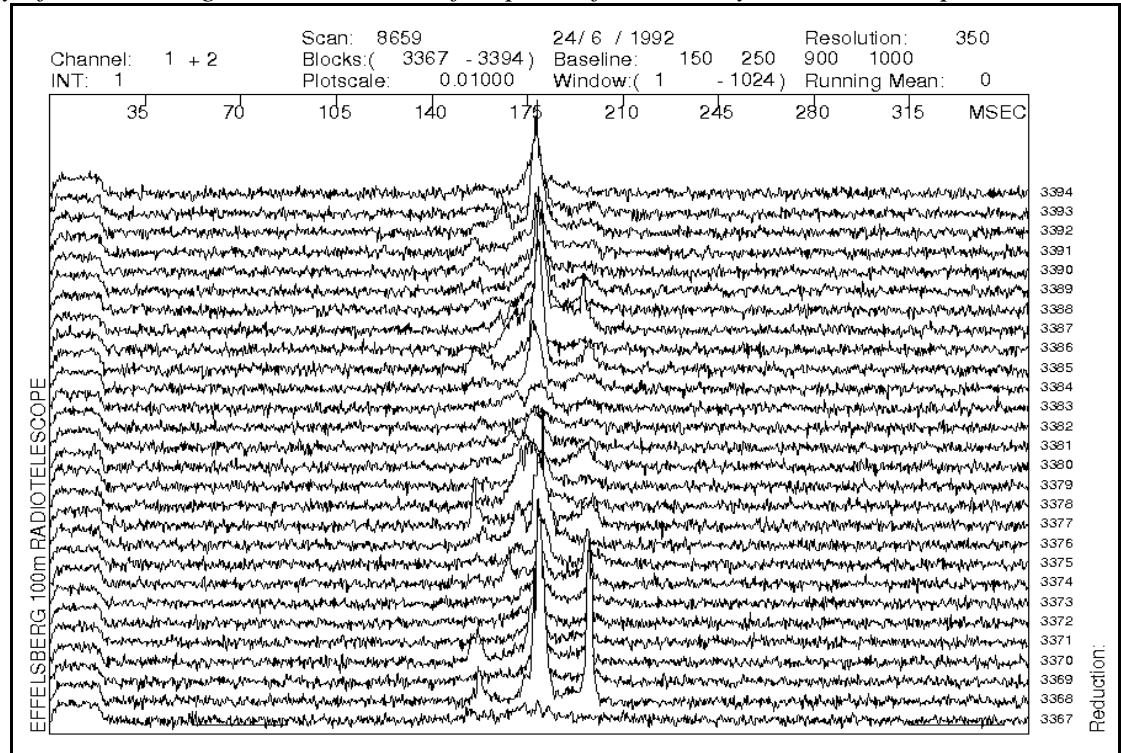


Figure 80: Sequence of pulses of Scan 8659

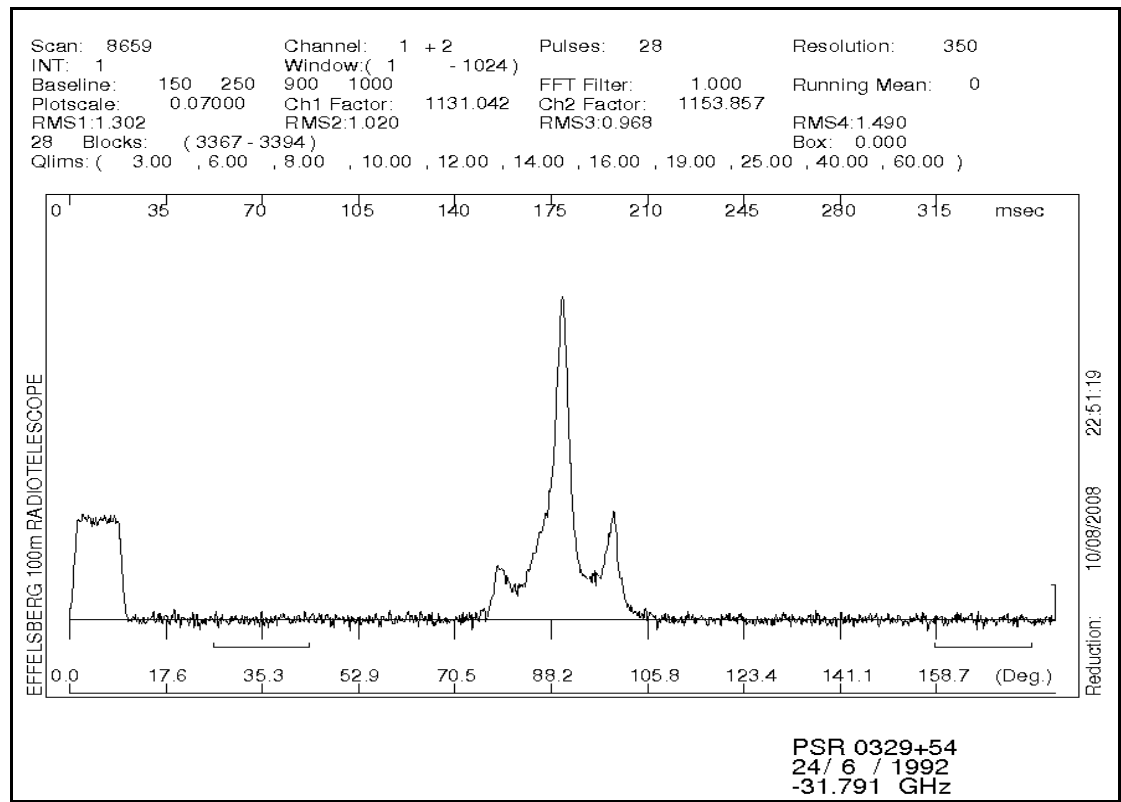
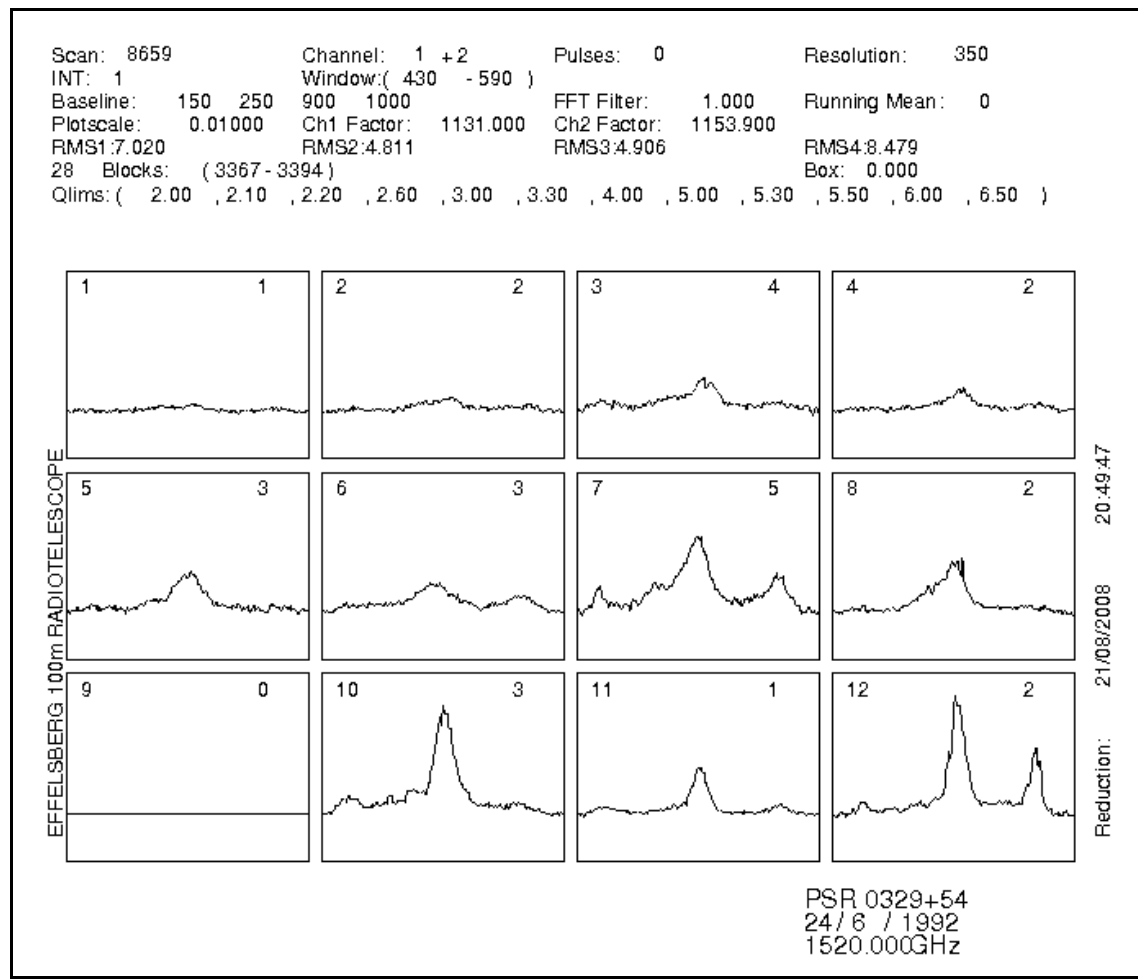


Figure 81: Integrated Profile of Scan 8659

A study of the quality graph shows that indeed there are too few pulses, since no more than 3 pulses per window can be seen in the graph below.



**Figure 82: Quality Graph of Scan 8659**

### Scan 8660

The sequence of pulses and the integrated profile of the scan can be seen below. A study of the sequence of pulses and the integrated profile reveal that they are well defined. It is obvious from the sequence of pulses that there is little noise present. A closer study of the sequence as well as the quality graph reveals that the intensity-noise ratio has a rather high value. That allows for accurate results to be drawn from its study. The main component is the pulse component with the highest values. So we assume that the main component (core component) is the central pulse, the first component the second “pulse” and the third component the first “pulse” in the integrated profile.

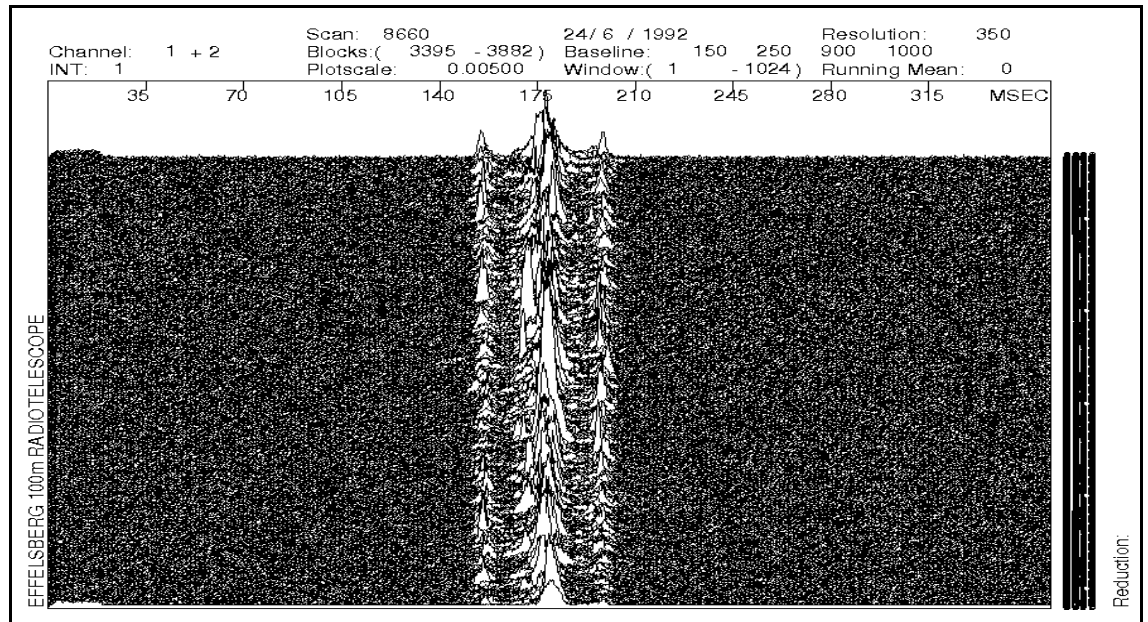


Figure 83: Sequence of pulses of Scan 8660

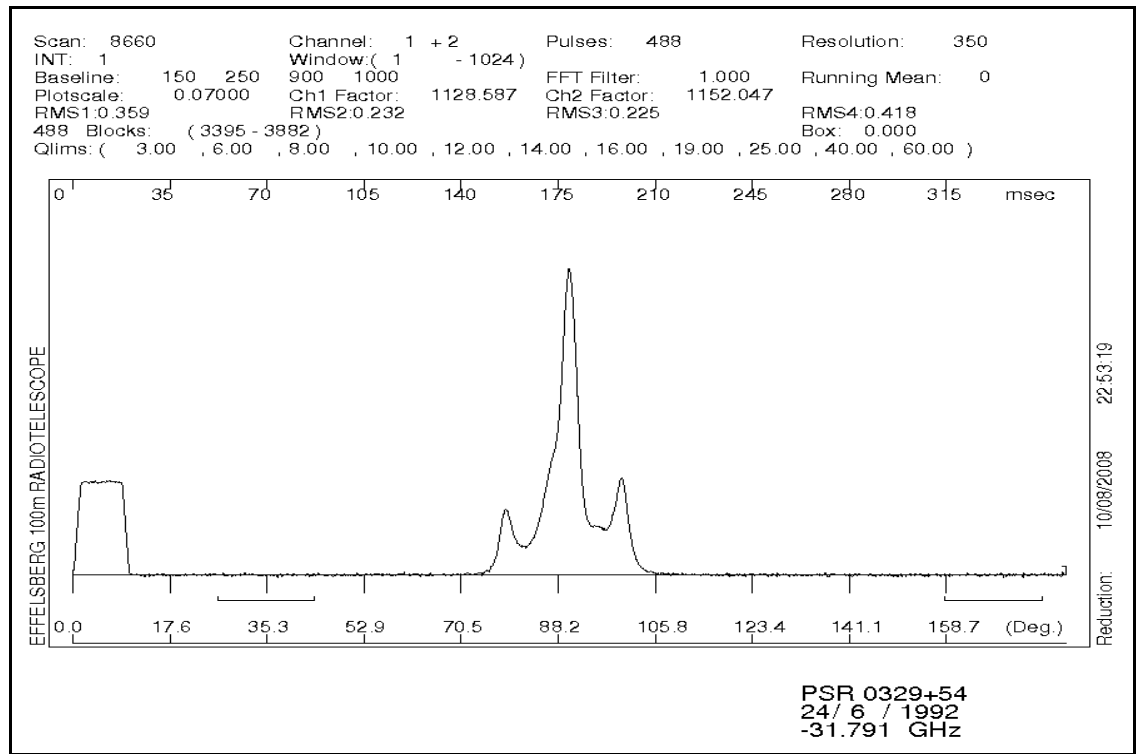


Figure 84: Integrated Profile of Scan 8660

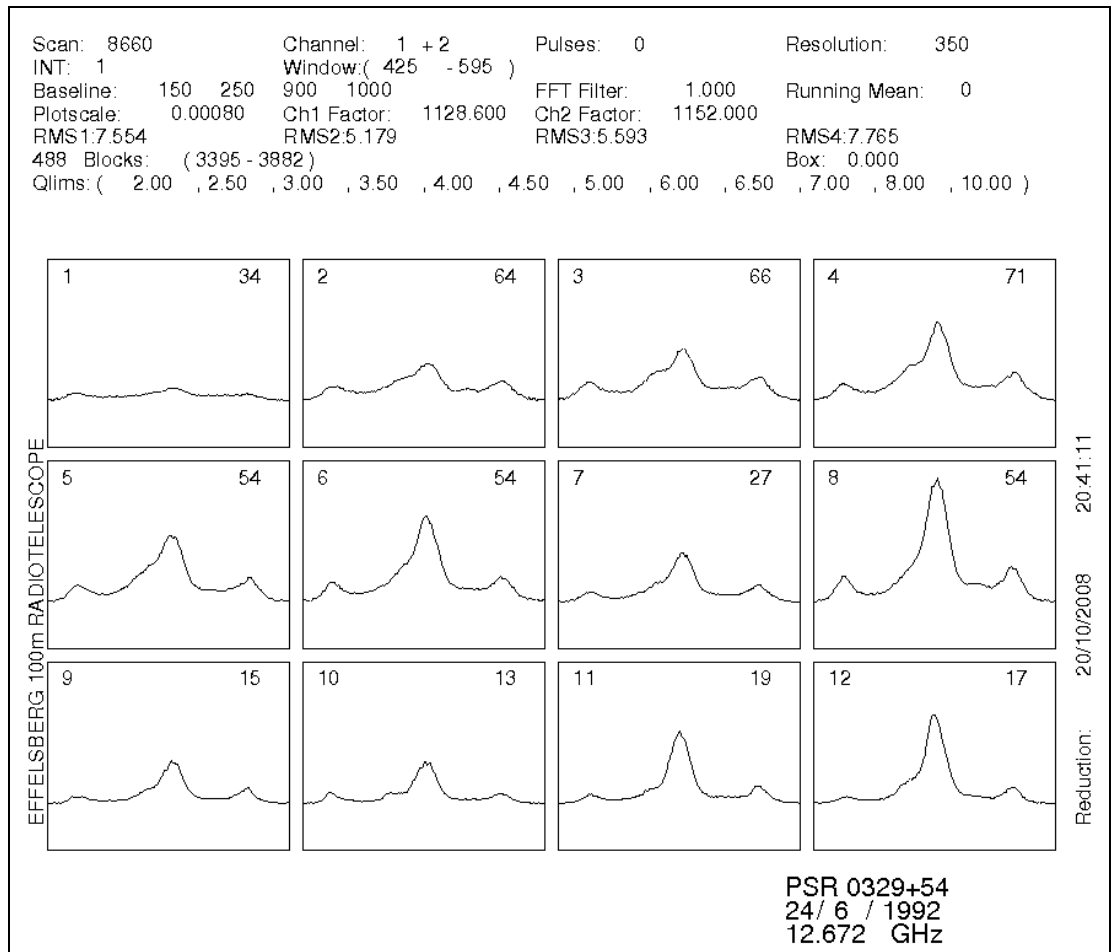


Figure 85: Quality Graph of Scan 8660

We can see the maximum values of each component for each window in the following table.

Table 11: Scan 8660

Channel	1	2	3	4	5	6
<b>Main Component</b>	1,03973E+03	3,01144E+03	4,25396E+03	6,36269E+03	5,32857E+03	6,91810E+03
<b>Component 1</b>	6,14979E+02	1,62098E+03	1,88704E+03	2,27436E+03	1,94950E+03	2,06001E+03
<b>Component 2</b>	6,55037E+02	1,14165E+03	1,53870E+03	1,36243E+03	1,35223E+03	1,60938E+03
<b>Main/Comp. 1</b>	<b>5,91480E-01</b>	<b>5,38274E-01</b>	<b>4,43596E-01</b>	<b>3,57453E-01</b>	<b>3,65858E-01</b>	<b>2,97771E-01</b>
<b>Main/Comp. 2</b>	<b>6,30007E-01</b>	<b>3,79104E-01</b>	<b>3,61710E-01</b>	<b>2,14128E-01</b>	<b>2,53770E-01</b>	<b>2,32633E-01</b>
<b>Comp.2/Comp.1</b>	<b>1,06514E+00</b>	<b>7,04296E-01</b>	<b>8,15404E-01</b>	<b>5,99039E-01</b>	<b>6,93629E-01</b>	<b>7,81249E-01</b>
Channel	7	8	9	10	11	12
<b>Main Component</b>	3,99572E+03	1,00268E+04	3,49303E+03	3,40538E+03	5,85361E+03	7,14527E+03
<b>Component 1</b>	1,39190E+03	2,85347E+03	1,30524E+03	8,13183E+02	1,39988E+03	1,33220E+03
<b>Component 2</b>	<b>8,28276E+02</b>	<b>2,06222E+03</b>	<b>5,90691E+02</b>	<b>8,96497E+02</b>	<b>7,93443E+02</b>	<b>5,26870E+02</b>
<b>Main/Comp. 1</b>	<b>3,48348E-01</b>	<b>2,84584E-01</b>	<b>3,73670E-01</b>	<b>2,38794E-01</b>	<b>2,39148E-01</b>	<b>1,86445E-01</b>
<b>Main/Comp. 2</b>	<b>2,07291E-01</b>	<b>2,05671E-01</b>	<b>1,69106E-01</b>	<b>2,63259E-01</b>	<b>1,35548E-01</b>	<b>7,37369E-02</b>
<b>Comp.2/Comp.1</b>	<b>5,95069E-01</b>	<b>7,22706E-01</b>	<b>4,52554E-01</b>	<b>1,10245E+00</b>	<b>5,66794E-01</b>	<b>3,95489E-01</b>

From the tables above we get the following diagram:

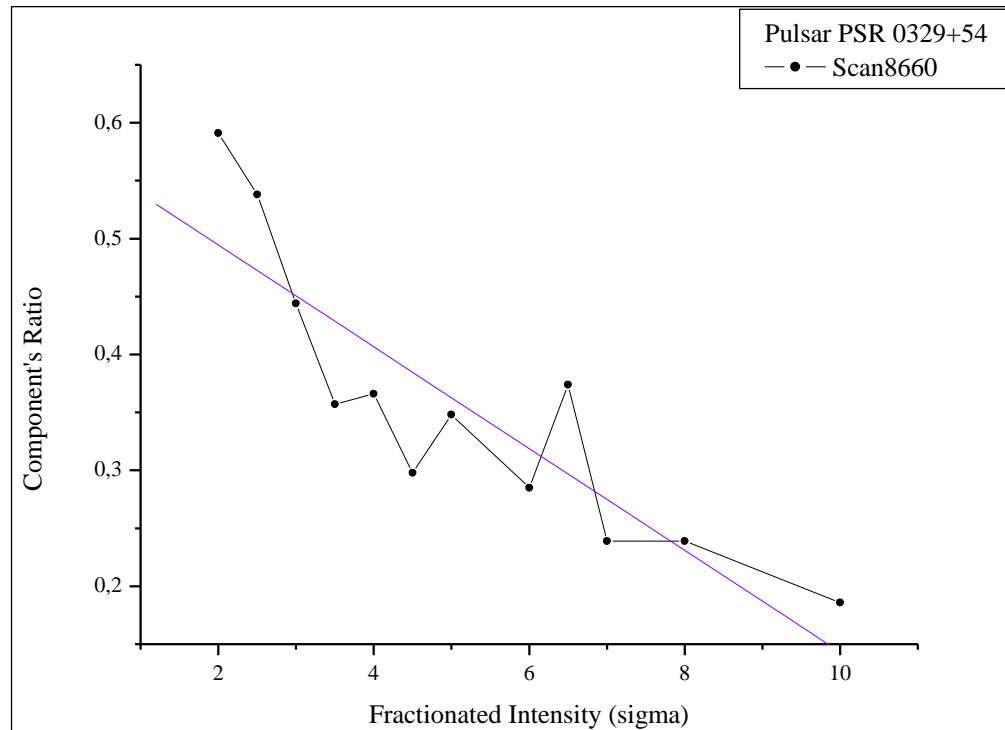


**Figure 86:** Main component, First component Ratio of Scans 8660

The linear fit gives us a descending line with the following equation:

$$y = 0,58234 - 0,04392x$$

A descending line means that the ratio of the main and first component decreases as the fractionated intensity (sigma) increases.

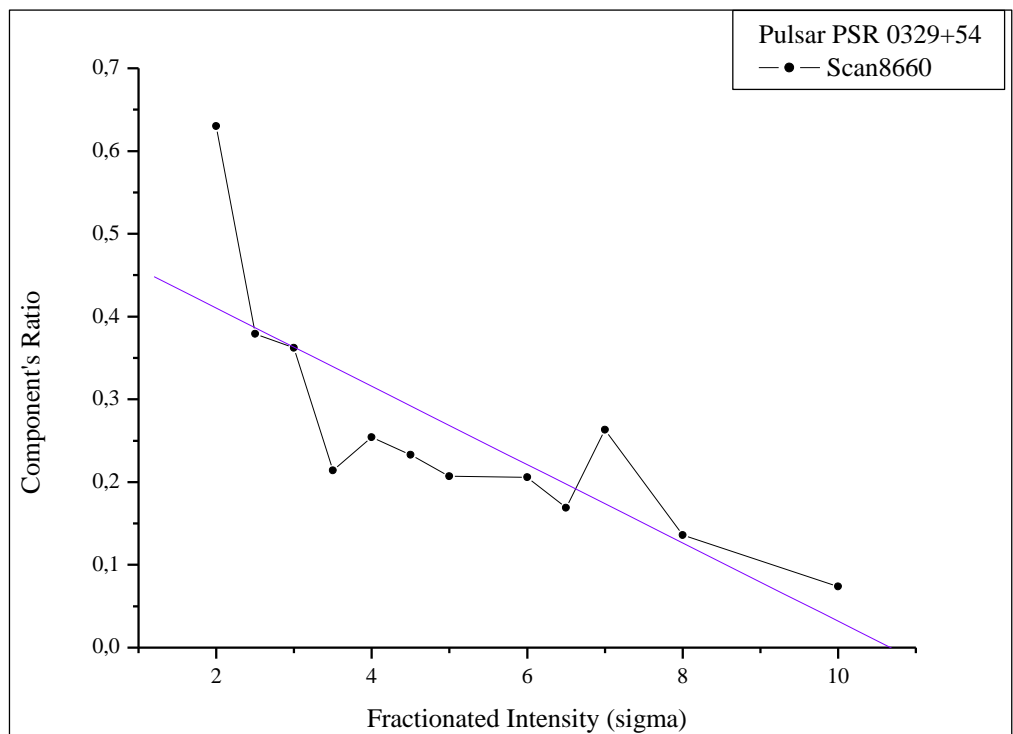


**Figure 87:** Second to Main component of Scan 8660

The linear fit gives us a descending line with the following equation:

$$y = 0,505 - 0,0473 \text{ lx}$$

A descending line means that the ratio of the main and first component decreases as the fractionated intensity (sigma) increases.

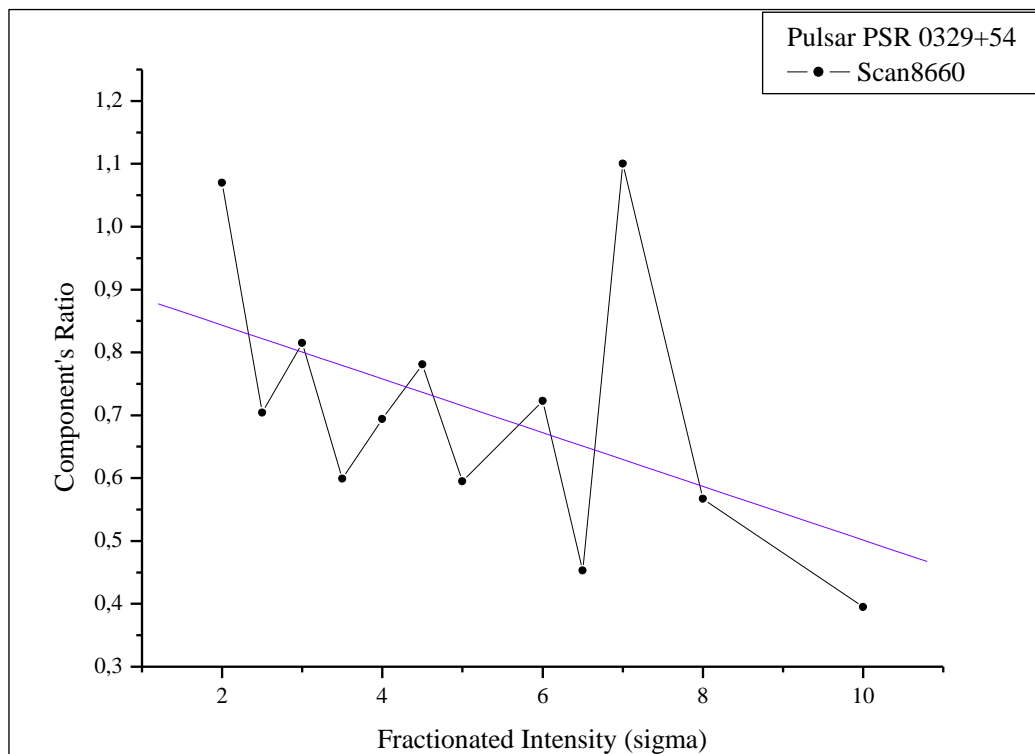


**Figure 88:** Second component, First component of Scan 8660

The linear fit gives us a descending line with the following equation:

$$y = 0,92877 - 0,04273x$$

A descending line means that the ratio of the main and first component decreases as the fractionated intensity (sigma) increases.

### (3.3)Pulsar PSR 0450+55

#### Scan 9038

The sequence of pulses and the integrated profile of the scan can be seen below. A study of the sequence of pulses and the integrated profile reveal that they are well defined. A spike can be seen in the sequence of pulses. It was probably caused by an accidental rebooting of the amplifier. A closer study of the sequence as well as the quality graph reveals that the intensity-noise ratio has a rather low value.

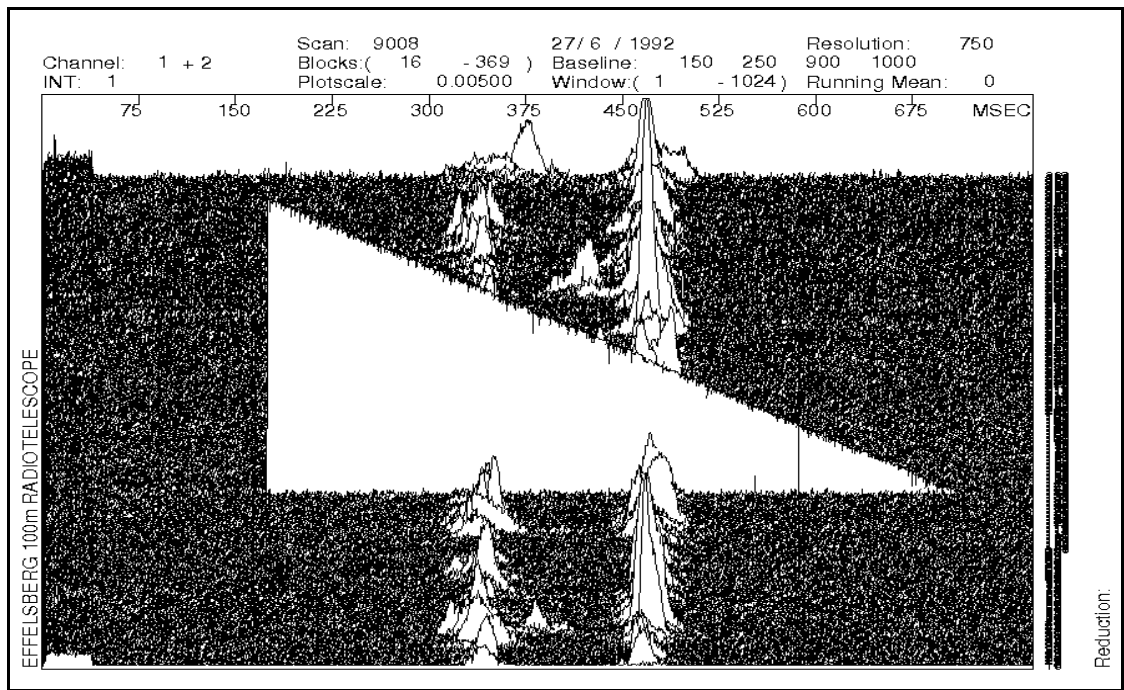


**Figure 89:** Sequence of pulses of Scan 9038

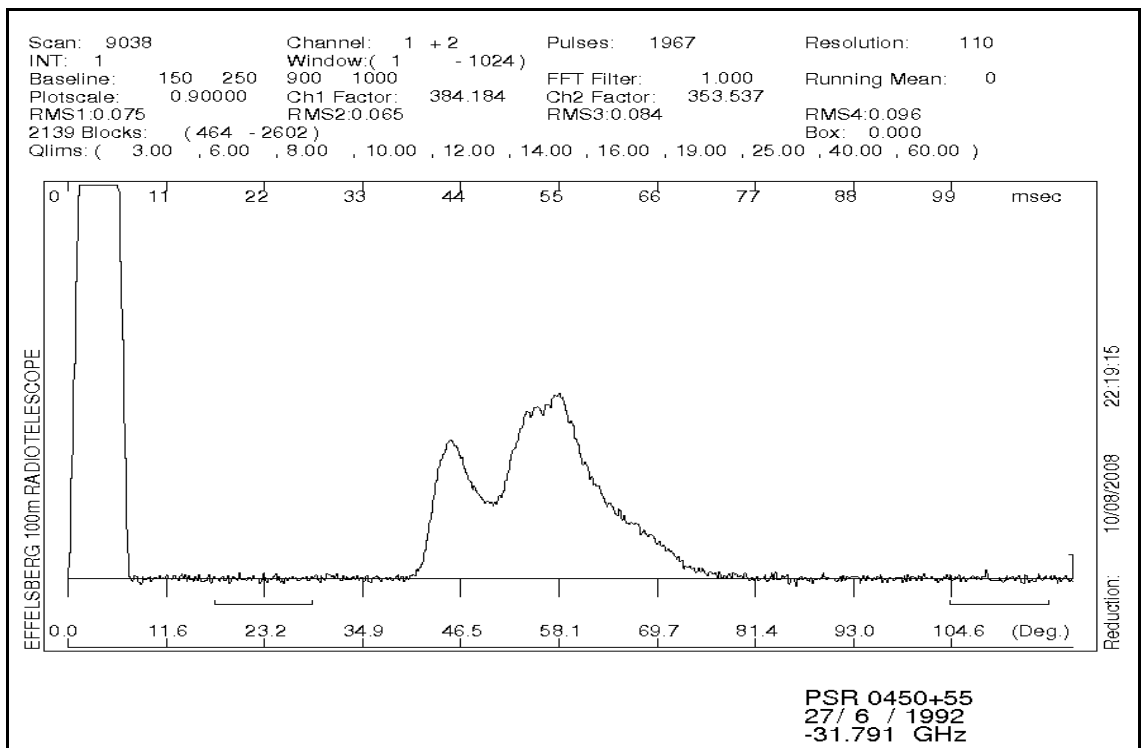


**Figure 90:** Integrated Profile of Scan 9038

As we can see below, the sigma is very low. That means, that what we really observe is noise. Therefore the results cannot be used.

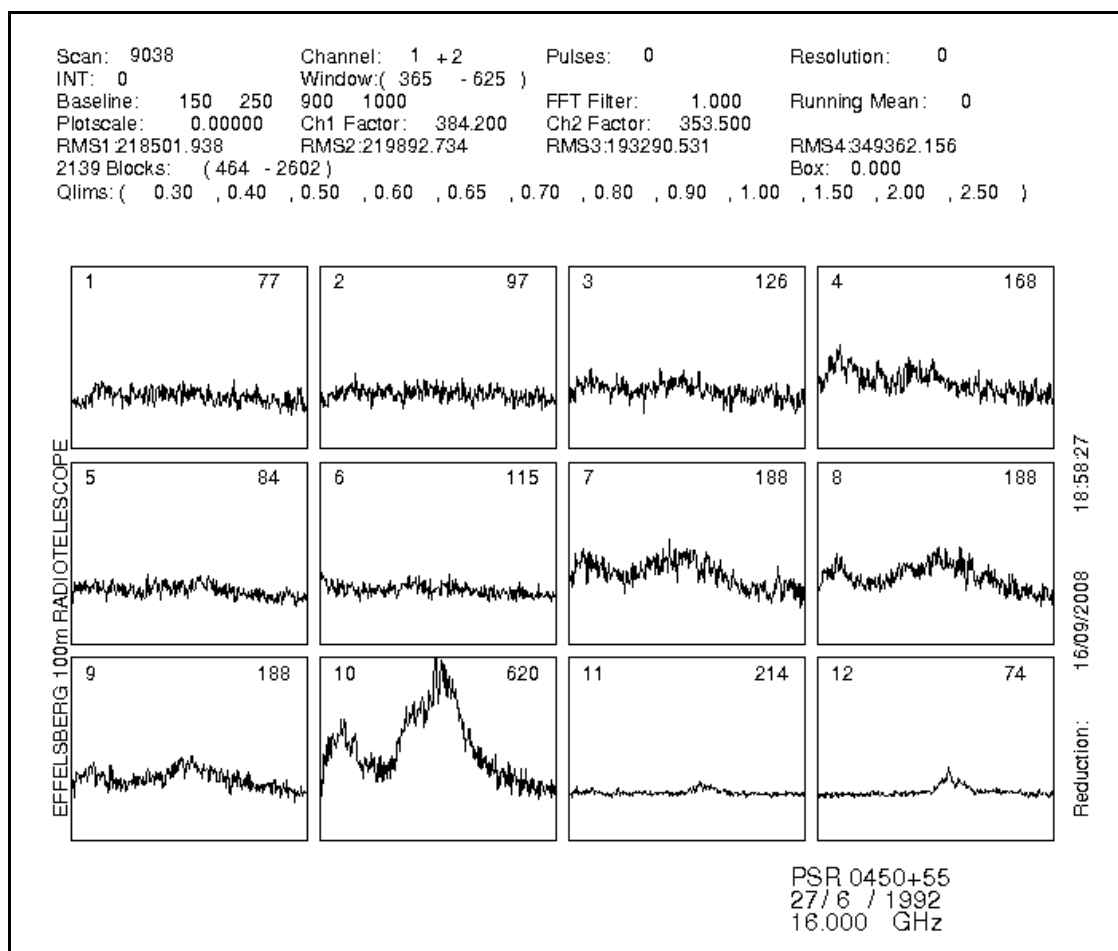


*Figure 9I: Quality Graph of Scan 9038*

### (3.4)Pulsar PSR 1822-09

#### Scan 9118

The sequence of pulses and the integrated profile of the scan can be seen below. A study of the sequence of pulses reveals that they are not well defined. It is obvious from the sequence of pulses that there is a lot of noise present. Enough so that no results can be drawn from the study of this scan.

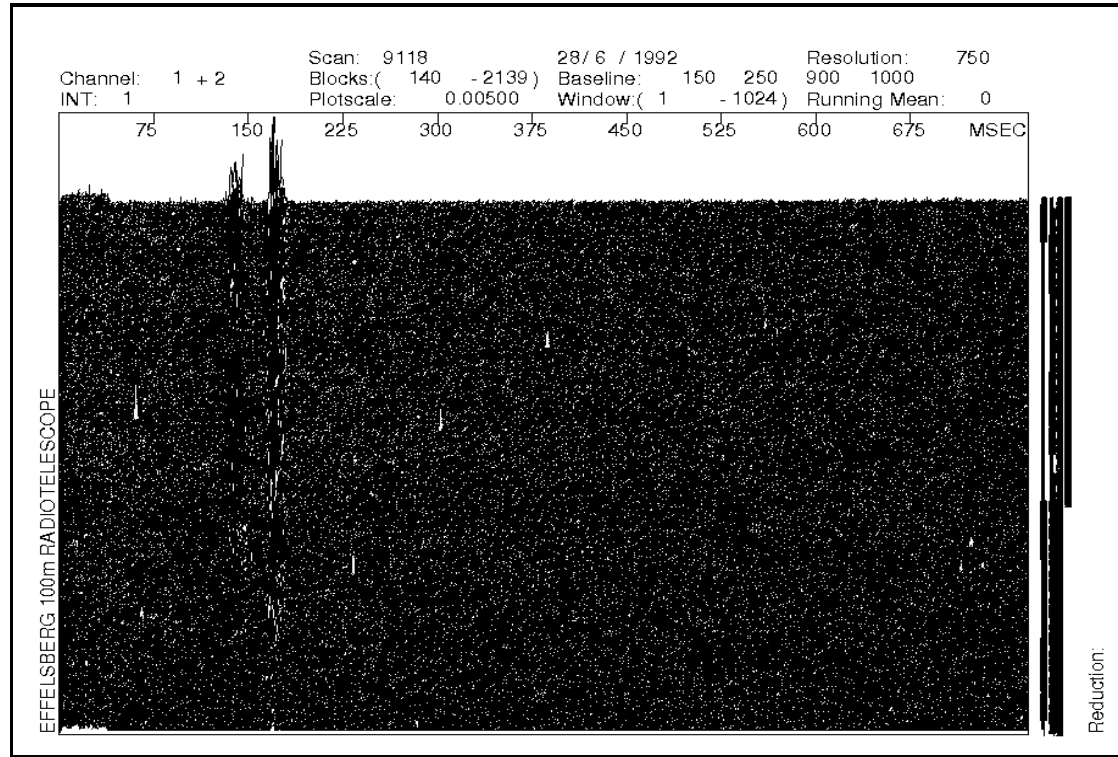


**Figure 92:** Sequence of pulses of Scan 9118

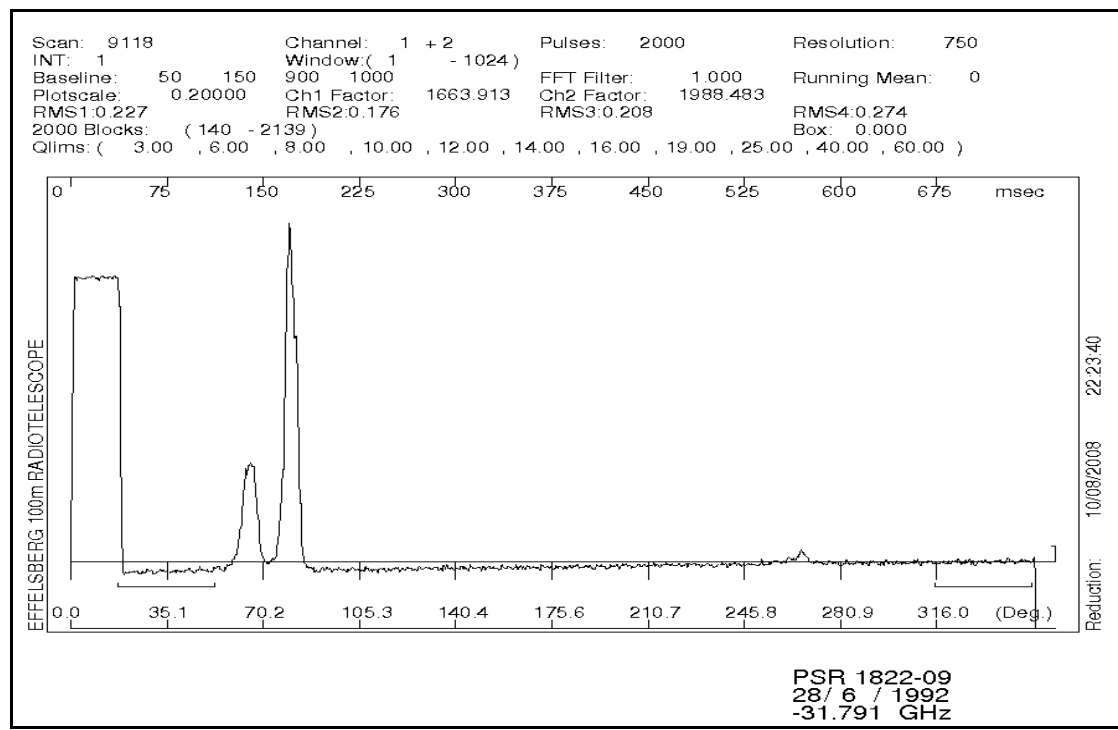


**Figure 93:** Integrated Profile of Scan 9118

As we can see the sigma takes low values and there are too few pulses in the last windows.

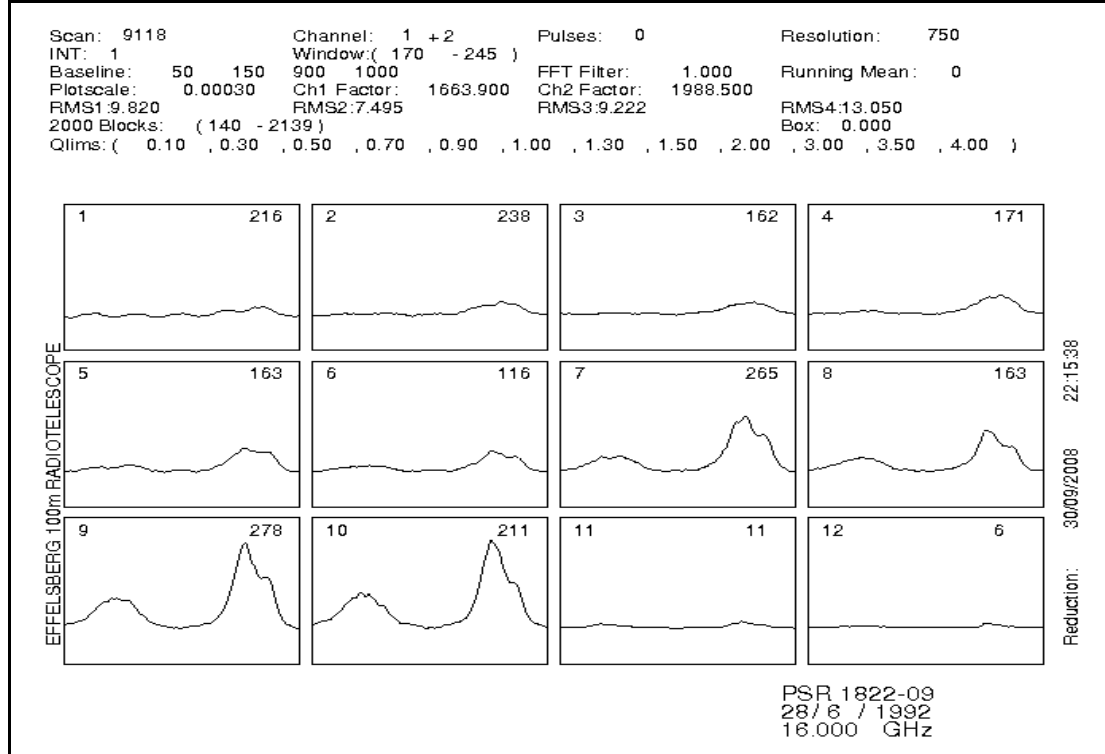


*Figure 94: Quality Graph of Scan 9118*

### Scan 9119

The sequence of pulses and the integrated profile of the scan can be seen below. A study of the sequence of pulses reveals that they are not well defined. It is obvious from the sequence of pulses that there is a lot of noise present. Enough so that no results can be drawn from the study of this scan.

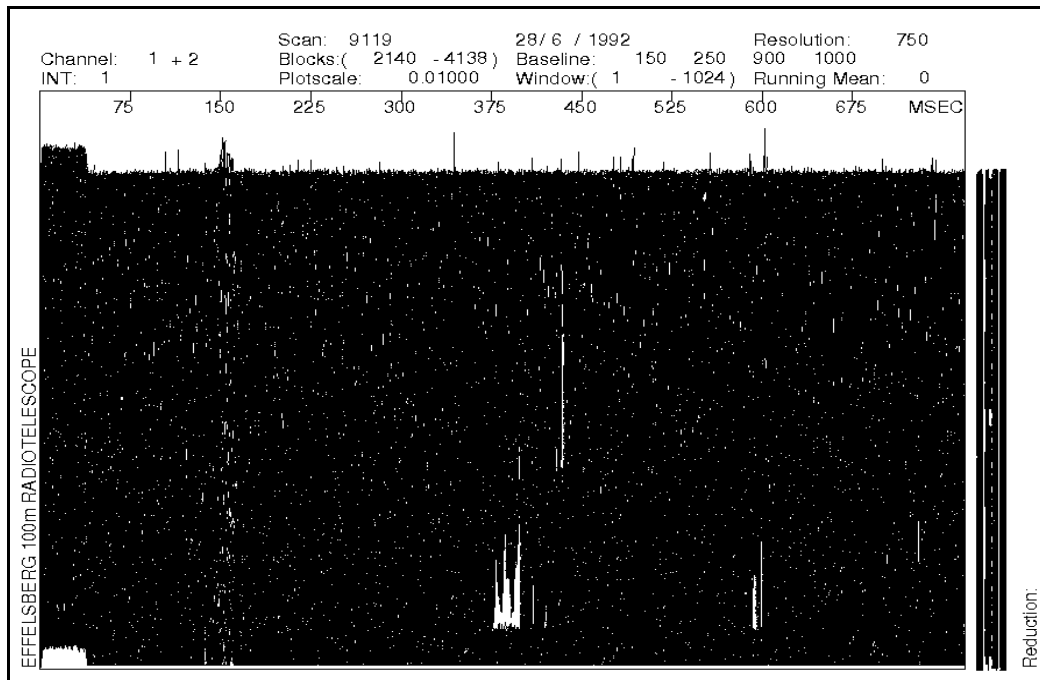


*Figure 95: Sequence of pulses of Scan 9119*

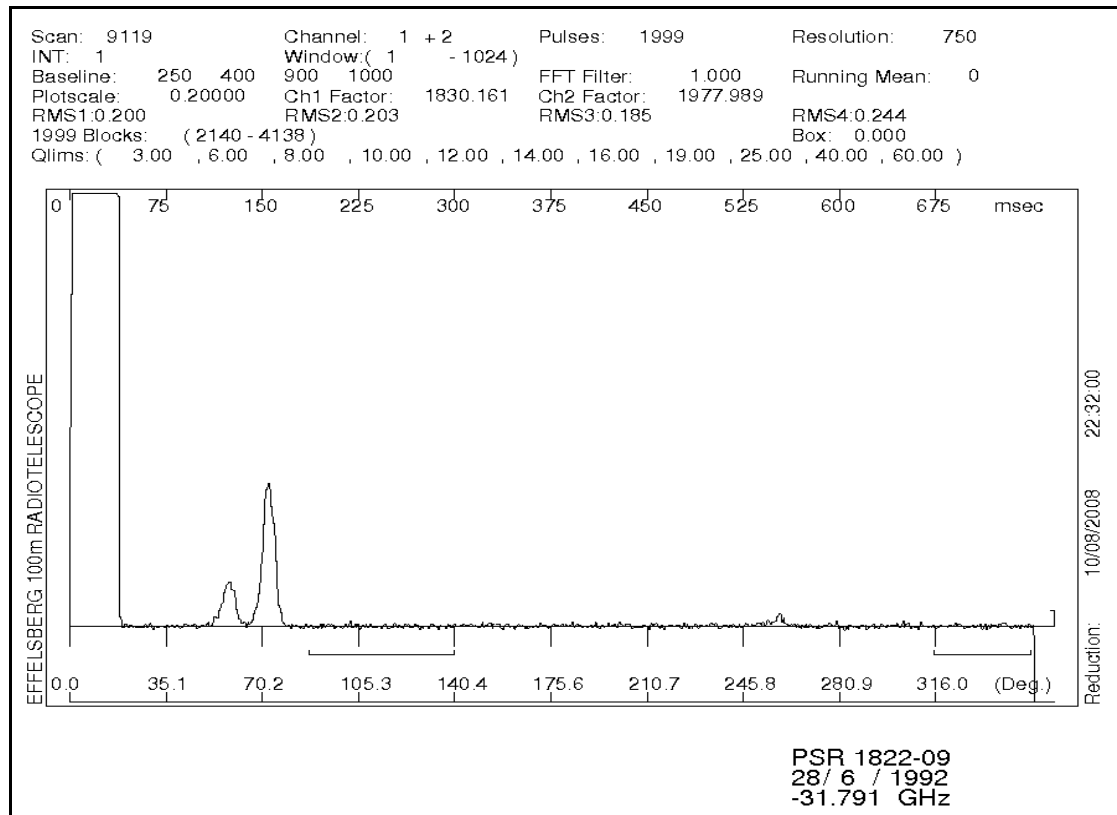


**Figure 96: Integrated Profile of Scan 9119**

As we can see below the sigma has very low values,

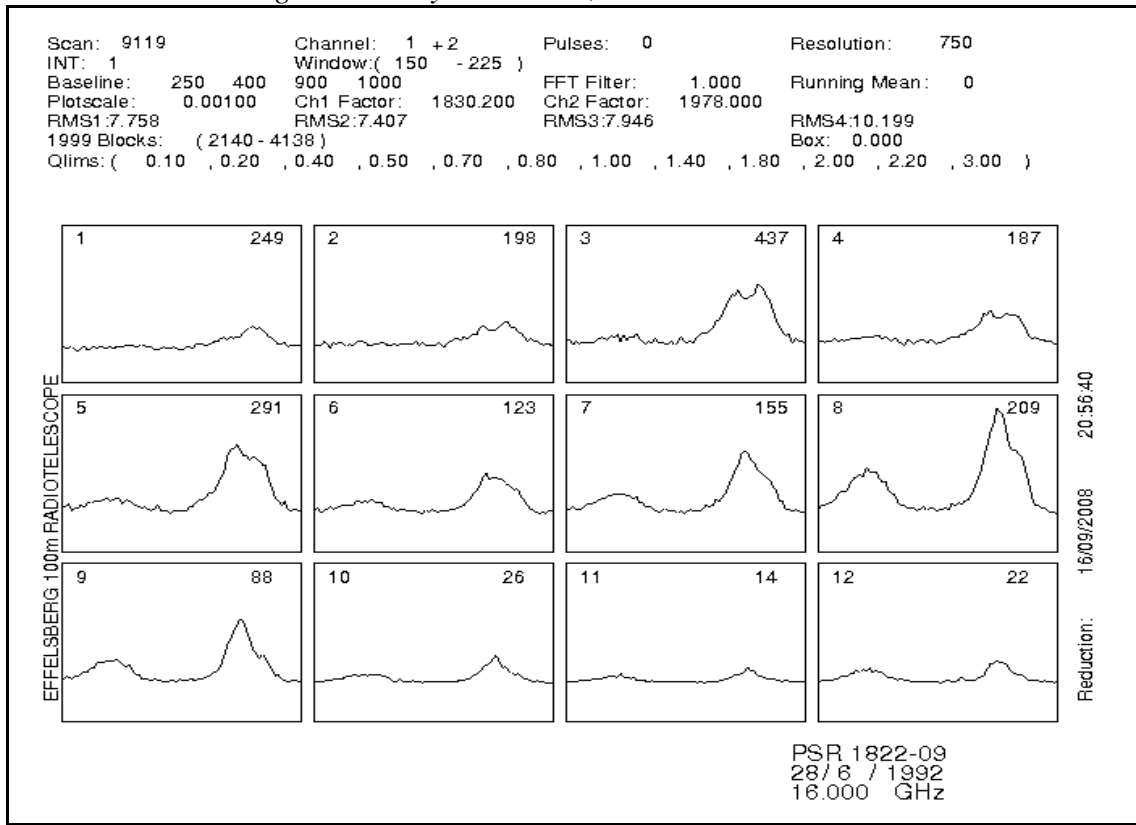


**Figure 97: Quality Graph of Scan 9119**

### (3.5)Pulsar PSR 0823+26

#### Scan 9175

The sequence of pulses and the integrated profile of the scan can be seen below. A study of the sequence of pulses reveals that the two pulses are not easily distinguishable. Therefore no results can be drawn from the study of this scan. The baseline of the left side of the intergrated profile is underneath the zero point average.

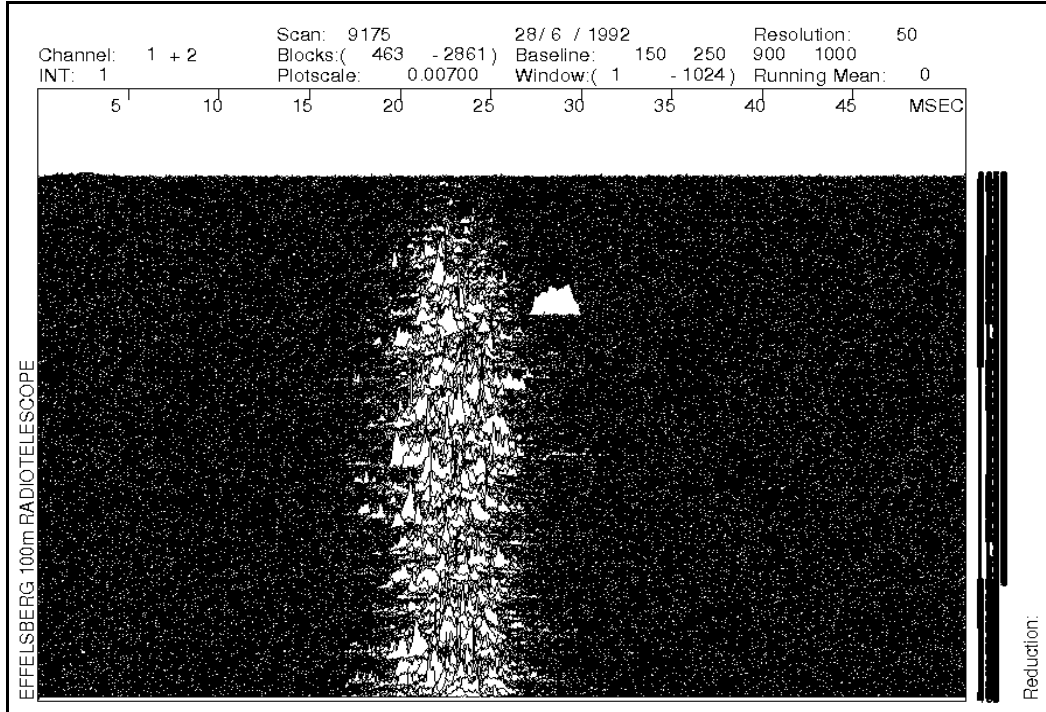


Figure 98: Sequence of pulses of Scan 9175

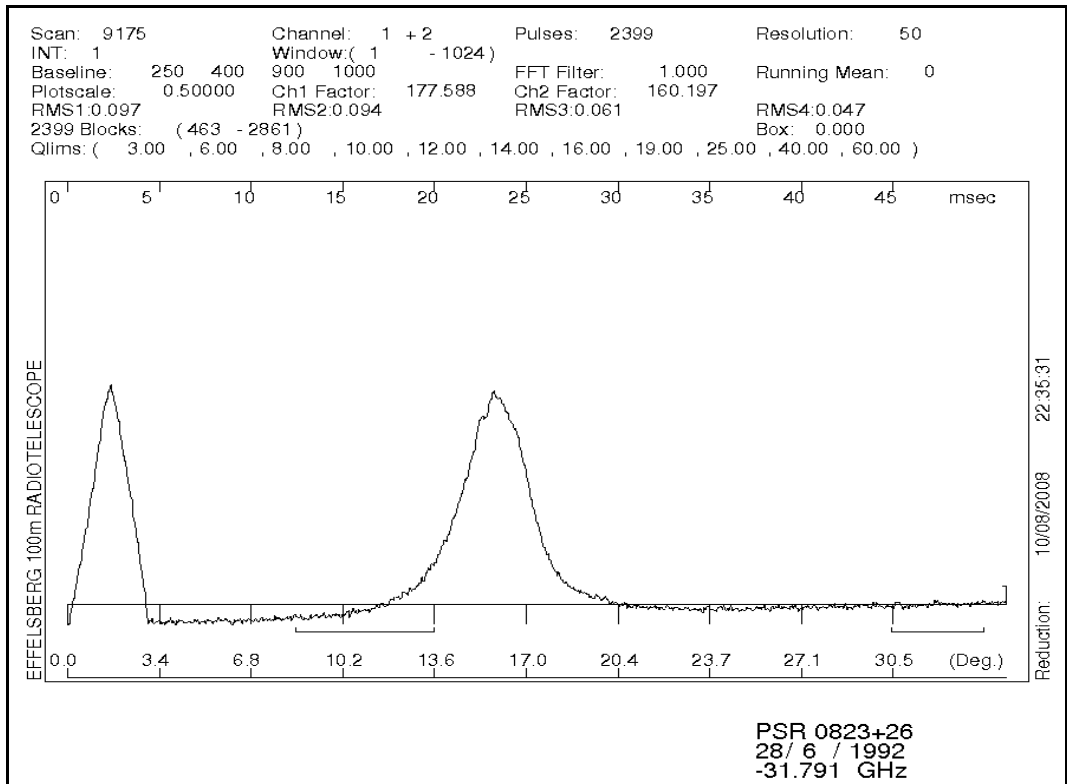
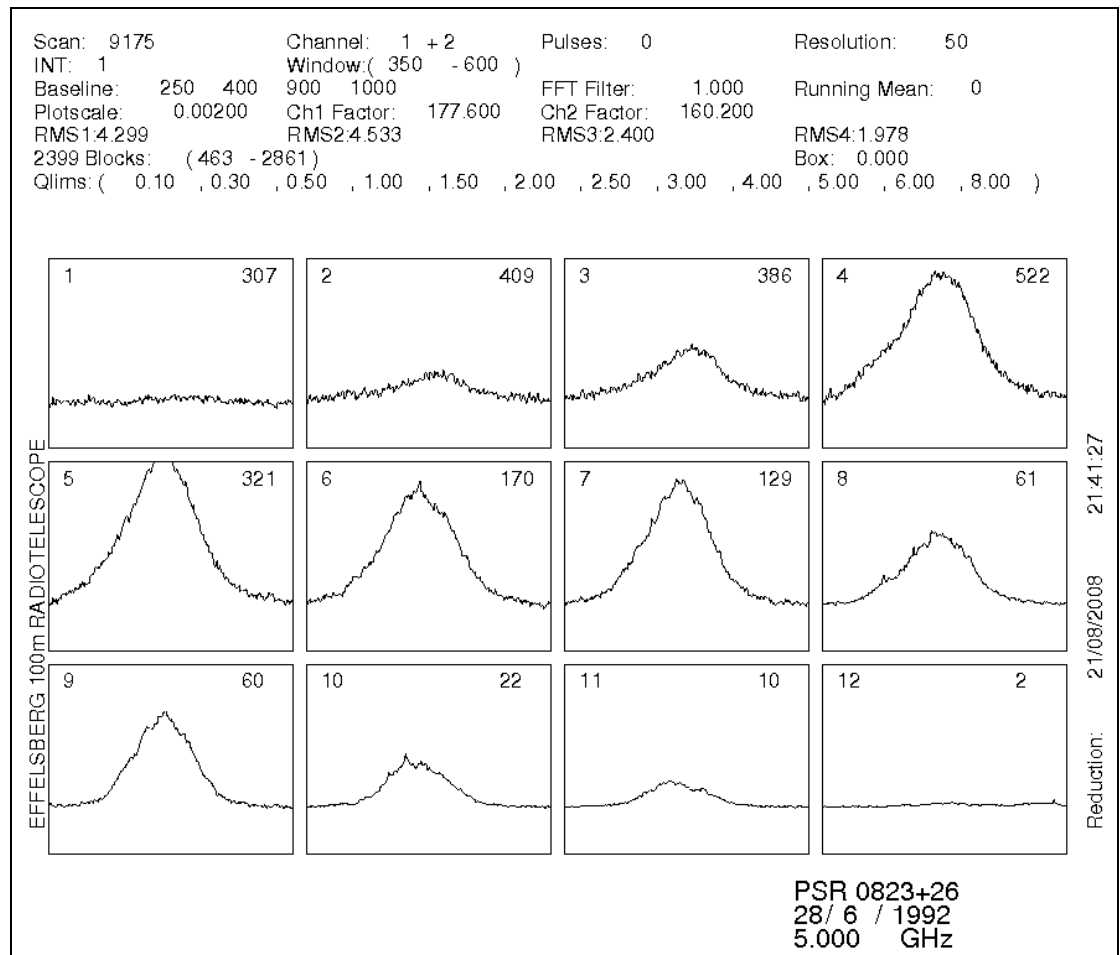


Figure 99: Integrated Profile of Scan 9175

The same conclusion can be drawn from the study of the Quality Profile, since it is obvious here as well that that only one component (the main component) is visible.



*Figure 100: Quality Graph of Scan 9175*

### (3.6)Pulsar PSR 1133+73

#### Scan 6160

The sequence of pulses and the integrated profile of the scan can be seen below. A study of the sequence of pulses and the integrated profile reveal that they are well defined. The pulses start strong and weaken as the recording progresses. It is obvious from the sequence of pulses that there is very little noise present. A closer study of the sequence, as well as the quality graph, reveals that the intensity-noise ratio has a high value. That allows for accurate results to be drawn from its study. The main component is the pulse component with the highest values. So we assume that the main component (core component) is the first in the integrated profile.

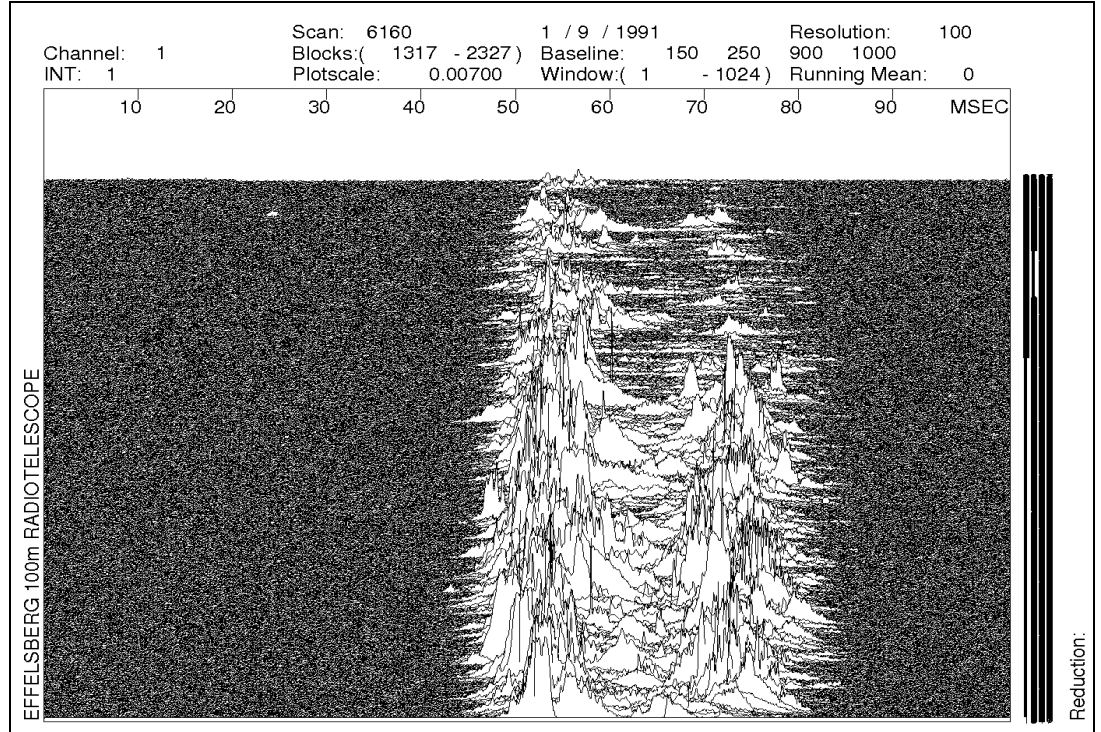


**Figure 101:** Sequence of pulses of Scan 6160

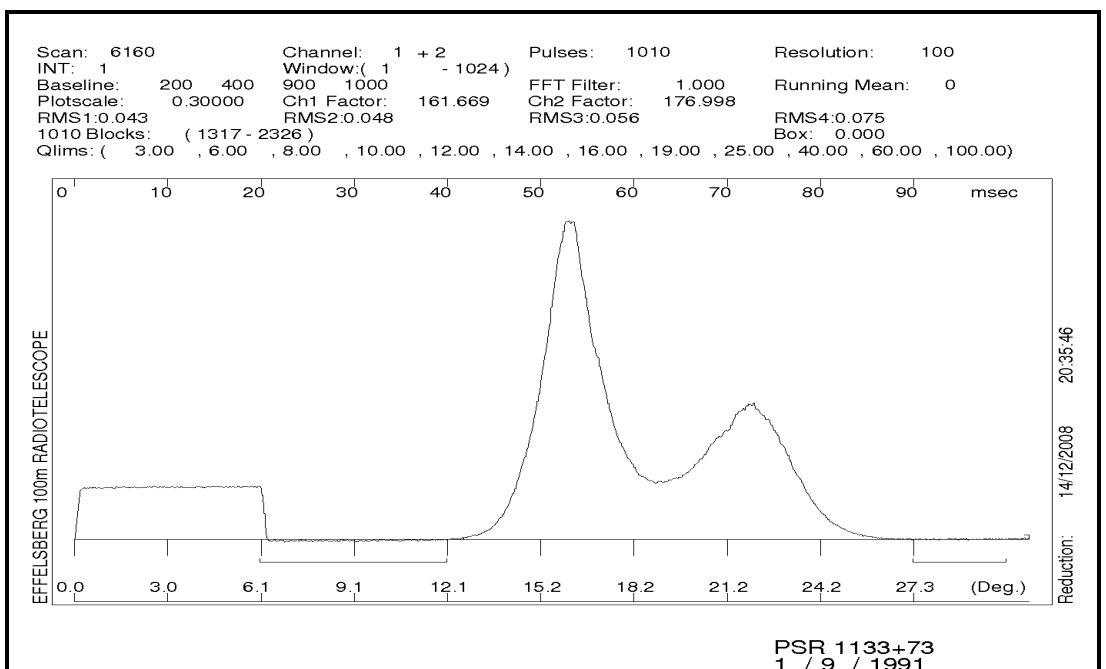


**Figure 102:** Integrated Profile of Scan 6160

The first window depicts the pulses with the lowest intensity, with a sigma equal to 2. We see that, the maximum pulse intensity of the main component is always greater to the maximum value of the first component.

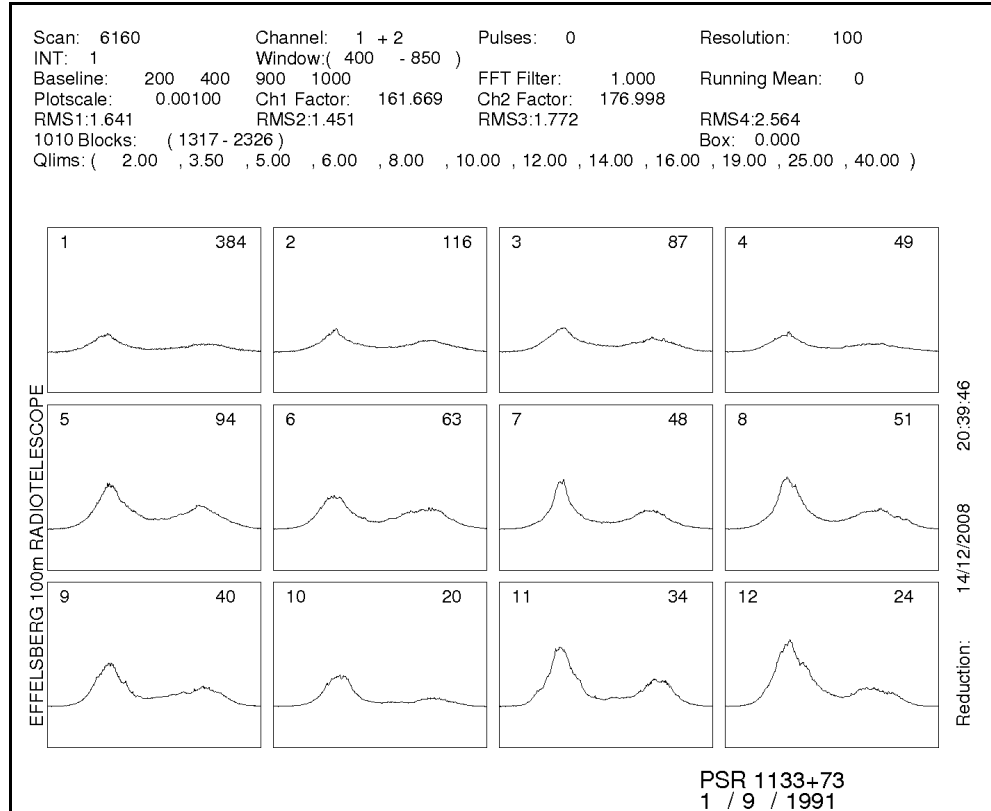


Figure 103: Quality Graph for Scan 6160

We can see the maximum values of each component for each window in the following table.

Table : Scan 6160

Channel	<b>1</b>	<b>2</b>	<b>3</b>	<b>4</b>	<b>5</b>	<b>6</b>
<b>Main Component</b>	1,33713E+03	1,71308E+03	1,77601E+03	1,51417E+03	3,38741E+03	2,48254E+03
<b>Component 1</b>	5,98323E+02	8,54395E+02	1,10737E+03	6,26553E+02	1,75230E+03	1,59936E+03
<b>Main/Comp. 1</b>	<b>0,447468085</b>	<b>0,498747869</b>	<b>0,623515633</b>	<b>0,413793035</b>	<b>0,517297877</b>	<b>0,644243396</b>
Channel	<b>7</b>	<b>8</b>	<b>9</b>	<b>10</b>	<b>11</b>	<b>12</b>
<b>Main Component</b>	3,61134E+03	3,84298E+03	3,15635E+03	2,34340E+03	4,35998E+03	4,89948E+03
<b>Component 1</b>	1,38095E+03	1,54634E+03	1,47555E+03	6,26881E+02	2,02957E+03	1,40058E+03
<b>Main/Comp. 1</b>	<b>3,82393E-01</b>	<b>4,02380E-01</b>	<b>4,67486E-01</b>	<b>2,67509E-01</b>	<b>4,65500E-01</b>	<b>2,85863E-01</b>

From the tables above we get the following diagram:

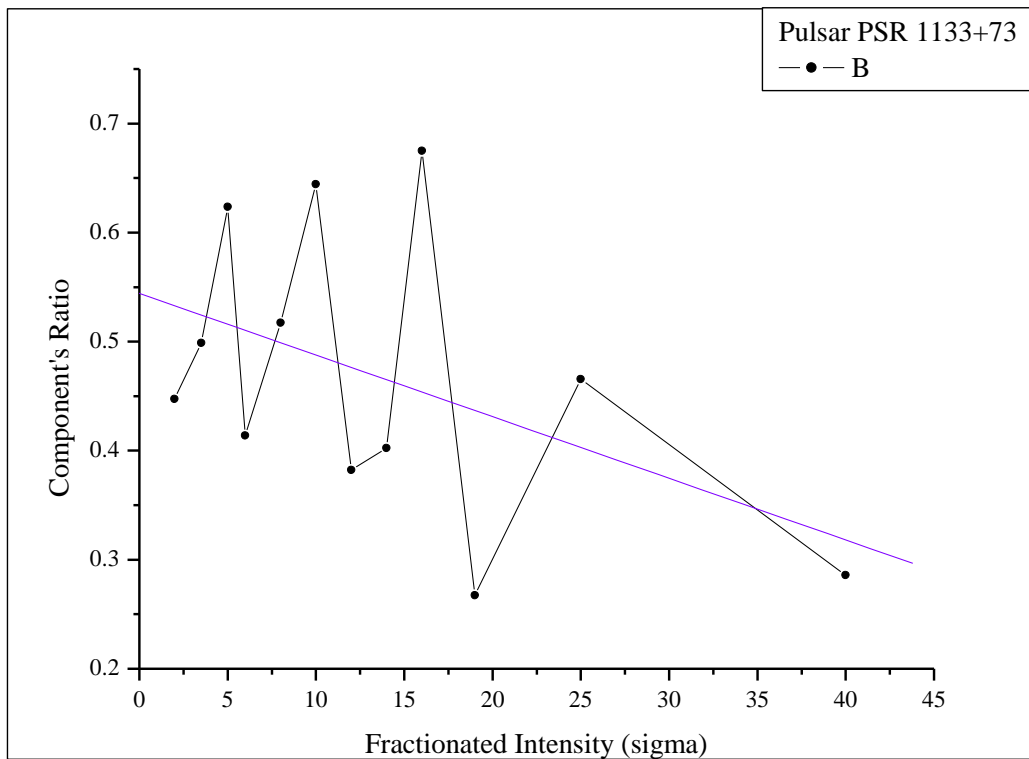


**Figure 104:** Main component, First component Ratio for Scan 6061

The linear fit gives us a descending line with the following equation:

$$y = 0.54427 - 0.00566x$$

A descending line means that the ratio of the main and first component decreases as the fractionated intensity (sigma) increases.

## VI. Conclusions:

- ❖ For pulsar PSR 0525+21:
  - The linear fit of the First to the Main component ratio has a negative slope. Therefore the ratio of the components decreases as the individual pulses get stronger..
  - The slope of the linear fit line has a much higher value in Scan 9008 compared to Scans 7702, 7827, 7833. This could be attributed to the fact that the observations were made in different frequencies (1,420 GHz for Scans 7702, 7827, 7833 and 1,6 GHz for Scan 9008)
- ❖ For pulsar PSR 0329+54:
  - The linear fits of the First to the Main component ratio and the Second to the Main component ratio have a negative slope.
  - The linear fit of the Second component to the Main component ratio has a negative slope for Scan 8653 and Scan 8660 but has a positive slope for Scan 8657.
- ❖ For pulsar PSR 1133+73:
  - The linear fit of the First to the Main component ratio has a negative slope. Therefore the ratio of the components decreases as the pulses get stronger.

The linear fit of the First to the Main component ratio and for the Second to the Main component ratio are similar (with a negative slope) to the results of Metallinou Fiori Anastasia's thesis.

Whereas the results of the linear fit for the Second to the First component ratio cannot be compared since she made no such study.

The negative slope of the linear fit of the First to the Main and of the Second to the Main components indicates that the observed components originate from different radiation sources within the radiation beam.

If the observed components originated from the same radiation source the component's ratio would either increase or remain stable with the increase of the fractionated pulse intensity ( $\sigma$ ).

A careful study of the integrated profiles of PSR 0329+54 of scans 8653 and 8657 reveals the mode changing that has occurred in the scan 8657. So the slope of the linear fit of the Second to the First component could be explained by the mode changing.

### **(C). Bibliography**

*Pulsars, Manchester, Richard N., Taylor, Joseph H. (Joseph Hooton) W. H. Freeman, c1977.*

*Pulsars, Graham-Smith, Francis, (Francis Graham), Sir, 1923-Cambridge University Press, 1977.*

*Pulsar astronomy, Lyne, Andrew. G., Graham-Smith, Francis, Sir, 1923-Cambridge University Press, 2006.*

*Cordes, James. M. (1975). *Astrophys. J.* 195, 193.*

*Craft, H. D., J. M. Comella, and Frank. D Drake. 1968. *Nature*, 218:1122*

*Craft, H. D. & Comella, J. M., (1968). *Nature*,. 220, 676.*

*Gold, Tommy. 1968. *Nature*, 218:731*

*Hesse, K. H., and Wielebinski Richard. 1974. *Astron. Astrphys.*, 31:409.*

*Huguenin, G. R., J. H. Taylor, R. M. Hjellming, and C. M. Wade. 1971. *Nature Phys. Sci.*, 243:50.*

*Komesaroff, M. M. 1970. *Nature*, 225:612*

*Ritchings, R. Timothy. 1976. *Mon. Not. Roy Astron. Soc.*, 176:249.*

*Robinson, B. J., B. F. C. Cooper, F. F. Gardner, R. Wielebinski, and Tom. L. Landecker. 1968. *Nature*, 218:1143.*

*Taylor, J. H., and G. R. Huguenin. 1971. *Astrophys. J.*, 167:273*

*Taylor, J. H., and R. N. Manchester. 1975. *Astron. J.*, 80:794.*

*Taylor, J. H. and R. N. Manchester, and G. R. Huguenin. 1975. *Astrophys. J.*, 195:513*

*Komesaroff, M. M, Morris, Dave. & Cooke, D.J., 1970. *Astrophys. Lett.*, 5, 37.*

*Dunkan. R. Lorimer, Max Planck Institut für Radioastronomie, Auf dem Hügel 69, D-53121, Bonn, Germany.*

[www.wikipedia.com](http://www.wikipedia.com)

*Γλώσσα Fortran 77 , Συγγραφέας: Shelley, John, 1940-, Νινής, N. (in greek)*

*FORTRAN 77:με στοιχεία του MS-DOS, Συγγραφέας: Λάζος, Κωνσταντίνος E. (in greek)*

*Fortran, Σωτήριος Κ. Περσίδης, Καθηγητής Πανεπιστημίου Θεσσαλονίκης, ΙΔΕΑ, Αθήνα*

*Manchester, R. N., Hobbs, G. B., Teoh, A. & Hobbs, M., AJ, 129, 1993-2006 (2005)*

*<http://www.atnf.csiro.au/research/pulsar/psrcat/>*

*<http://www.mpifr-bonn.mpg.de/survey.html>*